ALLIGATOR RIVERS ANALOGUE PROJECT

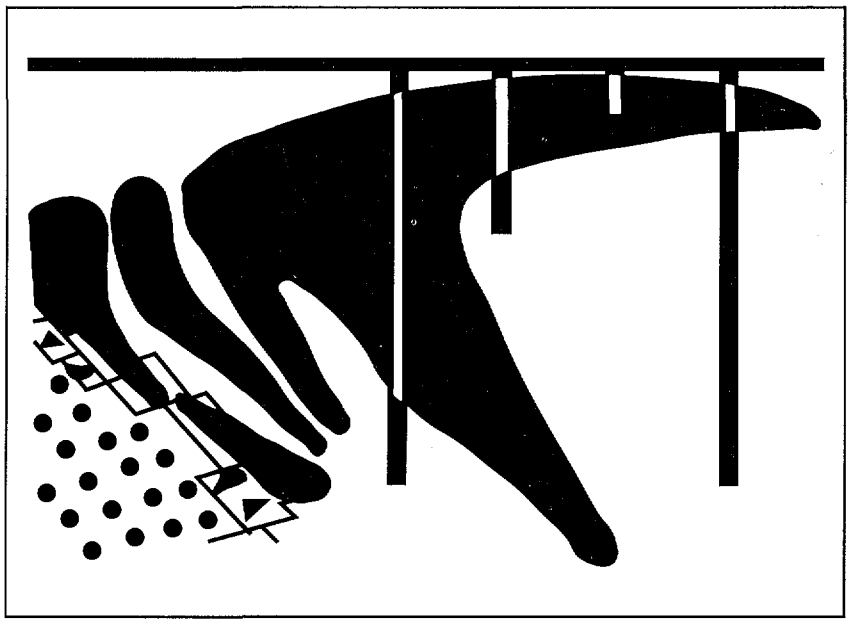

ISBN 0-642-59927-0

DOE/HMIP/RR/92/071

SKI TR 92:20-1

FINAL REPORT
VOLUME 1

SUMMARY OF FINDINGS

1992

AN OECD/NEA INTERNATIONAL PROJECT MANAGED BY:
AUSTRALIAN NUCLEAR SCIENCE AND TECHNOLOGY ORGANISATION

ALLIGATOR RIVERS ANALOGUE PROJECT
FINAL REPORT

VOLUME 1

SUMMARY OF FINDINGS

P. Duerden[1], D.A. Lever[2], D.A. Sverjensky[3] and L.R. Townley[4]

[1]Australian Nuclear Science and Technology Organisation
PMB 1, Menai, NSW 2234, Australia

[2]AEA Technology
B424.4, Harwell Laboratory, Oxfordshire, OX11 ORA, Great Britain

[3]Department of Earth and Planetary Sciences
The Johns Hopkins University, Baltimore, MD 212189, USA

[4]CSIRO Division of Water Resources
Private Bag, PO Wembley, WA 6014, Australia

CONTENTS

EXECUTIVE SUMMARY

The Koongarra uranium ore deposit is located in the Alligator Rivers Region of the Northern Territory of Australia. Many of the processes that have controlled the development of this natural system are relevant to the performance assessment of radioactive waste repositories. An agreement was reached in 1987 by a number of agencies concerned with radioactive waste disposal to set up the International Alligator Rivers Analogue Project (ARAP) to study relevant aspects of the hydrological and geochemical evolution of the site. The Project ran for five years.

The work was undertaken by ARAP through an agreement sponsored by the Organisation of Economic Cooperation and Development (OECD) Nuclear Energy Agency (NEA). The Agreement was signed by the following organisations: the Australian Nuclear Science and Technology Organisation (ANSTO), the Japan Atomic Energy Research Institute (JAERI), the Power Reactor and Nuclear Fuel Development Corporation of Japan (PNC), the Swedish Nuclear Power Inspectorate (SKI), the UK Department of the Environment (UKDoE), and the US Nuclear Regulatory Commission (USNRC). ANSTO was the managing participant.

The aims of the study were:

- to contribute to the production of reliable and realistic models for radionuclide migration within geological environments relevant to the assessment of the safety of radioactive waste repositories

- to develop methods of validation of models using a combination of laboratory and field data associated with the Koongarra uranium deposit, and

- to encourage maximum interaction between modellers and experimentalists in achieving these objectives.

It was anticipated that the substantial databases generated in the field and laboratory studies would then be used to develop and test geochemical and radionuclide transport models.

The uranium ore in the Koongarra No. 1 orebody is elongated over a distance of 450 m and persists to a depth of about 100 m. Secondary uranium mineralisation is present in the weathered schist zone to a depth of 25-30 m and has been mobilised downslope for about 80 m to form a dispersion fan.

Hydrogeological field investigations showed that the site was more complex than initially thought, hence a major site investigation of structures relevant to groundwater flow was also undertaken using geophysical techniques. The "simple" flow model that had been anticipated when initiating the project was seen to be inappropriate.

A geomorphological assessment of the development of the site and variations in the climate during the past million years, with their effect on the site hydrology, was undertaken to determine the time frame in which the uranium dispersion fan had developed, and to determine the timing of the dispersion fan formation.

Field measurement programs to measure chemical parameters of groundwater were carried out at the end of the Northern Territory wet and dry seasons, when water levels were at their highest and lowest levels. Colloids and particles were also collected and measurements were made of isotopes such as deuterium, tritium, ^{13}C and ^{14}C, which enabled groundwater mixing and flow paths to be studied.

An extensive study of the chemistry and mineralogy of the solid phase was also carried out on a large selection of materials sampled during the ARAP. This provided data on the early stages of weathering and the development of isotopic disequilibria under such conditions, the behaviour of rare earth elements, and the associations of uranium with mineral phases. A late finding in the mineralogical studies was the highly significant association of cerium and uranium in the weathered zone, a finding completely unexpected at the beginning of the project, and one which merits further investigation.

A two-phase study of sorption determined experimentally the factors that influence the sorption of U(VI) to well-defined mineral phases and to natural substrates from Koongarra and, on the basis of this experimental data, models of uranyl sorption were developed.

The groundwater and solid phase data provided a geochemical framework of the Koongarra system that was then used to develop and test transport and geochemical models. Initially, aqueous speciation models were used to calculate the composition of representative Koongarra waters. These showed that the present-day groundwaters were strongly undersaturated with respect to uranium-bearing minerals, hence should have been actively dissolving the uranyl phosphate zone. The geochemical modelling study was therefore extended to consider both present-day geochemical processes and those that operated in the geologic past.

A large number of radionuclide transport models were used to interpret the large database of concentrations of uranium series radionuclides in the groundwater and in the solid phases. Although the work focused on the ^{238}U series, and to a lesser extent on the ^{232}Th and ^{235}U series, there were also studies of ^{239}Pu, ^{129}I, ^{99}Tc and ^{36}Cl. All of these radionuclides are found in radioactive wastes, therefore the estimates of radionuclide mobility obtained in this study are of relevance to performance assessment modelling.

The modelling approaches had to deal with many uncertainties in representing the Koongarra site and its evolution with time including the hydrogeology, the effect of climatic variations, and the heterogeneity of the weathered zone. Consequently, it was found that a number of models fit the available data, and it was not possible to conclude that any one particular model was correct and that the others were

incorrect. Rather, it was possible to identify important processes affecting uranium transport and then apply a broad variety of modelling approaches.

Uranium transport in the secondary dispersion fan was found to have taken place over fairly short distances during a timescale of the order of millions of years. However, it was not possible to exclude the loss of some uranium bearing fluids from the system along flow paths through now eroded rocks. The fact that most of the uranium has moved only of the order of 50 to 100 m over a timescale of the order of millions of years suggests that the uranium is not very mobile, even in a chemically active system with relatively high groundwater flow.

The findings from the technical studies are discussed in the context of assessments of the long-term performance of geological repositories for radioactive wastes, which are being undertaken in many countries. They are also considered in an integrated "Scenario Development" approach, aimed to understand the formation of the ore deposit. Despite their inherent uncertainties, the findings provide a basis for assessing the way in which radionuclides will migrate in environments with a variety of geologic settings and over a range of different geologic timescales.

One of the great challenges of the ARAP, and therefore one of the great benefits because of the successful completion of the project, was that so many contrasting scientific disciplines had to work together to develop an understanding of the system. This was a valuable experience that similar teams will have to develop for the assessment of repositories, which will have to be founded on the characterisation of real sites.

This summary report, which highlights the work and findings of the Alligator Rivers Analogue Project is one of a series of 16 volumes, listed below. Detailed descriptions and results are provided in Volumes 2 to 16. Although an attempt has been made to make the individual reports self-sufficient, in many cases the results and conclusions overlap with other volumes. In these cases, comprehensive cross-referencing should allow the work to be fully accessed. Full acknowledgment to individual contributions is provided in the individual reports, and in Appendix I of this report.

No.	Title	Lead Author(s)
1	Summary of Findings	P Duerden, D A Lever, D A Sverjensky and L R Townley
2	Geologic Setting	A A Snelling
3	Geomorphology and Paleoclimatic History	K-H Wyrwoll
4	Geophysics, Petrophysics and Structure	D W Emerson

5	Hydrogeological Field Studies	S N Davis
6	Hydrogeological Modelling	L R Townley
7	Groundwater Chemistry	T E Payne
8	Chemistry and Mineralogy of Rocks and Soils	R Edis
9	Weathering and its Effects on Uranium Redistribution	T Murakami
10	Geochemical Data Bases	D G Bennett and D Read
11	Geochemical Modelling of Secondary Uranium Ore Formation	D A Sverjensky
12	Geochemical Modelling of Present-day Groundwaters	D A Sverjensky
13	Uranium Sorption	T D Waite
14	Radionuclide Transport	C Golian and D A Lever
15	Geochemistry of ^{239}Pu, ^{129}I, ^{99}Tc and ^{36}Cl	J T Fabryka-Martin
16	Scenarios	K Skagius and S Wingefors

ACKNOWLEDGEMENTS

We gratefully acknowledge the financial support of the organisations which sponsored the Alligator Rivers Analogue Project (ARAP). We also acknowledge the support provided by Denison Australia in allowing access to Koongarra and to scientific and technical data from the original Koongarra leaseholders. We also thank Grant Watt for his support in the field.

We wish to thank Robin Lowerson for her dedicated support of all administrative and organisational matters that were the basis of the project's success.

1 INTRODUCTION

Derivation of data for performance assessment studies of nuclear waste repositories over long timescales and distances on the basis solely of the extrapolation of laboratory-derived data leaves some uncertainties not addressed. As a result, procedures are being developed in many countries to develop the datasets for performance assessments based on the modelling of the results of laboratory studies, field experiments and natural analogue studies. The basis for the latter is reasoning by analogy, which Petit (1992) concluded might be the only means available for obtaining unique qualitative and, in some cases, quantitative information on systems of equivalent complexity to a nuclear waste repository. Although laboratory experiments can be designed to identify individual processes and evaluate the influence of specific properties they can only be run for a comparatively short time period. Field measurements allow more complex systems on a medium spatial scale, such as *in situ* fractures, to be studied and modelled; however, these experiments are also limited by having a fixed study period. By considering a natural system which contains processes relevant to a repository design study, such as radionuclide transport, we can increase our knowledge of the significant processes involved in the complex real system and evaluate their relative importance. Natural systems are also useful for testing uncertainties in models and parameters.

A major review by Chapman et al. (1984) discussed in detail the application of natural analogue studies to a range of potential problems at all stages of a waste disposal strategy. More recently, in outlining a rational foundation of such reasoning by analogy, Petit (1992) commented that although Chapman et al. "were looking for the best criteria to identify among natural objects those which were analogues", provided "similarity exists with a disposal or part of it (e.g. nature of materials, geological or geochemical situation), it is only the way information is derived from a natural object, that defines an analogue."

Birchard (1989) suggested that analogue studies could allow the testing of models for the most important processes controlling performance and provide a basis for determining the relative importance of processes to long-term radionuclide transport. He noted that although analogues may provide only a first order validation of radionuclide transport over the thousand to million year timescale, this level of validation may be sufficient for high-level waste performance assessment. Analogues may also have an additional role in establishing a scientific basis for model simplification. In this way unnecessary complexity that could increase modelling uncertainties might be avoided by judiciously simplifying models. Similarly, cost savings may result from not designing repository components to counteract insignificant processes.

A major difficulty confronted when modelling natural systems is the uncertainty in defining the timeframe and initial and boundary conditions to be applied. However, the difficulties presented to a modeller when trying to establish the behaviour of a system over the past hundreds of thousands of years are only marginally more

complex than those presented to the designer of a nuclear waste repository, who has to assess its long term evolution into an uncertain future.

By considering a complex system such as a uranium orebody as a natural analogue of a waste repository, it may be possible to conceptualise and test individual models of processes and ultimately combine them to represent the complete natural system. It may also be possible to test performance assessment models and other strategies to evaluate repositories such as scenario development studies. The natural analogue may also allow the results of performance studies to be presented in a more acceptable manner to wider audiences of non-specialists and the general public.

Petit (1992) noted that an analogy should be "used with caution and only in conjunction with laboratory and *in situ* experiments as well as with modelling". At the same time, he stressed that "the role of analogy should not be underestimated, notably for the safety assessment of a disposal concept in a geological formation and for the communication of scientific results to the general public, who are not trained to the scientific method".

Section 2 of this report discusses the concept of using uranium deposits as natural analogues and refers to a number of such studies, including those at the Koongarra deposit in the Alligator Rivers Region of the Northern Territory of Australia. Section 3 reviews early scientific work in the Alligator Rivers Region and summarises the results of the analogue studies undertaken between 1981 and 1987 that were funded by the US Nuclear Regulatory Commission (USNRC) and the UK Department of the Environment (UKDoE).

Section 4 describes the objectives of ARAP and the manner in which the study was conducted and provides a general outline of the project and a summary of the findings. A general description of the Koongarra ore deposit, the focus of ARAP, is provided in Section 5, with Sections 6-13 providing summaries of the work carried out to characterise the site in detail and provide data for modelling. Sections 14-18 discuss how this data was used in modelling and how the results may be applied for performance assessment studies. Finally, Section 19 considers the implications of the work for performance assessment modelling.

2 URANIUM ORE DEPOSITS AS NATURAL ANALOGUES

Uranium orebodies contain a wide range of radionuclides and heavy metals of direct interest to waste repository design. These include actinides, radium isotopes, lead isotopes and rare earth elements, as well as ultra-low levels of significant transuranic elements (^{239}Pu, ^{237}Np) and fission products (^{99}Tc, ^{129}I). Hence, they provide the opportunity for direct measurement of the migration of relevant radionuclides that has occurred over geological time and allow a reduction of uncertainties in the assessment of long-term transport of these radionuclides. The accessible timescales range from <1 year to about 500,000 or more years, depending on the process being studied. As uranium series elements are ubiquitous and can be measured at very low levels, there is also the possibility of transferring information from the analogue to any proposed repository site.

A number of uranium ore deposits have been considered as the basis of such studies. These include the Oklo deposits in Gabon, ore deposits near Poços de Caldas in Brazil, the Tono Mine in Japan, the Alligator Rivers Region of the Northern Territory of Australia and numerous smaller uranium deposits including those at Palmottu in Finland, South Terras in England and Needle's Eye and Broubster in Scotland. All these studies have been carried out with the aim of improving the basis for understanding natural rock-water interactions and their effect on radionuclide transport; however their focus has varied as a result of the different nature of the sites. Descriptions of a number of national natural analogues have been reported by von Maravic and Smellie (1992).

2.1 Oklo

A study of samples from the Oklo uranium mine in the Republic of Gabon (Cowan et al., 1975) showed that 2 Ga ago nuclear fission was sustained for a period of a few hundred thousand years in discrete volumes of rock. The extent of the elemental changes resulting from this sequence of reactions has been the focus of extensive scientific investigations since the phenomenon was first identified in 1972. Initial measurements showed that uranium isotope concentrations had continuous distributions and it was concluded that the configuration had changed very little since the time of the reactions; ie. the uraninite potentially exhibited some of the characteristics of "spent fuel" stored in a high-level waste repository. High-precision mass spectrometry techniques allowed the relative amounts of (fission product) isotopes originating from the "reactors" (and non-nuclear sources) to be measured and compared with reactor physics calculations of isotopic and elemental abundances of uranium and long lived fission products. Reports by Curtis et al. (1989) and Loss et al. (1989) discussed the retention of fission products showing that the relative abundances were different from those produced by fission. This was attributed to the stability of "putative" minerals under physiochemical conditions established by the geological environment over the last 2 Ga and their ability to retain the nuclear products. Curtis et al. (1989) and Loss et al. (1989) concluded that their work demonstrated the utility of the Oklo uranium ore deposit as a long-timescale analogue for radioactive waste repositories.

2.2 Poços de Caldas Project

The foci of this study were the Osamu Utsumi uranium mine and the Morro do Ferro thorium/rare earth orebody, located near the town of Poços de Caldas in the State of Minas Gerais, Brazil. The notable features of the sites are prominent redox fronts contained in the host rock at the Osamu Utsumi mine and the shallow, very high thorium ore-grade present at Morro do Ferro. The four main objectives of the project were:

1. to assist in the validation of equilibrium thermodynamic codes and databases used to evaluate rock/water interactions and solubility/speciation of elements
2. to determine interactions of natural groundwater colloids, radionuclides and mineral surfaces with respect to radionuclide transport processes and colloid stability

3. to produce a model of the geochemical evolution of redox fronts, specifically with the aim of understanding long-term, large-scale movements of redox-sensitive natural series radionuclides (including, if possible, natural Pu and Tc), and
4. to model the migration of rare earth elements (REE)/U-Th series radionuclides during hydrothermal activity (similar to that anticipated in the very near-field of some spent fuel repositories).

The results of this international project were described in a series of 14 reports and summarised in Volume 15 of the series by Chapman et al. (1991).

2.3 Cigar Lake

This ore deposit, situated at a depth of ~430 m, has exceptionally high concentrations of uranium which have not been significantly affected by surface-controlled processes such as remobilisation by oxidising recharge waters. Although the deposit has been water-saturated since its formation, the high-grade mineralisation has existed for about 1 By without significant dispersion of the uranium ore, and with secondary uranium mobilisation being restricted to migration along fractures. Many of its features are considered to be analogous to components of a high-level waste repository.

The objectives of the investigations were to develop improved assessment models and data for a disposal system, and to provide validation support for aspects of the models. The investigations included studies of the groundwater to identify processes and parameters controlling uranium fixation, and involved collection of data on solution, redox, colloid and organic chemistry and microbial activity. The information was then used to analyse the dissolution of the natural uranium minerals (an analogue of fuel dissolution) and to study the effects of solution and redox chemistry, microbial activity and colloids on the migration of radionuclides and trace elements. Cramer and Smellie reported the final results of this study in 1994.

2.4 Alligator Rivers Region

In 1981 the USNRC began to sponsor research by the Australian Atomic Energy Commission (now the Australian Nuclear Science and Technology Organisation - ANSTO) and sub-contractors on the four uranium deposits of the Alligator Rivers Region. To ensure that generic, rather than site-specific, properties of uranium and radionuclides migration were being studied, all the deposits were investigated. The work involved both field and laboratory studies. However, as the USNRC-funded project progressed, the efforts became almost entirely directed towards studying the Koongarra deposit.

Beginning in 1986, a complementary collaborative study of colloids in groundwater at Koongarra was also undertaken by ANSTO and Harwell Laboratory (United Kingdom Atomic Energy Agency - UKAEA) staff. The study was funded by the UKDoE and reported by Ivanovich et al. (1988).

In the context of studying geochemical alteration and radionuclide transport in the far-field of a repository, the most important feature of the Koongarra ore deposit is

the distribution of ore-grade uranium in the near surface water-saturated zone. This extends 100 m from the assumed position of original accumulation. The remobilisation is assumed to have resulted from the movement of uranium by groundwater away from the primary ore zone. The period of this migration was calculated during the preliminary project to have been approximately 1-2 million years (Airey et al. 1986); ie, a timescale relevant for repository safety assessments.

As a result of the findings of the earlier work, the international Alligator Rivers Analogue Project (ARAP) was set up to understand the processes which have contributed to the formation of the secondary uranium mineralisation and the dispersion fan. The work has comprised site characterisation studies and the development and testing of models, including those used in performance assessment studies.

3 REVIEW OF EARLIER WORK IN THE ALLIGATOR RIVERS REGION

There had been little scientific study of the Alligator Rivers region of the Northern Territory prior to the discovery of uranium in 1953. Although the first European explorers came to the region in 1845, early efforts to develop a pastoral industry in the Northern Territory had little impact. The area around Oenpelli, where recording of climatic data commenced in 1910-11, was included in an Aboriginal reserve in 1920 with a mission station being opened in 1925. After World War II, efforts were made to obtain more information about the region. A land resource survey was carried out in 1946 by the Commonwealth Scientific and Industrial Research Organisation (CSIRO) and a 1948 American-Australian scientific expedition to Arnhem Land reported on the existence of Aboriginal paintings and provided information about vegetation and wildlife.

Following the 1953 discovery of uranium at El Sherana in the Alligator Rivers Region, there were extensive searches for further deposits, although the poor accessibility meant that the region was still preserved in a near natural state. Airborne spectrometer surveys in 1969, followed by ground exploration of anomalies, led to the discovery of the Koongarra, Nabarlek, Ranger and Jabiluka uranium deposits. A systematic geological and geophysical survey was then begun by the Bureau of Mineral Resources (BMR) and in 1972 the Australian Government and the mining companies initiated a series of fact-finding surveys and investigations as part of a baseline study of the Alligator Rivers Region. A major aim of this study was to investigate the sensitivity of the region to various kinds of development, a direction which eventually led to the Government deciding that mining should only proceed at two of the deposits (Ranger and Nabarlek).

3.1 Noranda Uranium Exploration

From 1970 to 1973, Noranda Australia Ltd carried out an intensive program of fieldwork at Koongarra. This involved detailed geological mapping and auger, rotary/percussion and diamond drilling. Hydrological monitoring of rainfall and standing water levels throughout the area was also started and measurements of *in situ* permeability and of the effects of pumping on water levels in nearby monitoring wells were carried out. An Environmental Impact Statement (EIS) was then

prepared for submission to the Australian Government (Noranda Australia Limited, 1978). This work and the university research thesis of Snelling (1980a) have formed the foundation for all the subsequent studies at Koongarra, including the current Alligator Rivers Analogue Project.

The overall aim of the work carried out by Noranda was to investigate the commercial value of the uranium resource, plan the mining operation, including, the construction of a pit, and evaluate potential ingress of water to the pit. Data were collected from the vicinity of the ore deposit to facilitate the design and construction of tailings dams, evaporation ponds and associated roads and structures, and assess the environmental impact of such a mining operation.

3.2 USNRC Project

From 1981-1987, in the USNRC-funded study, a number of new investigations were started. In contrast to the earlier work, the natural analogue project was focussed on identifying processes in the ore deposit that might be significant over long timescales in the behaviour of a high-level waste repository. Initially the work looked at the four ore deposits in the region, though by this time the mining operations at Ranger and Nabarlek were underway, while the other two at Koongarra and Jabiluka were, and still are, in the planning and approval phase. In the final stages of the USNRC project all work was focussed on the Koongarra ore deposit.

Four main themes were developed:

1. *A study of solid phases, with particular emphasis on the distribution of uranium.* Sequential extraction schemes were developed to study mineral phases and the associated uranium series distribution. Adsorption-desorption experiments were also carried out on Ranger and Koongarra solids.

   Major findings of this work included the importance of the iron-rich phase in the distribution of uranium; the substantial fraction of uranium (~25%) associated with the amorphous iron rock phase that appeared to be accessible to (exchangeable with) the uranium in the groundwater; and the accumulation of daughter radionuclides in the clay/quartz phases.

2. *Groundwater and colloids.* A limited program of groundwater chemistry had been carried out by Noranda to locate a source for potable and industrial water supply. The data were generally expressed as trilinear plots and were used to class the water's chemical evolution as it passed from rainfall/runoff, through major aquifer paths, to discharge into streams or billabongs. Tritium measurements were also initiated for groundwater dating. During the USNRC study these measurements were continued in a selected number of wells and were extended to D/H, ^{14}C, $^{234}U/^{238}U$ and $^{230}Th/^{234}U$ as well as trace elements and tritium. However, these measurements and those of Giblin and Snelling (1983) (see below) were made with samples collected either by a flow-through sampler or by sampling with a submersible pump; ie, the depth of the source of groundwater was undefined.

An Amicon™ ultrafiltration system was adapted to concentrate the colloid fraction in groundwater sampled from three wells at Koongarra, collected out of contact with air. Uranium concentrations in both the solute and the concentrate fractions were analysed to estimate the fraction of uranium and thorium associated with colloids. It appeared that negligible uranium isotopes were associated with the groundwater colloids from the deposits, though significant amounts of thorium were present.

3 *Fission products (technetium-99 and iodine-129), plutonium-239 and chlorine-36.* Preliminary work was carried out to extend the geochemical natural analogue to fission products and transuranic elements (^{239}Pu). Groundwater samples were collected for ^{129}I and ^{36}Cl analysis, and chemical procedures were developed to separate environmental levels of ^{36}Cl and ^{129}I. The aim was to compare the measurements of ^{129}I in the host rock and groundwater with production rates from neutron induced and spontaneous fission. However, this task was not completed during this phase of work at Koongarra.

Field techniques were also developed to separate ^{239}Pu from volumes of groundwater up to 10000 L in size. During the duration of the project, measurement of these samples was not possible; however, values of ^{239}Pu/U were successfully measured on rock samples from Koongarra containing primary and altered pitchblende.

4. *Modelling.* An open system uranium model was developed to describe the gross features of the ore deposits. Initially, this was used to model the rate of advance of the weathering front at Ranger, Jabiluka and Nabarlek (on the basis of this approximately balancing the rate of surface erosion). It was then extended to a multiphase system that had been defined on the basis of the results of the sequential extraction measurements. The open system model was then used to quantify the rate of redistribution of uranium at Koongarra, with the model being calibrated against uranium series data. The work suggested that the time period for the secondary mineralisation was in the range 1-3 million years. Two transport models typical of those used in repository safety assessments were developed to estimate the time that uranium has been migrating in the system. Although simplifications were made, an estimate of the time that migration has been taking place was in the same range as that given by the open system concept.

On the basis of the observed alteration in the primary ore zone above the fault, Snelling (1980b) postulated that flow of groundwater in the weathered zone was responsible for the weathering and dispersion of the primary ore. Recharge of groundwaters was believed to occur via downflow parallel to the reverse fault, with some water flowing from the sandstone into the schists via cross fractures.

In their work on applying hydrogeochemistry to uranium exploration in the region Giblin and Snelling (1983) had identified areas of magnesium dominance in groundwaters sampled around all the uranium mineralisations. On the basis of the ratio [Mg^{2+}] to [Ca^{2+} + Mg^{2+} + Na^{+} + K^{+}], they identified a region to the south of the Koongarra No. 1 orebody which had similar characteristics to that of the orebody

itself. Using the limited information available to the USNRC study, Payne continued this work and also noted that the groundwater character closely resembled the groundwater of the mineralised zones (see also Volume 7 of this series).

The Koongarra colloid study, funded by the UKDoE in 1986, extended the earlier work. Equipment was developed for *in situ* concentration of the colloids and fractionation into size ranges whilst ensuring that outgassing of CO_2 did not occur and that the groundwater chemistry and dissolved oxygen levels were unchanged. The physical, chemical and radionuclide parameters of the colloid concentrate and the solution phase were determined, and electron microscopy analysis was used to determine the shape and composition of individual colloids.

4 THE INTERNATIONAL ARAP PROJECT

4.1 Introduction

The results of the early studies in the USNRC- and UKDoE-funded projects had demonstrated the potential value of research at Koongarra as a natural analogue for a waste repository. Individual processes had been studied to varying degrees, with some of them, such as the fission product and transuranic work, being delayed because of the necessity of developing "state-of-the-art" ultra-trace isotopic techniques of analysis.

Preliminary models of radionuclide migration in the dispersion fan suggested that the time of its formation was in the order of 1-3 Ma ago. However, the one-dimensional models had been restricted to K_d or leaching-deposition concepts with little real basis for the data used and there had been no geochemical modelling of either the formation of the ore deposit or the processes currently occurring.

Examination of groundwater chemical data from the ~65 wells scattered through the site had also suggested that the present-day groundwater flow was not in the direction traditionally studied in the modelling. However, by necessity, sample data used to calibrate the migration modelling were only available from the original Mine Grid section that appeared from the outline of the commercial ore grade to have been the greatest extent of uranium dispersion.

Continuation of this work in an OECD Nuclear Energy Agency (NEA) sponsored project was agreed in 1987. Funding was provided by the Australian Nuclear Science and Technology Organisation (ANSTO), the Japan Atomic Energy Research Institute (JAERI), the Power Reactor and Nuclear Fuel Development Corporation of Japan (PNC), the Swedish Nuclear Fuel Inspectorate (SKI), the UKDOE and the USNRC. In the final two years of the project, the US Department of Energy also provided financial support and the Central Research Institute for Electric Power Industry (CRIEPI) supported a borehole TV investigation of the site. The Government of the Northern Territory of Australia provided funding for drilling new wells at Koongarra.

Detailed results of project findings are provided in Volumes 2 to 16 of this series of reports. Although an attempt has been made to make the individual reports self-

sufficient, in many cases the results and conclusions overlap with other volumes. In these cases, comprehensive cross-referencing should allow the work to be fully accessed. Full acknowledgment to individual contributions is provided in the individual reports, and in Appendix I of this report.

4.2 Project Objectives

The Alligator Rivers Analogue Project has been focussed on the geochemical alteration of the Koongarra No. 1 uranium orebody, radionuclide migration in the weathered zone and the formation of the secondary uranium mineralisation dispersion fan. Although other important features, such as the initial alteration of uraninite in the unweathered zone, might provide additional analogue information on near-field alteration of fuel element disposal. These were omitted from the study.

The aims of the study were:

- to contribute to the production of reliable and realistic models for radionuclide migration within geological environments relevant to the assessment of the safety of radioactive waste repositories
- to develop methods of validation of models using a combination of laboratory and field data associated with the Koongarra uranium deposit, and
- to encourage maximum interaction between modellers and experimentalists in achieving these objectives.

Initially the planned investigations were grouped into six technical sub-projects:

I Modelling of Radionuclide Migration
II Hydrogeology at Koongarra
III Uranium/Thorium Series Disequilibria Studies
IV Colloid and Groundwater Studies
V Fission Product Studies, and
VI Transuranic Nuclide Studies

with the research investigations being carried out by an extensive group of researchers both in the field and at the laboratories of the participating organisations. Other organisations involved included:

- Australia - CSIRO Division of Water Resources - Perth and Adelaide; Northern Territory - Power and Water Authority, and Department of Mines and Energy; Andrew Snelling; The University of Sydney (Departments of Geology and Geophysics, and Crop Sciences); and The University of Western Australia
- Sweden - KEMAKTA Consultants
- UK - AEA Technology's Harwell Laboratory and W S Atkins, and
- USA - University of Arizona, the Johns Hopkins University, the University of New Mexico, Los Alamos National Laboratory (LANL), Pacific Northwest Laboratories (PNL), and the US Geological Survey (USGS) Menlo Park.

The work was reviewed annually by a Joint Technical Committee of representatives of the participants and there were regular technical workshops to facilitate interaction between the principal investigators. The results of the study were also presented to meetings of the NEA/OECD international INTRAVAL project. Through this collaboration, additional input by the National Institute of Public Health and Environmental Hygiene of the Netherlands (RIVM) was made to understanding the regional hydrogeology, radionuclide transport and geochemical modelling (van de Weerd et al. 1994).

4.3 Conduct of the Study

The initial research tasks were undertaken to:

- characterise the host rock properties and mineralogy
- investigate the hydrogeology and evaluate groundwater flow as an input to radionuclide transport modelling, and
- study the geochemistry of water and rocks, including the geochemistry of fission products and transuranics.

It was anticipated that the substantial databases generated in the field and laboratory studies would then be used to develop and test geochemical and radionuclide transport models.

Although the overall direction of the work was unchanged throughout the study, it was necessary as the project developed to put effort to areas that had not been considered initially.

For example, the hydrogeological field investigations showed that the site was more complex than initially thought, hence a major site investigation of structures relevant to groundwater flow was begun, using geophysical techniques. The "simple" flow model that had been anticipated when initiating the project was seen to be inappropriate.

A re-evaluation of the work was also needed following the early findings of the geochemical modelling study. This work was begun with the aim of modelling the formation of the secondary mineralisation, the uranyl phosphate zone. However, it was found that the present-day groundwaters were strongly undersaturated with respect to uranium-bearing minerals and should have been actively dissolving the uranyl phosphate zone. Hence, the analysed groundwaters were not responsible for the formation of the (high-grade) uranyl phosphate zone but rather with its alteration and removal into the dispersion fan. In addition, modelling of the formation of the uranyl phosphate zone suggested that this was most likely to have taken place in an unsaturated zone; ie, uranyl phosphate may have formed in a more arid climate when the groundwater table was lower than at present.

This suggested that the work at Koongarra needed to be divided into two categories. One should focus on their relevance to present-day geochemical processes and the other on those that have operated in the geologic past. It was also noted that the

geomorphological development of the site and variations in the climate during the past million years, with their effect on the site hydrology, would need to be considered.

The geochemical modelling also stressed the importance of better understanding the mineralogy of the "non-commercial" dispersion zone down-flow of the uranyl phosphate. This had earlier been classed as a zone of dispersed uranium absorbed on clays. It seemed possible that micro-minerals of uranyl phosphates were present here but they had not been identified in the earlier work. A late finding in the mineralogical studies was the highly significant association of cerium and uranium in the weathered zone, a finding completely unexpected at the beginning of the project, and one which merits further investigation.

It was also decided that the Scenario Development technique should be adapted to Koongarra in order to not only trial the technique in modelling the dispersion fan development but also to facilitate the exchange of information and ideas between the different scientific disciplines and modellers. As the ARAP involved a full spectrum of detailed studies it was considered appropriate to utilise methodologies developed for performance assessments to evaluate the analogue and ensure that the proper questions were being asked and that investigations were focussed on phenomena relevant to validation objectives.

4.4 General Project Outline and Summary of the Findings

The ARAP concentrated on investigating:

- the original weathering of the Koongarra region
- groundwater flow
- alteration of the host rock and primary uranium
- rock-groundwater interactions, including adsorption and desorption
- radionuclide transport, including the relative distribution of the uranium/thorium radionuclides in the multi-phase system
- the continued development of the dispersion fan, and
- *in situ* production and mobility of long lived fission products such as ^{99}Tc and ^{129}I and transuranic nuclides such as ^{239}Pu.

The experimental programs resulted in substantial drillcore and groundwater databases for all the distinctive geologic units in the vicinity of Koongarra. Hydrogeological data were also obtained in selected parts of the area from both field and laboratory measurement programs. Although field pumping tests provided information on the present-day (not paleo) flow system, flow patterns derived from the measurements should agree with the results of the hydrochemistry sampling and provide some validation of the techniques used. Borehole TV surveys and other surface geophysical measurements also supported these measurements.

It was, therefore, possible to test various aspects of geochemical models and databases such as radionuclide solubility/speciation calculations, the formation of specific secondary uranium minerals and surface complexation modelling. The latter work used the results of sorption of uranium to single minerals and to substrates from the leached and deposited zones in the weathered zone.

A number of independent methods of estimating how the system has evolved have also been used to provide reassurance that an adequate understanding of radionuclide transport has been gained. These have included a study of the geomorphology and time evolution of the site, so that the times that key geological events took place and their effects on transport could be understood. A second approach was to try to gain an understanding of elemental transport at the site, and how the present-day groundwater flow (and that which has taken place in the past) was related to the geochemistry of key elements. This involved laboratory experiments similar to those employed in the characterisation of sites being considered for a waste repository, such as sorption measurements using intact samples. The last method made use of the distinctive information yielded by disequilibrium in the uranium series and provided data for calibration of site radionuclide transport and performance assessment models. Evolving interpretations of hydrogeology and geochemistry were particularly challenging to the transport modelling, where a range of approaches was adopted.

Much evidence has been gathered to suggest that the development of the uranium dispersion fan at Koongarra occurred in two stages. The first stage, during the development of the uranyl phosphate mineralisation, occurred in an unsaturated zone above the water table with atmospheric values for O_2 and CO_2. The climate at this time may have been more arid than the relatively recent monsoonal climate. In the second stage, the development of the low level uranium concentration dispersion fan, it is possible that oxidising waters reached the unweathered schist, where flow was governed by the macroscopic fracturing seen in the borehole television mapping. This led to weathering of the fracture walls and eventually to complete weathering of the rock to a mixture of clay minerals.

5 GENERAL DESCRIPTION OF THE SITE

The Koongarra uranium deposit lies about 25 km south of the small town of Jabiru in the Northern Territory of Australia (Figure 5.1). The geographical and geological area is known as the Alligator Rivers Region due to it being drained, and geographically dominated, by two major river systems, the South Alligator and East Alligator Rivers. The headwaters of these river systems are in the Arnhem Land Plateau. The major uranium deposits in the Alligator Rivers Region are situated either in valleys between eroded outliers of the Arnhem Land Plateau or on the edges of the lowland floodplains in the lower reaches of the major river systems. All are adjacent to prominent sandstone escarpments.

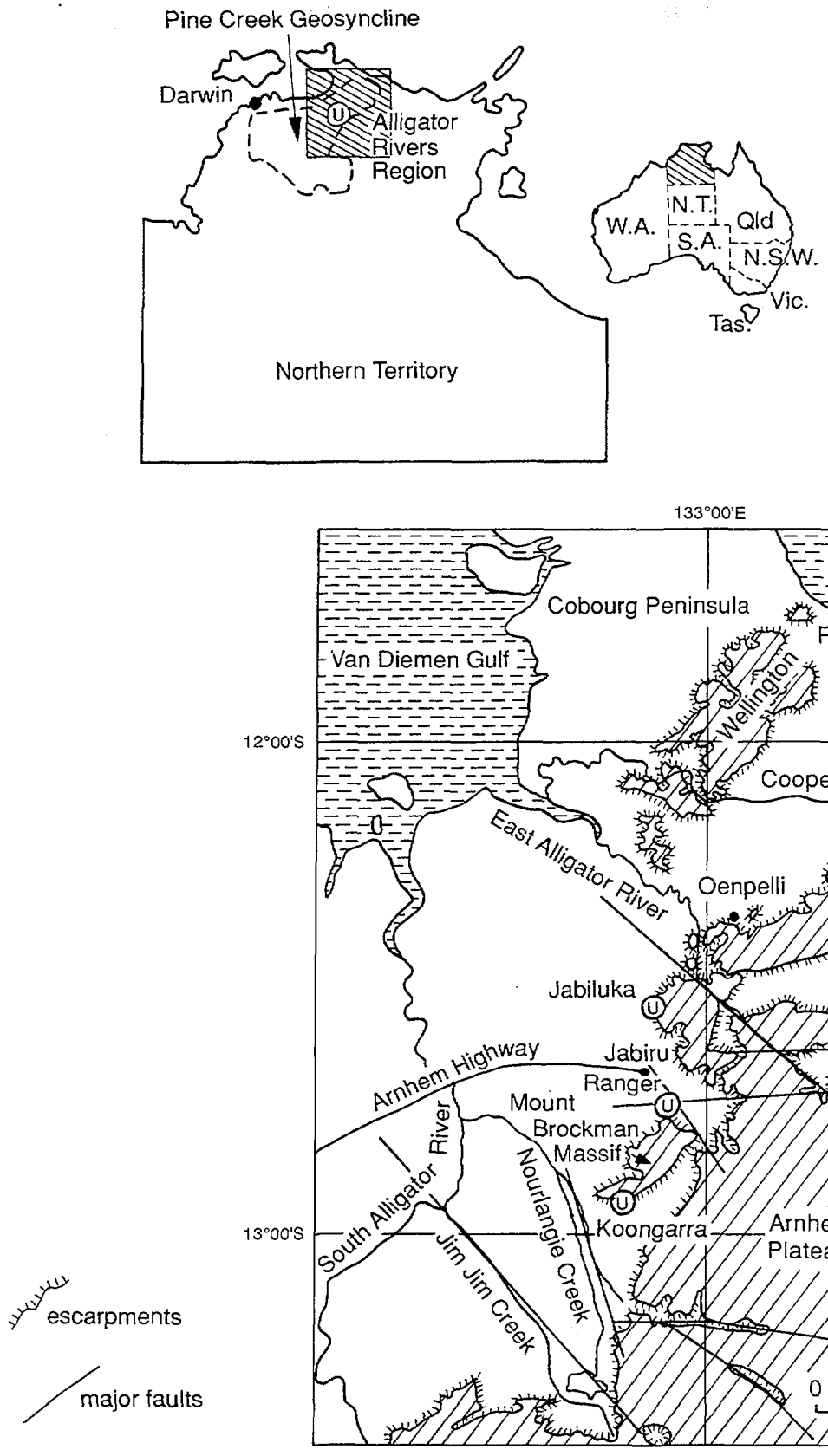

FIGURE 5.1 Location map showing the four uranium deposits of the Alligator Rivers Region, sandstone escarpments and major faults. (Adapted from Needham and Stuart-Smith, 1976)

Well-defined escarpments bound the Arnhem Land Plateau and Mount Brockman Massif, reaching broken heights of up to 200 m. The escarpments separate the plateau terrain of the Kombolgie Sandstone from the seasonally flooded wetlands and northern lateritic plains of low relief, which make up much of the land surface of this part of northern Australia (Figure 5.2). The plains rise from heights of a few metres above sea level to reach elevations of up to 60 m at the edge of the Arnhem Land Plateau. These plains are often sandy and are associated with deeply weathered soil profiles. Koongarra is situated in the valley between the main Arnhem Land Plateau and the Mount Brockman Massif outlier adjacent to the escarpment.

The drainage network that has developed in the region is well defined, with alluvial plains bordering the streams. The region has a strongly seasonal tropical monsoonal climate, which results in strong seasonal variations in the surface hydrology. An interpretation of the local lithology and structure at Koongarra, based on aerial photography and field observations, is shown in Figure 5.3; the position of the ore deposit is given.

The presence of extensive wetlands for part of the year is a characteristic feature of the region. Streamflow is much reduced during the dry season and many streams cease to flow by the end of winter. Most of the Koongarra region forms part of the South Alligator Catchment. Only the northern part of Koongarra Valley drains into the adjacent East Alligator Catchment via Magela Creek.

Vegetation is an open forest dominated by evergreen eucalyptus trees. About 30% of the area is made up of small patches of open grasslands and low shrubs. Rugged sandstone outcrops north of the site are generally devoid of vegetation except along deep fracture zones in the rock. Air photographs show slightly denser vegetation along the base of the outcrop and also along Koongarra Creek. Figures 5.4-5.6 are oblique aerial photographs of the Koongarra area, while Figures 5.7-5.9 are ground photographs looking across the orebody and surrounding areas where ARAP investigations were conducted.

The Koongarra orebody is situated entirely within the catchment of Koongarra Creek, which flows into Nourlangie Creek and then into the South Alligator River. Runoff from the uplands north of the ore deposits crosses the lowlands to enter Koongarra Creek south of the deposits. The creek flows during the wet season. Standing water in small seasonal ponds will persist into the dry season but is completely gone before the end of the season.

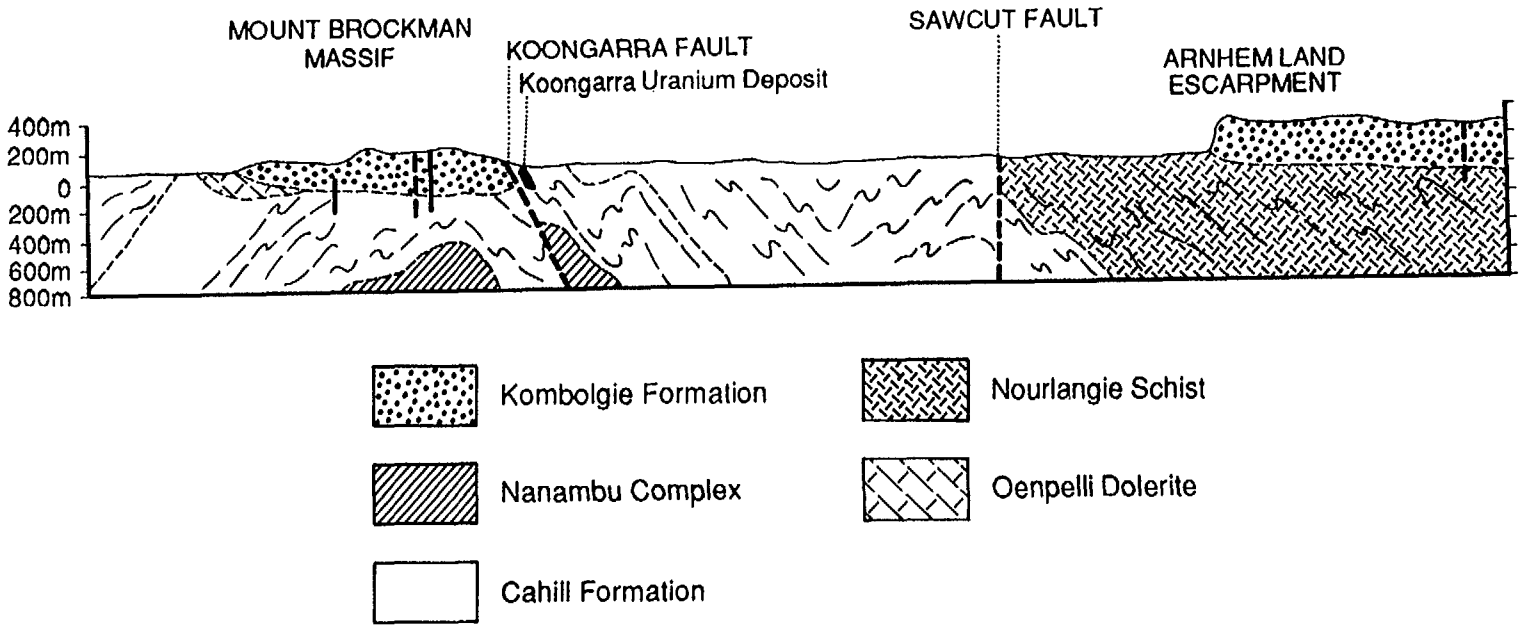

FIGURE 5.2 Geological cross-section of the Koongarra region (After Needham, 1982)

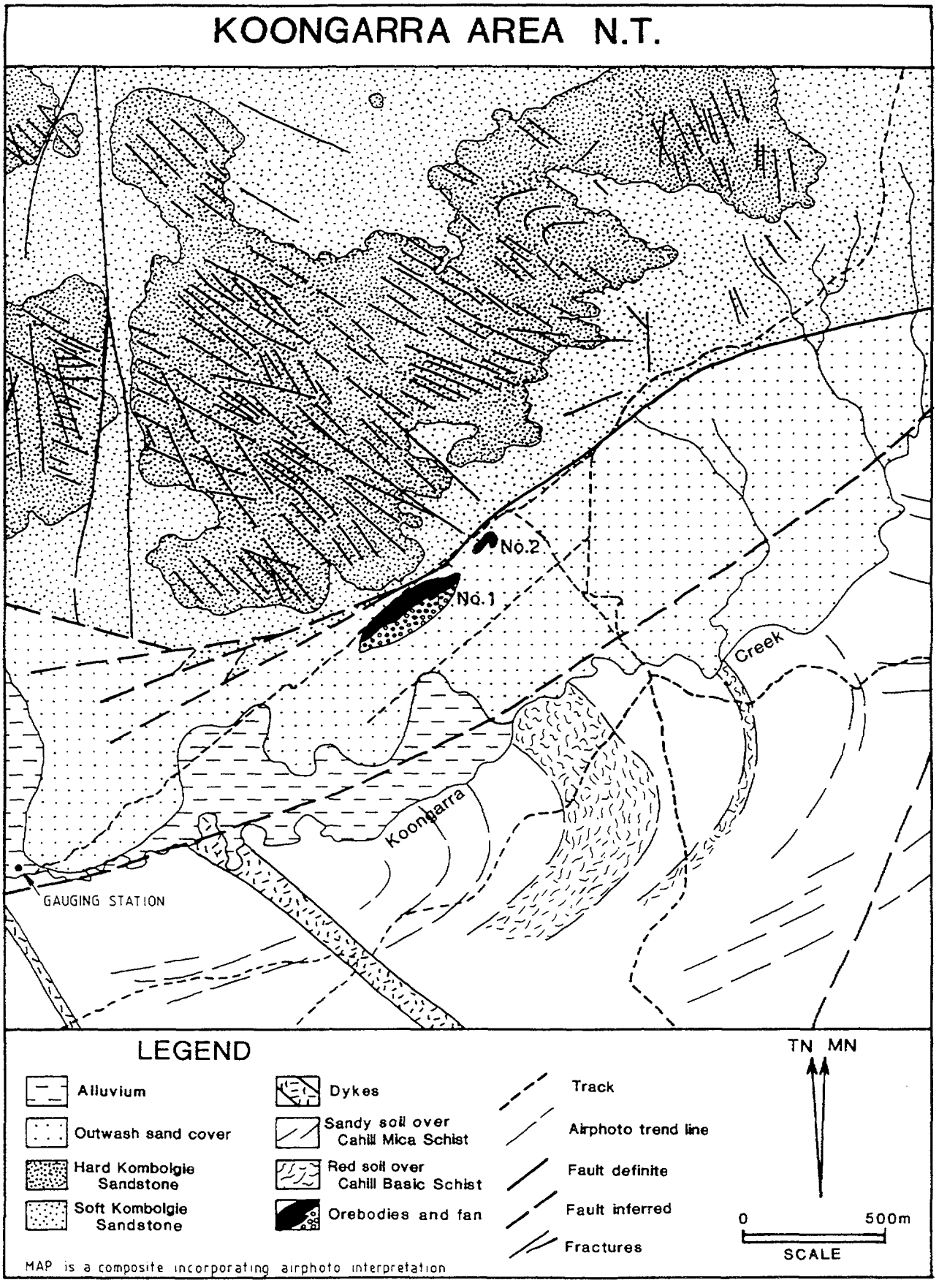

FIGURE 5.3 An interpretation of local lithology and structure at Koongarra based on aerial photography.

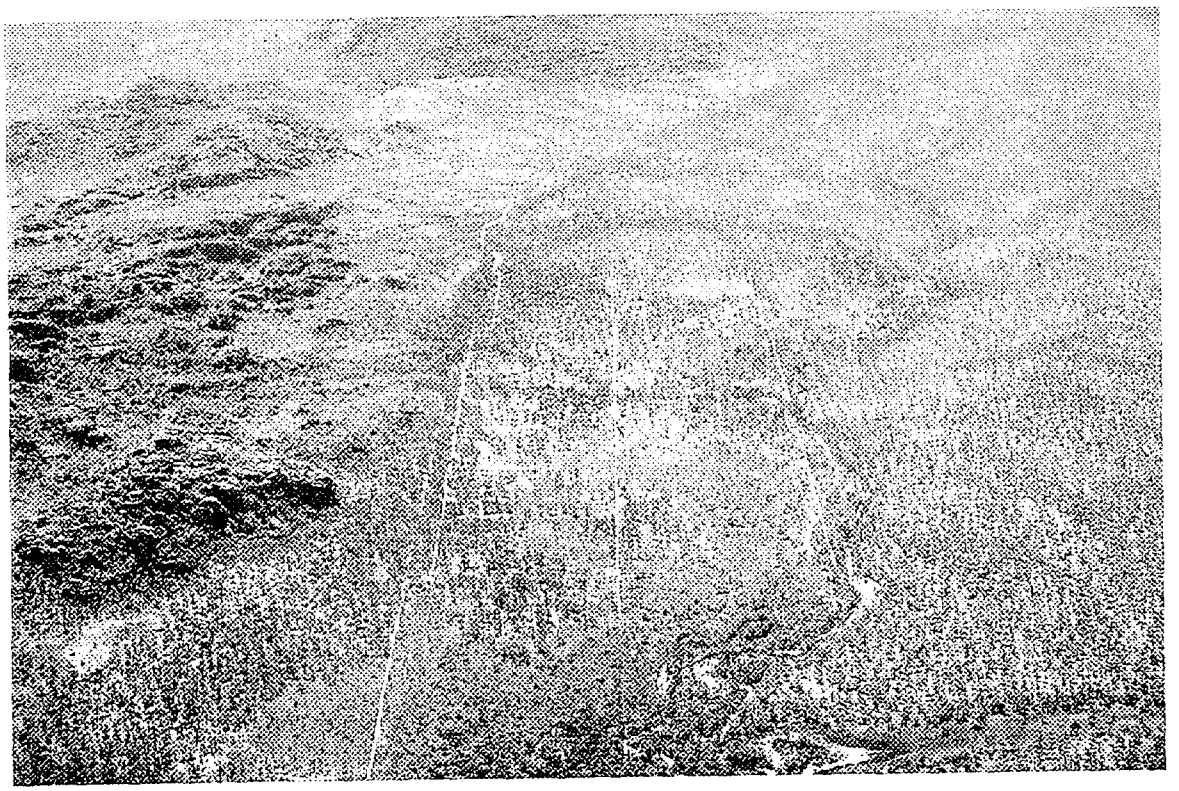

FIGURE 5.4 Oblique aerial photograph of the Koongarra area looking northeast along the mine grid. The tracks running cross-wise in the centre view are the grid-lines along which cross-sections through the orebodies were drilled. To the left (northwest) are the Kombolgie sandstone cliffs of Mt Brockman and to the right (southeast) is Koongarra Creek

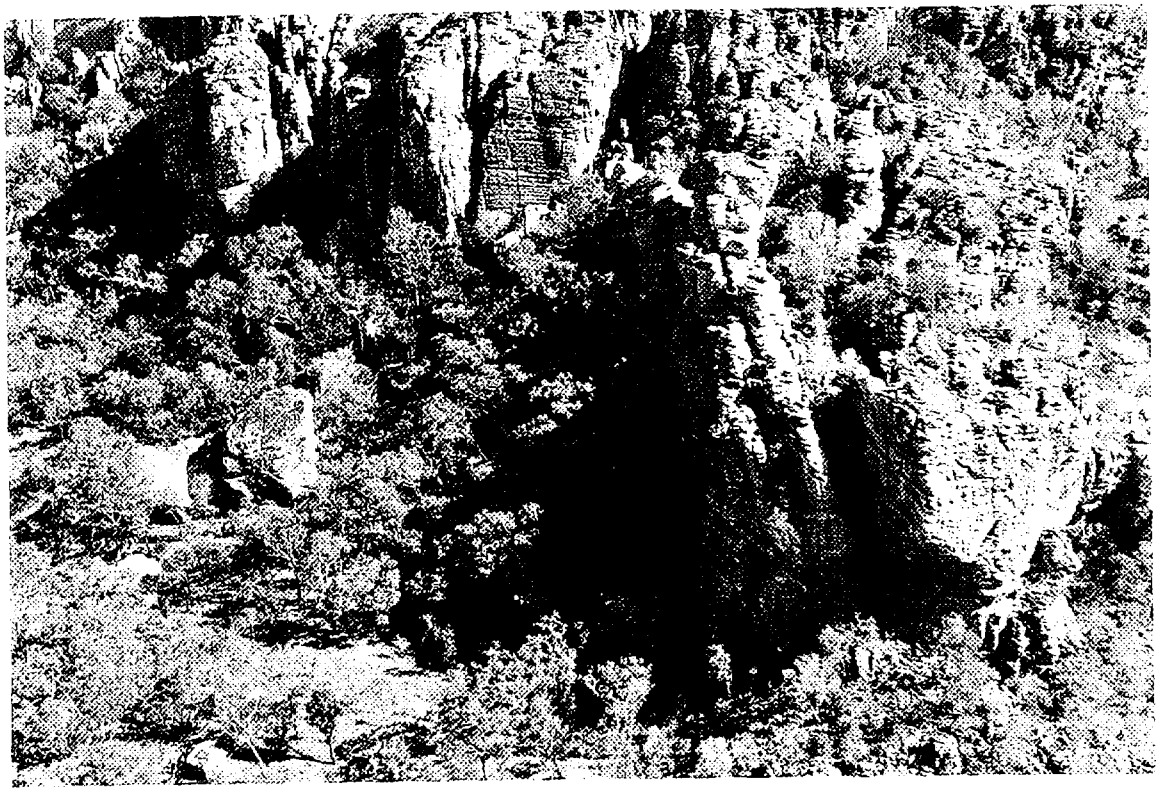

FIGURE 5.5 Oblique aerial view of the Kombolgie sandstone cliffs of Mt Brockman just to the northwest of the Koongarra No. 1 orebody.

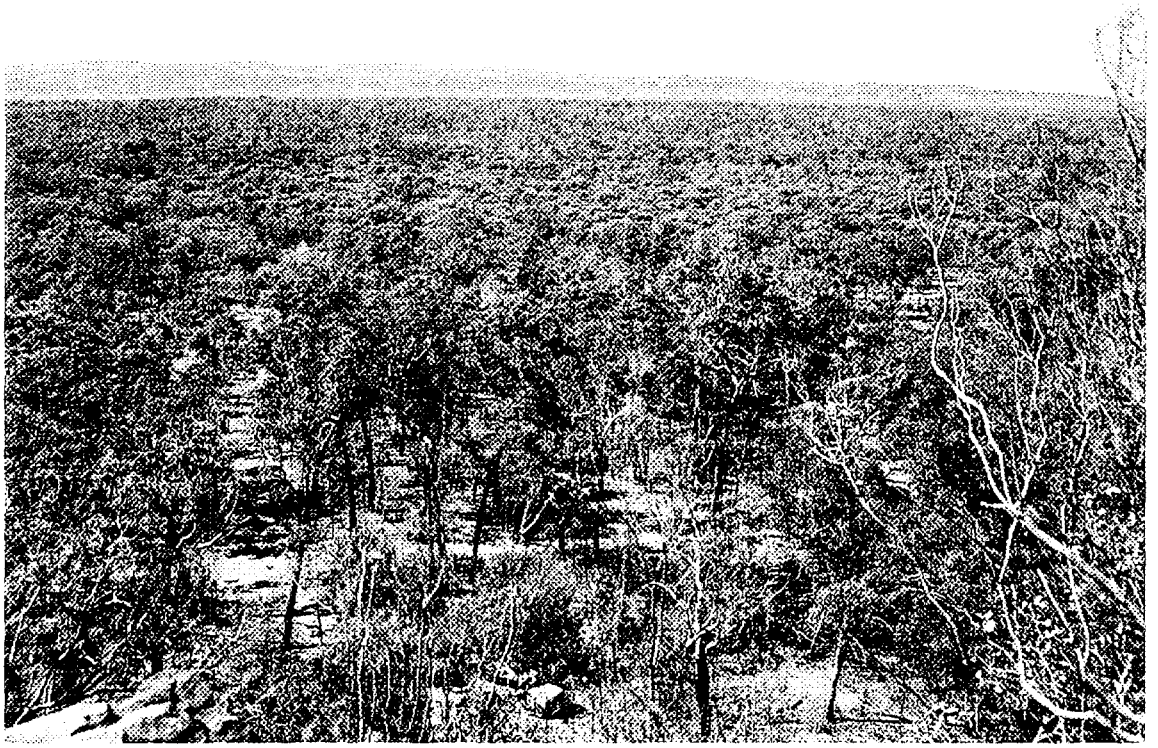

FIGURE 5.6 View of the Koongarra No. 1 orebody area (across the centre of the photograph) as seen from Mt Brockman. In the distance is the line of Kombolgie sandstone cliffs that mark the edge of the Arnhem Land Plateau.

FIGURE 5.7 Ground level photograph looking across the Koongarra No. 1 orebody area along Section 6109 mN towards Mt Brockman.

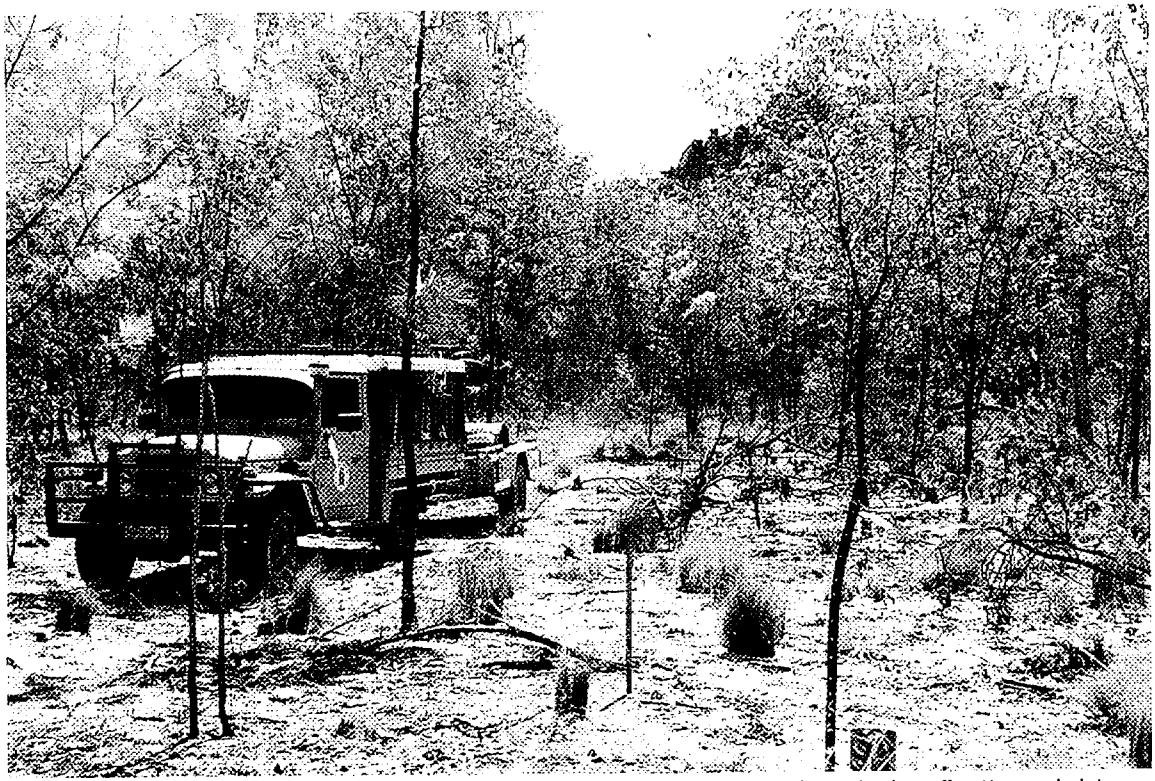

FIGURE 5.8 Negotiating the sand terrain is not easy. Open boreholes (bottom right and centre right) can be seen along Section 5865 mN. During torrential downpours in the "wet" season access is difficult as water can run off faster than it infiltrates the sand.

FIGURE 5.9 Various methods of obtaining water samples were used. Here a double packer (black sections at each end) pump system is being prepared for lowering down PH15 on Section 6048 mN. Work was mostly done during the "dry" season – the dry brown "spear" grass attests to the intense seasonal aridity and high temperatures (around 35°C).

6 GEOLOGY

6.1 Geologic Description

Comprehensive descriptions of the Koongarra ore deposit can be found in Volumes 2 and 4 of this series. Volume 2 also provides cross-sections through the orezone showing geology, drill holes and outlines of economic mineralisation grades.

The uranium mineralisation occurs in a layered Lower Proterozoic sequence which was metamorphosed or changed by heat and pressure to schists and dolomite between 1,870 and 1,800 Ma ago, accompanied by severe folding. This was followed by a ~150 Ma period of uplift, weathering and erosion which produced a new land surface on which thick layers of sandstone (the Kombolgie Formation) were then deposited (probably between 1,690 and 1,600 Ma).

The movement of the Koongarra Fault has reversed the normal sequence of strata by bringing the overlying younger sandstone down underneath the older tilted schist layers. This fault zone forms the lower boundary (or footwall) to the uranium ore zone. The strongest mineralisation, with grades in excess of 1% U over several metres, occurs just below a distinctive sheared graphite-quartz-chlorite schist unit that forms the hanging wall to the ore.

The Koongarra deposit today lies beneath a gently sloping ground surface below the sandstone escarpment of the Mount Brockman Massif (Figure 6.1). Beneath a sand cover is the zone of weathered schist. Between this weathered zone and the unweathered (fresh) schists is what has been called the transitional zone. In this region there is marked change in colour of the rock - from the reddish and yellowish browns of the weathered schist to a greenish light grey - which is still distinct from the dark greys of the fresh schists. Fractures in this zone, as well as the schistosity surfaces, are still often coated with yellowish-brown iron oxides. This zone thus reflects the onset of the weathering process on the fresh schists, but the process is not yet complete.

In the unweathered (fresh) schists there are both high grade and medium-low grade ores and areas of uraninite-dominated and uranyl silicates-dominated ore, described as the primary ore. It should be noted that the use of the word "primary" in this context does not necessarily imply timing and/or genesis, although of course the primary ore at Koongarra, being in the unweathered schists, was in place before weathering occurred. Immediately above, and up-dip of, this primary ore in both the transitional zone and the weathered schist is ore that was obviously once primary but now is weathered. Consequently it is here designated as weathered primary ore. Adjacent to it and downslope, again within the weathered schist and transitional zone, is ore that represents uranium which has been mobilised from the weathered primary ore and dispersed downslope to form what has been designated as the dispersion fan. The weathered primary ore and the dispersion fan together are here called the secondary ore. Figure 6.1 shows a simplified geological cross-section through the Koongarra No. 1 orebody, including the distribution of uranium minerals and alteration.

A 1,650-1,550 million year age for the primary ore has been suggested on the basis of Sm-Nd isotopic data on uraninite. This is consistent with the observation that the mineralisation occupies the breccia zones generated by the post-Kombolgie reverse faulting.

A distinct and extensive primary hydrothermal alteration halo has been observed about the mineralisation extending for up to 1.5 km from the ore. Uranium mineralisation is only present within the inner halo, where pervasive chlorite-dominant replacement of the schist fabric and removal of quartz has occurred with the result that magnesium-rich chlorite is the principal gangue mineral. The inner halo extends to nearly 50 m from the ore. The bulk rock geochemistry reflects this alteration and is characterised by magnesium enrichment and silicon depletion. The primary ore is enriched in copper, lead, sulfur, arsenic and vanadium, while nickel and cobalt form an enrichment halo about the deposit.

The uranium occurs in two distinct orebodies, separated by about 100 m of barren schists, and consists of partially coalescing lenses that are elongated and dip at 55° broadly parallel to the reverse fault breccia. The No.1 orebody is elongated over a distance of 450 m and persists to a depth of about 100 m. Secondary uranium mineralisation, derived from leaching of the primary mineralised zone, is present from the surface down to the base of weathering over some 25-30 m and forms a tongue-like body of ore-grade material dispersed down-slope for about 80 m to the southeast. In the No.2 orebody the mineralisation is elongated over a distance of about 100 m and persists down dip at 55° to at least 250 m.

Oxidation and alteration of uraninite within the primary ore zone have produced a variety of secondary uranium minerals, and uraninite veins have been completely altered *in situ*. The secondary mineralisation of the dispersion fan in the weathered schists above the No.1 orebody is characterised by uranyl phosphates. Away from the tail of the dispersion fan, the uranium appears to be dispersed in the weathered schists and is apparently adsorbed onto the surfaces of clay and iron oxide minerals. Uranyl phosphates have not yet been identified in this area, although they have been the focus of an extensive mineralogical study. Figure 6.2 shows a map of the local geology of the No. 1 and 2 orebodies.

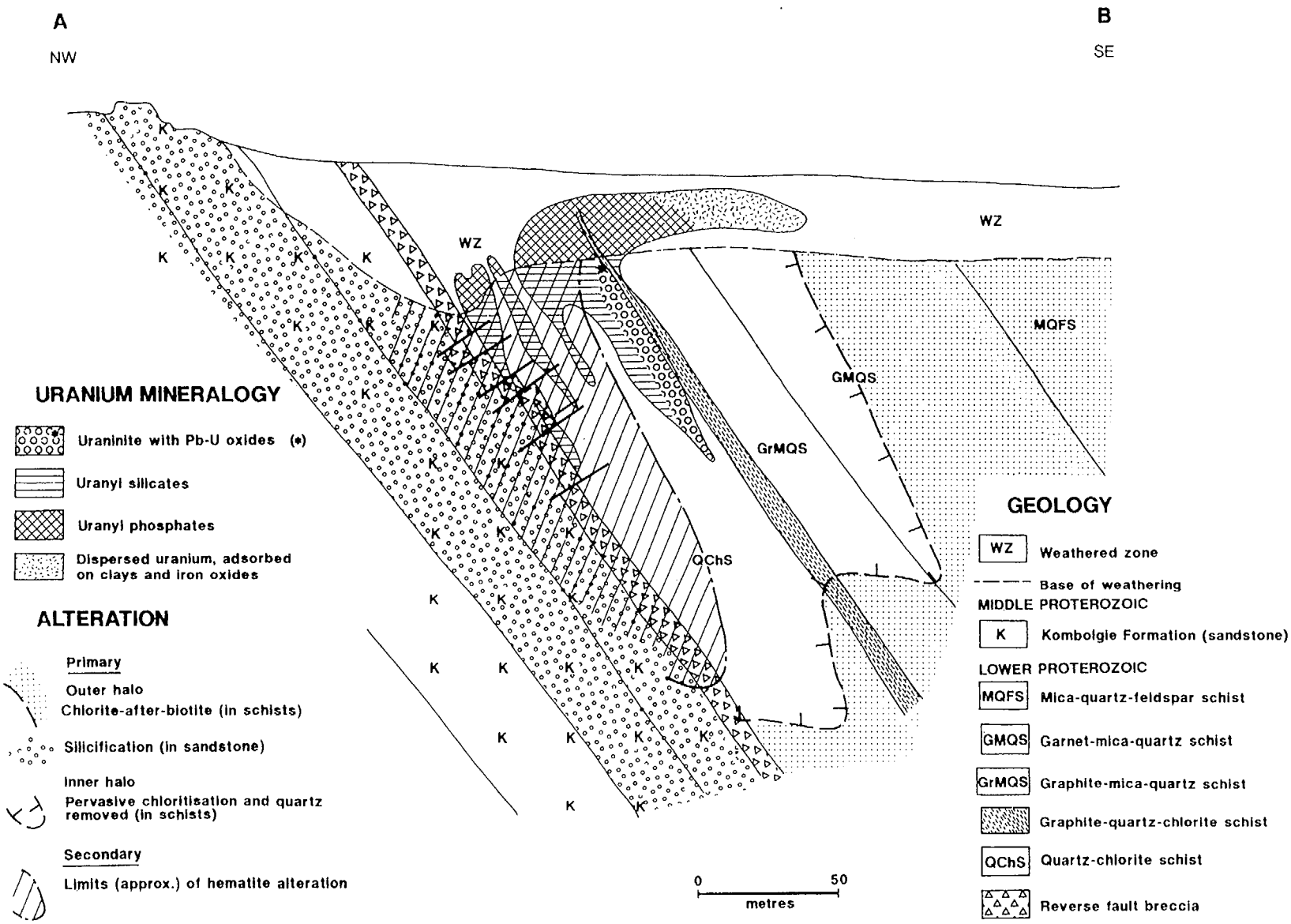

FIGURE 6.1 Simplified cross-section through the Koongarra No. 1 orebody showing the geology and the distribution of uranium minerals and alteration (after Snelling, 1990).

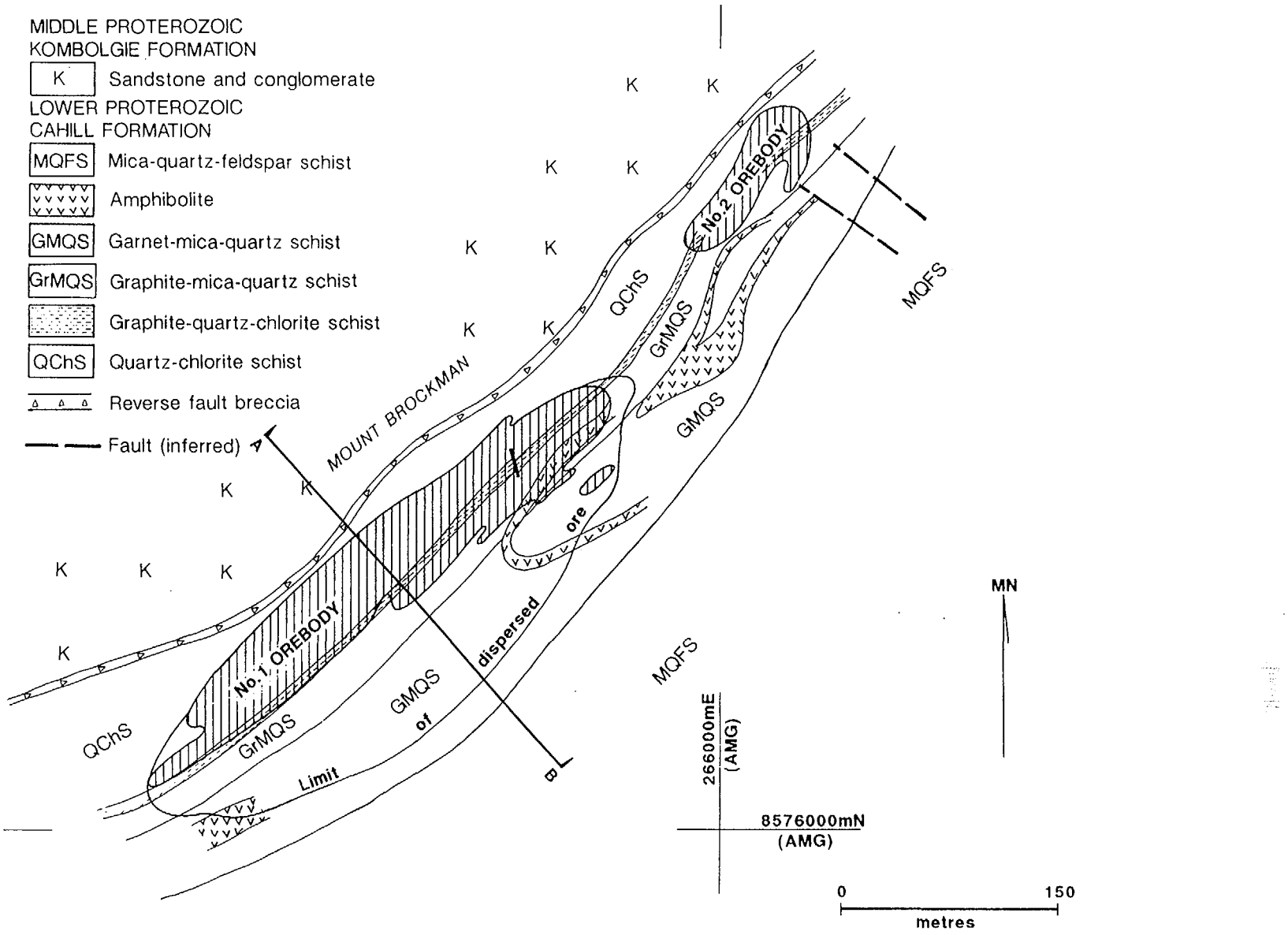

FIGURE 6.2 Local geology map of the Koongarra No. 1 and No. 2 orebodies. Because of the surficial cover the geological units and the outline of the mineralisation are projected to the surface from the base of weathering (after Pedersen, 1978).

6.2 Sampling for the Natural Analogue Study

All company records on drillholes, including assay and geological data, were made available to the ARAP. Core and crushed core samples were selected from the inclined diamond drill holes that were drilled by Noranda, Australia, in the initial site evaluation on cross-sections 30.5 metres apart through the No.1 orebody. At the southwestern end of the orebody, particularly, and beyond, vertical percussion holes also provided drill chips for study.

At the time of the initial program of fieldwork at Koongarra, 83 holes were drilled for core using diamond drilling and 62 holes were drilled with a rotary percussion drill. The latter holes were vertical and allowed the sampling of groundwater.

Figure 6.3 is an aerial photograph of Koongarra taken in June 1981 showing the camp and site development, the Koongarra Fault scarp and the rugged Kombolgie Sandstone exposures of the southern edge of the Mt Brockman Massif. Surficial trends south of Koongarra Creek indicate a dyke and broadly folded rock units. The Koongarra Creek can be seen towards the bottom of the photograph. The position of a number of boreholes is indicated; tracks running down the photograph follow Mine Grid sections.

At the beginning of the ARAP some 32 of the vertical percussion holes were still open, allowing water-sampling gear to be lowered to desired depths and measurements made of standing water levels. However, as the work progressed it was found that:

- detailed coverage of the southwestern half of the No.1 orebody and its environs was not as complete as was necessary for hydrogeological characterisation of the site, and monitoring and modelling of the groundwater chemistry and flow
- core samples drilled by Noranda in 1970-73, which had been stored in sheds at Koongarra, were now oxidised and degraded, and
- coverage of the weathered zone dispersion fan, the principal modelling objective of the analogue study, was in places quite sparse, particularly in its top half where there were either large core losses or the core was very degraded.

Consequently, late in 1988 twenty-two new holes were drilled. These provided samples through the weathered zone, additional water sampling holes and holes for pump tests and the monitoring of standing water levels. Additionally, late in the field program a number of shallow holes were drilled with an auger rig for the monitoring of standing water levels and for shallow groundwater chemistry samples. Figure 6.4 is a plan of Koongarra showing the mine grid and all drill hole locations. Details of the Reference Grid and pre-ARAP and ARAP drilling programs are also provided in Volume 2 of this series.

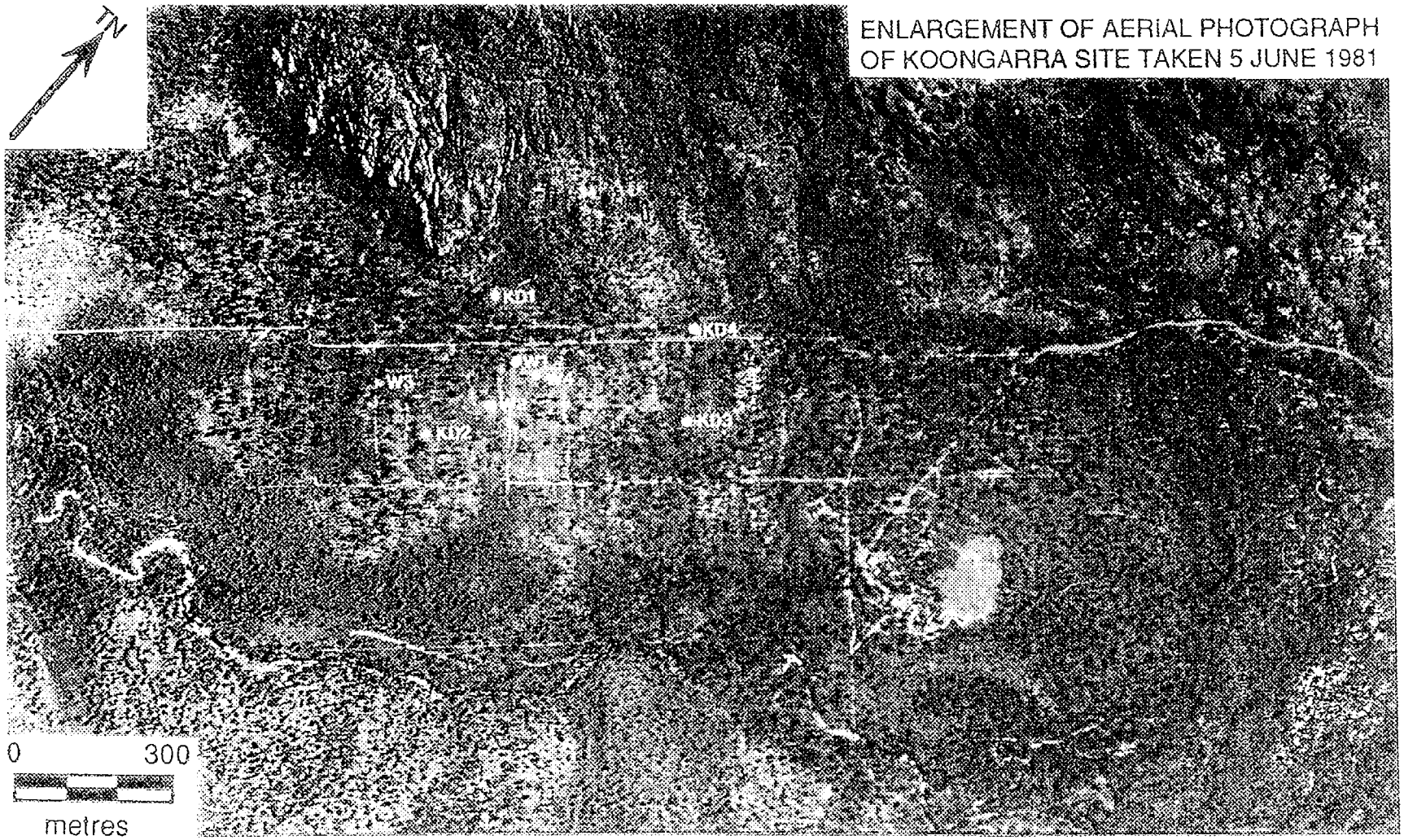

FIGURE 6.3 Aerial photograph of the Koongarra site taken 5 June 1981.

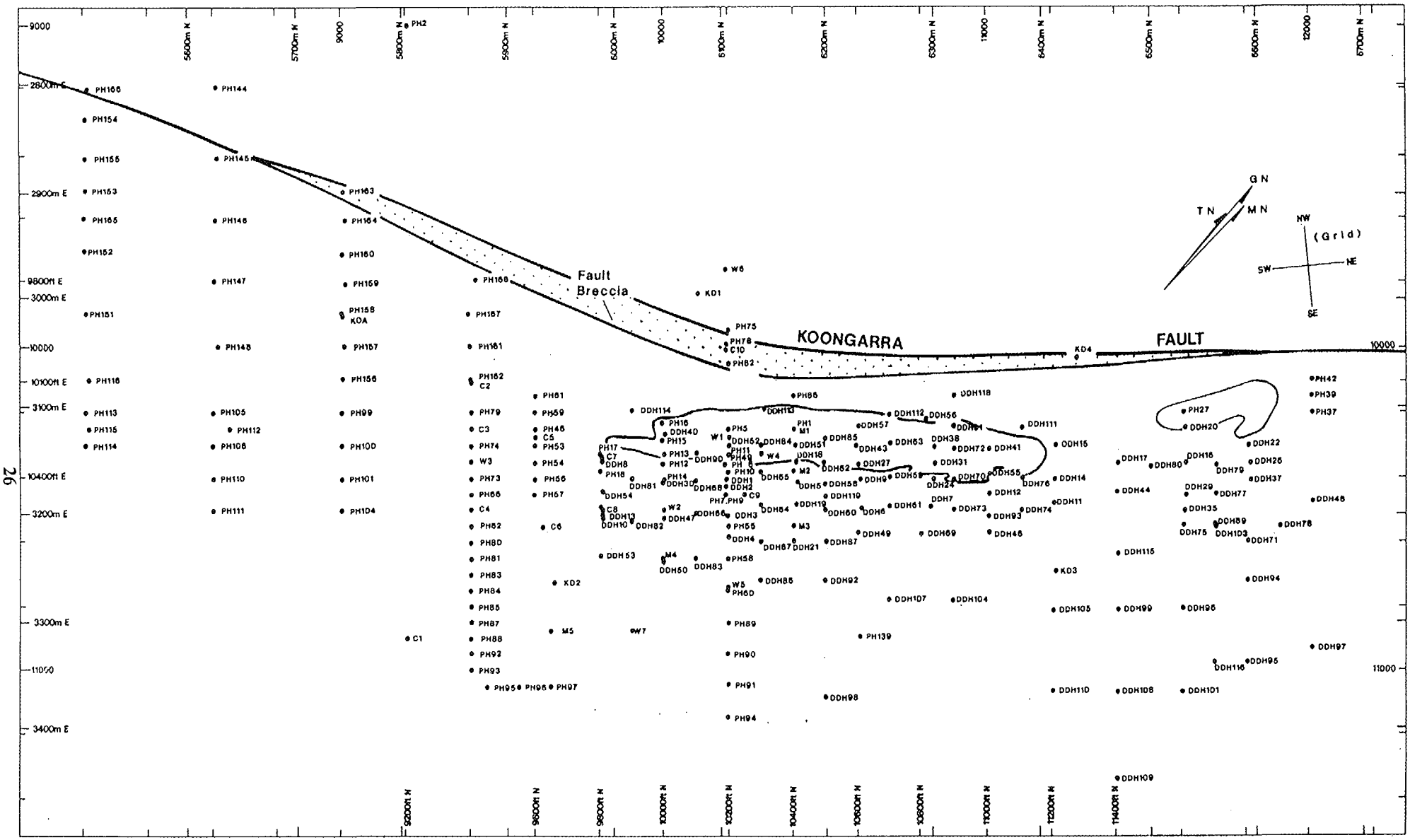

FIGURE 6.4 Koongarra site showing the locations of the exploration diamond drill and percussion boreholes. The diamond drillholes were inclined (50° to the northwest, the percussion holes were drilled vertically. Both the original exploration grid in feet, and the metric (mN, mE) Mine Grid used in the ARAP are shown.

7 GEOMORPHOLOGY

The objectives of this study were to determine from geomorphological evidence the time frame in which the uranium dispersion fan at Koongarra had developed, and to provide an independent method for validating the radionuclide transport modelling (reported below) and its determination of the timing of the dispersion fan formation.

The work, reported in Volume 3 of this series, discusses the current understanding of the geomorphological and paleoclimatic controls that are likely to have played a role in the development of the secondary dispersion fan. The fact that the available data are tentative and only provide an incomplete outline of events is acknowledged. A major problem which remains is of obtaining precise measures of rates of erosion and weathering - those reported are poorly constrained and can be treated only as "first estimates".

7.1 Erosional Processes and Rates of Denudation

The subaerial denudation history of Koongarra spans the Phanerozoic. From the structural geology it is clear that during that time a significant cover of Kombolgie Sandstone must have been removed to expose the Cahill Surface. The spatial arrangement of large-scale structural lineaments and the regional joint and fault patterns clearly facilitated the denudation of the rock mass over what is now the Koongarra Valley. The outcome of this was the separation of the Brockman Massif from the Arnhem Land Escarpment.

Once the Kombolgie Sandstone cover was removed, the exposed Cahill Surface was lowered by erosion. The present topographic position of the Kombolgie/Cahill unconformity along the western margins demonstrates that the Cahill Surface must have been lowered by more than 100 m. The actual amount of lowering of the Cahill Surface at Koongarra cannot be established because the vertical displacement of the reverse fault is not known. Through this lowering of the Cahill Surface, the orebody was "placed" in a weathering environment, which could lead to the development of the secondary dispersion fan.

In the early stages of the ARAP two possible geomorphological controls on the initiation of the development of the uranium dispersion fan were proposed. The first was that the retreat of the Kombolgie sandstone escarpment had uncovered the orezone and allowed oxidising groundwaters to interact and commence the alteration of the host rock and uranium mineralogy. The alternative possibility was that there had been continuing erosion, which eventually brought the top of the No. 1 orebody to a depth suitable for the development of the dispersion fan. Which of these scenarios has taken place and the timing of the events is obviously relevant to the formation of the orezone.

Following an evaluation of the structural geology of the site it now appears that the retreat of the escarpment has played no part in the development of the dispersion fan. Of greater importance in trying to ascertain the rate of surface lowering is the role of the sand apron which fronts the escarpment and forms a partial cover over

the orebody. Unfortunately, this was not resolved during the time of the project, although quartz samples from the sub-surface of Koongarra that might have been dated via measurements of the production of ^{10}Be and ^{26}Al, were collected.

From the possible range of surface lowering/erosion rates that was established for the Koongarra region it seems likely that the arrival of the No. 1 orebody at a depth suitable for the development of the dispersion fan occurred some time in the last 1-6 Ma. This is still a very tentative estimate. The estimate is derived from sediment yield data and more general geomorphological considerations. The incomplete understanding of how rates of weathering front advance and erosion could have varied through time compounds the lack of accuracy. Most important in this respect is our tentative knowledge of the timing and character of Late Cenozoic deep weathering events.

During the time in which the orebody was located in a "weathering environment", climates and hydrology would have varied significantly. Again, the details of Late Cenozoic climatic states remain largely unknown. But some guide for much of the Pleistocene can be obtained by using the climatic conditions of the Late Quaternary interglacials and glacials. This leads to the suggestion of dry glacial stages lasting for some 100 Ka, and shorter wet interglacials lasting for some 10 Ka.

In summary, given the estimate of the range of denudation rates over the past few millions years and the wider geomorphological considerations, it is likely that only in the last 1-6 Ma did the orebody come into a geochemical environment suitable for the development of a secondary dispersion fan. During this time the climate of the area would have changed profoundly. The resulting regional hydrological changes must be incorporated into an understanding of the processes that controlled the development of the secondary dispersion fan.

The suggested range of development of 1-6 Ma is considered a "safe" range given the present data. With better stratigraphic control and a more thorough understanding of the geomorphological and weathering processes operating in the area today, this range could be considerably refined.

8 CLIMATE

Discussions of past and present-day climates can be found in Volumes 3, 5 and 6 of this series, which discuss respectively the paleoclimatic history, hydrogeological field studies, and modelling.

8.1 The Present Climatic Regime of the Area

At present the area has a climate which has a Koeppen classification of A_w - a hot moist climate with a marked dry season in winter. About 95% of the rainfall occurs between November and April, during which time the relative humidity is most commonly above 80%. All indications are that past climates of the Late Cenozoic differed significantly from the climate regime presently prevailing in the region.

The controls on the dynamic climatology of the region are essentially the northern Australian monsoon, which determines the summer climates, and the Subtropical High Pressure Cell, which largely influences the winter situation. October is adopted as the starting point of the monsoon cycle as this month is the transition period between the cessation of the Asian summer monsoon and the Australian winter trades, and the Australian-Indonesian summer monsoon and the Asian winter monsoon. By May, the seasonal reversal is complete: the heat low over Western Australia and the monsoon shear line over the Southern Hemisphere have disappeared, the trades have strengthened over the Coral Sea and Indian Ocean and a southeast to east flow prevails over the near-equatorial latitudes. The summer monsoon has commenced over Malaysia and is moving into Southeast Asia.

The climatic statistics available for Koongarra are summarised in Figures 8.1 and 8.2. Because of the limited length of the Koongarra record, climate data from Oenpelli, which has a much longer record, have also been considered.

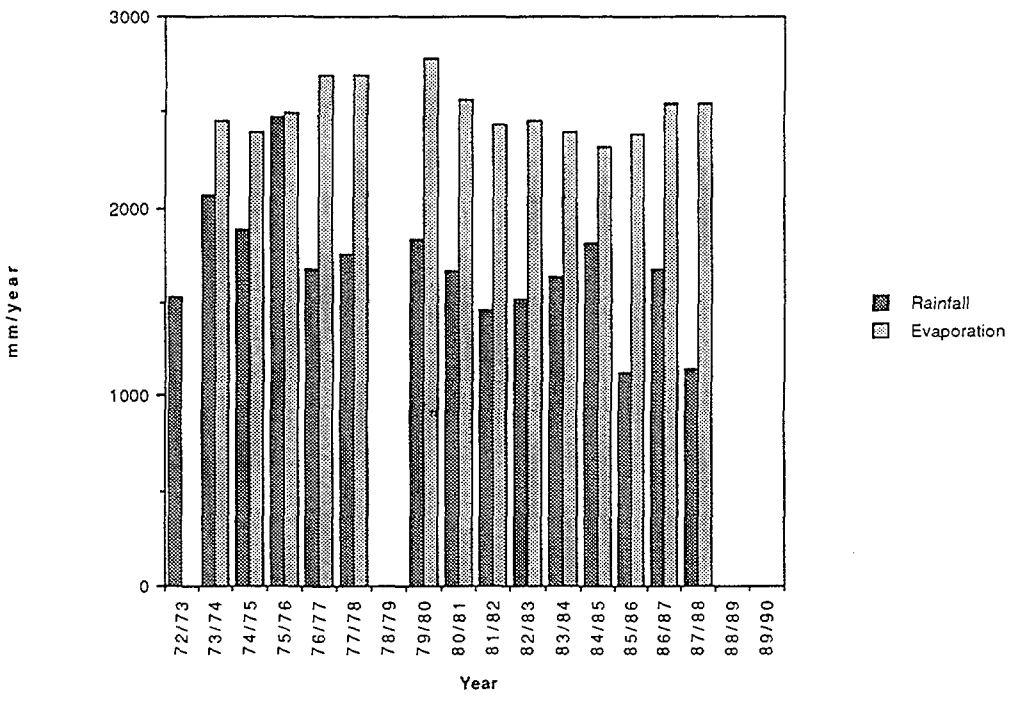

FIGURE 8.1 Rainfall and pan evaporation at Koongarra for water years.

The region has two quite distinct seasons - a dry warm winter and a hot, wet summer. At Oenpelli the mean monthly temperature varies from 24.6°C in July to 30.2°C in November. The extremes of temperature are up to 10°C higher and more than 10°C lower than the corresponding means.

The mean annual rainfall for Koongarra is shown in Figure 8.1. The rainfall is almost totally confined to the summer period of late October to early April. At the height of the wet season, December to March, monsoonal trough and tropical cyclones are the dominant rain-producing systems. Rainfall variability is low (Table 8.1). Two features of the local climate are illustrated in Figures 8.1 and 8.2. The first feature is variability in annual totals of rainfall and pan evaporation, and the second is the strong seasonal cycle in the same variables.

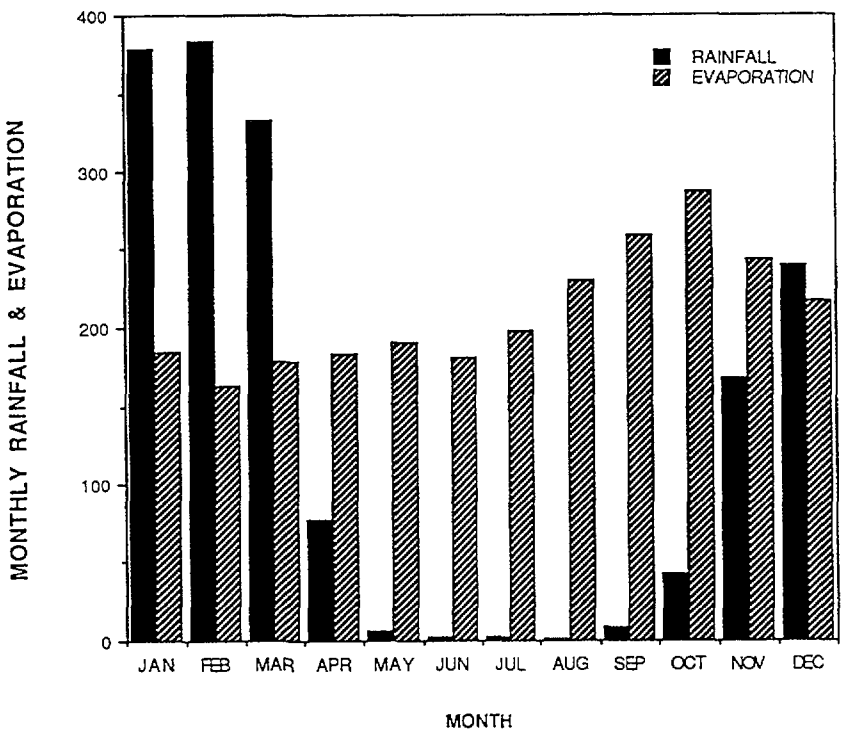

FIGURE 8.2 Monthly average rainfall and pad evaporation at Koongarra.

Table 8.1 presents the statistics of the annual totals for water years. There are 15 complete years of record for rainfall between 1972-73 and 1987-88 and 14 years for evaporation. Of particular interest is the fact that pan evaporation is significantly larger than rainfall. At the same time, the coefficient of variation for evaporation is considerably less than that for rainfall.

TABLE 8.1

CLIMATE STATISTICS FOR KOONGARRA

	Annual rainfall (mm)	Annual pan evaporation (mm)
Average	1685	2509
Standard deviation	335	135
Coefficient of variation	0.20	0.05

Seasonal variations in rainfall and pan evaporation show that about 90% of the rainfall occurs in the five months from November to March, whereas pan evaporation is relatively uniform throughout the year. During the wet season, evapotranspiration probably occurs at close to the potential rate. During the dry season, pan evaporation is significantly larger than rainfall, thus evapotranspiration must be controlled by soil moisture availability (at the surface and in the root zone), rather than by atmospheric demand.

8.2 Past Climates

Our understanding of Tertiary climate events is very limited. From present knowledge it is clear that there were climates during the middle and late Tertiary which would have led to more intense chemical weathering than occurs at present, but such weathering may also have taken place during the Pleistocene.

The most comprehensive Quaternary climate record of northern Australia comes from Lynch's Crater in northern Queensland (Figure 8.3) which is thought to cover the last two glacial/interglacial cycles. The pollen record obtained from this core indicates significant climate changes, and especially precipitation variations, during this period. The overall summary of likely precipitation changes shows very low precipitation values at the height of the last glacial maximum (LGM). A similar trend is evident for the previous glacial and interglacial stages. Reliable dates are only available for the upper part of the core, while the older dates are inferred.

Some unpublished preliminary findings of Late Quaternary climates come from northwestern Australia, where a limited number of thermoluminescence dates on desert sand dunes suggest that more arid conditions prevailed in this area for much of the Late Pleistocene (Wyrwoll, unpublished).

While the Holocene climate record of northern Australia is generally better known, problems of interpretation still remain. Wasson and Donnelly (1991) reviewed the relevant Australian literature and concluded that over the last c.13 Ka the Australian monsoon has essentially "tracked" the behaviour of its Northern Hemisphere counterparts. In their reconstruction, monsoon activity was already significant by 13 Ka BP, was more intense at 9 Ka BP and fell to present levels after 4 Ka BP. However, the data on which this conclusion is based are limited.

From the evidence now available it is reasonable to conclude that precipitation levels similar to that of today have prevailed in the Koongarra area for the last c.10 Ka. In tropical Australia there may have been times during the middle Holocene when mean annual precipitations were somewhat higher than those of today.

Another factor of significance to water balance considerations and paleohydrology in general, is temperature. Unfortunately, it is more difficult to obtain indications/ estimates of temperature differences for northern Australia at the LGM. It is obvious that mean annual temperatures over northern Australia at the time of the LGM can be expected to be lower than at present.

Evidence from the New Guinea Highlands (Bowler et al., 1976) suggests that at the LGM, mean annual temperatures were some 6°C lower than at present, while estimates of sea surface temperatures show differences of little more than 2°C.

It is concluded that the climates of the Koongarra area during full glacial stages were characterised by significant decreases in precipitation and lower temperatures. Estimates of likely relative reduction in the mean annual precipitation of the Koongarra area over the last c.100 Ka can be gauged from a comparison with the data provided by Kershaw (Figure 8.3).

In reconstructing the climates of the last 700 Ka the most limited approach that can be taken is to use the Middle-Late Quaternary record as a guide. Following this, and using the Lynch's Crater record, a "working" paleoclimate framework for this time period consists of:

(1) drier glacial periods lasting for the most part of 100 Ka, with extreme dryness prevailing at glacial maxima; and

(2) interglacials lasting in the order of 10 Ka, during which precipitation levels were similar to those which prevail today.

The sequence of paleoclimatic events for the last 700 Ka is an idealised scheme based on the direct hindcasting of the Late Quaternary record. Although the problems and inconsistencies inherent in hindcasting the Late Quaternary record should be apparent from the previous comments, this scheme nevertheless has merit for paleo-hydrological modelling. The sequence can be used to set the limits of the climatic boundary conditions for the last c.1 Ma. The two climate states can be set as end members and the effect of variable duration and intensity of these climate scenarios could be modelled in a random variate context. For such an exercise to have any physical meaning, the sensitivity of hydrological and geochemical processes to climate variations needs to be understood.

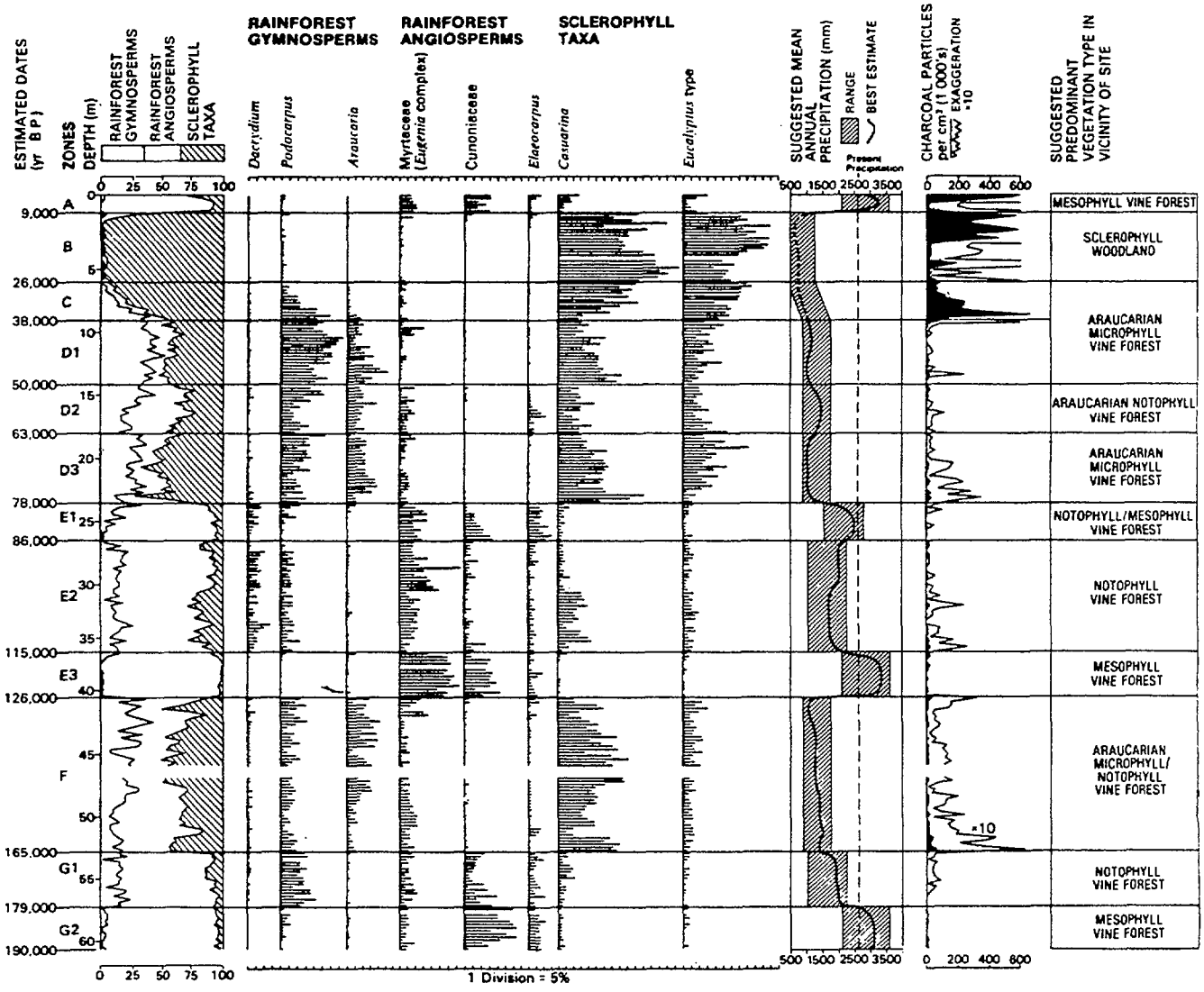

FIGURE 8.3 Pollen record and climatic reconstruction from Lynch's Crater, northeast Queensland (after Kershaw, 1986).

9 GEOPHYSICS, PETROPHYSICS AND STRUCTURE

The Koongarra site was studied by geophysical, geological and geotechnical techniques to determine lithological and structural features relevant to ancient and current groundwater flow. These techniques ranged from measurements on regional scales to measurements on sample scales to evaluate:

- how groundwater has moved and is moving through the orezone region
- the source of the water - natural recharges or flows across the fault
- how the groundwater drains out of the site
- whether fluid flow is through fractured or porous media or both, and in particular,
- how this has influenced the transport of uranium and the formation of the dispersion fan.

Details of these investigations are provided in Volume 4 of this series.

9.1 Petrophysical Measurements

The physical properties of 306 core samples from 29 drillholes penetrating the various units were measured for dry bulk density, apparent porosity, intrinsic permeability, galvanic (water saturated) resistivity, ultrasonic compressional wave velocity and magnetic susceptibility values. Figures 9.1 and 9.2 show examples of the results with density and permeability values plotted as a function of depth. The clayey (upper) weathered zone has very low density, very high porosity and very low permeability. The (lower) weathered and transition zones have low density, high porosity and low-to-moderate matrix permeabilities. The deeper, unweathered schist zone has typical metasedimentary densities, low porosities and very low permeabilities.

These results show that macro-fracturing in the bedrock does exist and presumably continues into the upper zones. The only way in which the deeper zones could hold significant quantities of water is by extensive fracturing. Significant fracturing and interconnectivity should be seen as a decrease in both *in situ* resistivity and velocity. The shallower zones have a high intrinsic water bearing capacity, and hence should be more conducive to matrix fluid flow than the unweathered zones.

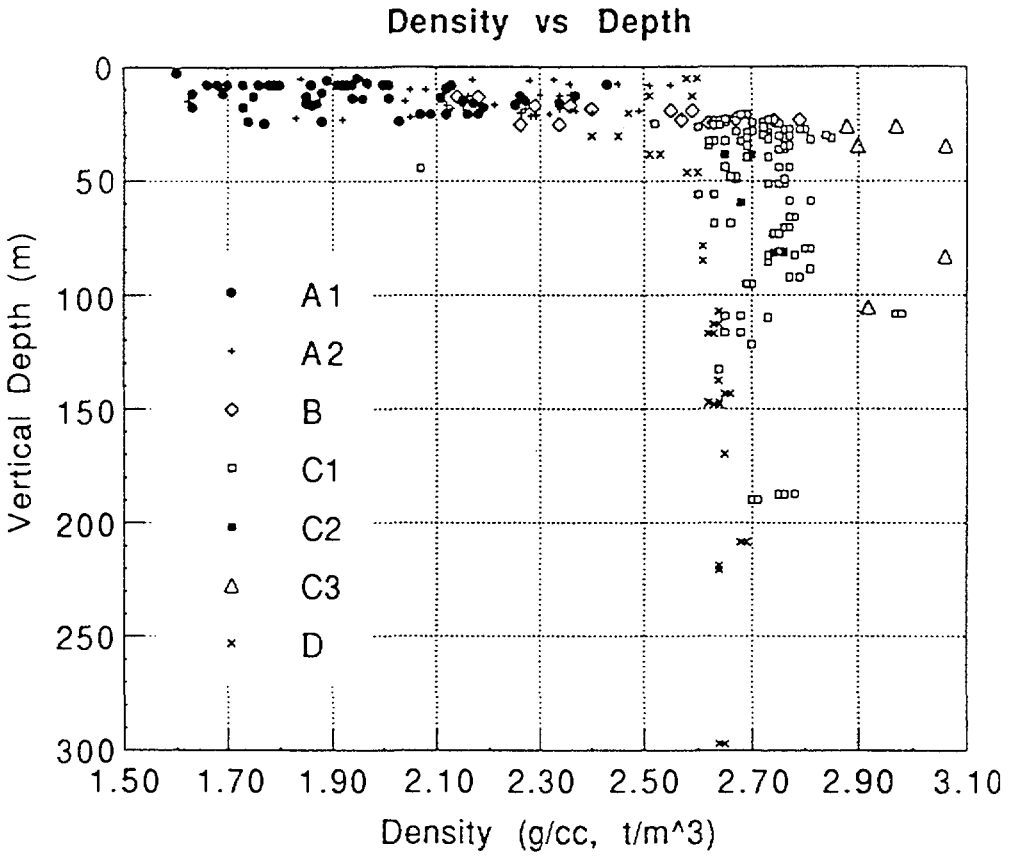

FIGURE 9.1 The relationship of the Koongarra samples' dry bulk density with depth.

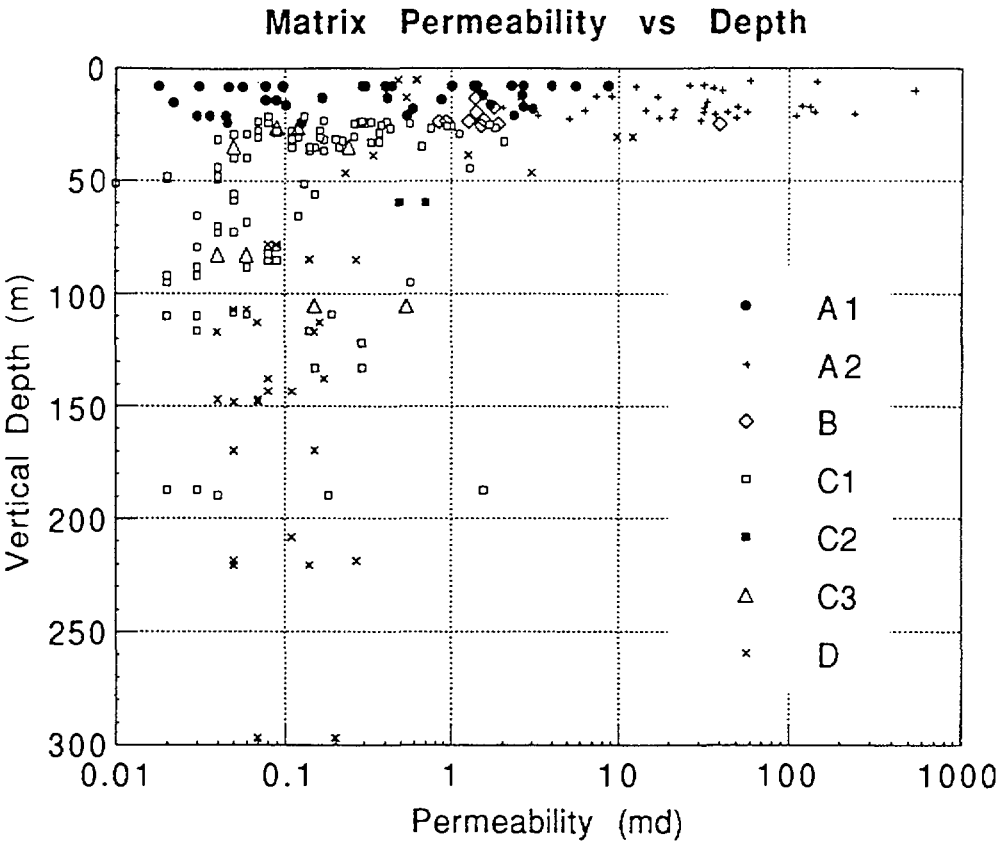

FIGURE 9.2 The relationship of the Koongarra samples' permeabilities with depth.

9.2 Study of Fractures

Since the results of laboratory tests can only assess the contribution of matrix porosity (including microfracturing) to permeability, macro- and micro-fracturing studies were carried out on an entire drillcore to try to quantify the nature and extent of fracturing and their implication for the flow of subsurface fluids. The implications for unweathered rock are that:

- extensive fracturing exists in the schist lithologies with a greater intensity in the graphitic horizons
- the deeper Kombolgie Sandstone appears to be sound and tight
- major fracture zones other than the Koongarra Fault appear to exist in the schists
- more fractured zones are expected to have enhanced hydraulic conductivities
- cross-foliation fracturing does occur on a relatively minor scale, and
- if the weathered zone has inherited any fracture patterns these would enhance hydraulic conductivities if they were not in-filled with clay and debris.

9.3 Geophysics

Geophysical field programs were undertaken to locate anomalies related to the subsurface geology and structure. The measured properties are not uniquely related to hydrogeological features, but could be assessed with the hydrogeology in mind. Twelve kilometres of geophysical traverses were completed. Magnetic, gravity, radiometric, spontaneous potential (SP), electrical resistivity and electromagnetic techniques were used to identify lateral and vertical lithological information, structural trends and discontinuities, and infer hydrogeological characteristics.

9.3.1 Streaming potentials

The SP method is based on the measurement of naturally occurring subsurface electrical potentials. It has a shallow depth of investigation, about 15 to 20 m, and responds to electrochemical phenomena associated with sulfidic, graphitic orebodies and/or electrofiltration currents generated by subsurface lateral and/or vertical fluid flow. The application of this method proved to be very informative and led to a map of interpreted streaming potentials associated with subsurface water flow.

Away from the No. 1 orebody, positive zones were considered to indicate water sources or upwellings, and negative zones were considered to indicate seepages along shears, faults or channels. Noting that the technique only investigates shallow depths, it appears that most responses away from the orebody reflected dynamic weathered zone hydrogeology and that the Kombolgie Sandstone on the northwest side of the Koongarra Fault acts as a water source.

Distinct electrofiltration trends were seen to the southeast and to the south of the orebody's southwest tip. This southerly trend agrees well with contours of uranium in shallow rock samples (see below), whilst the southerly SP zone overlapped a

relatively highly transmissive bedrock zone established by pumping tests (see below). It is interesting to note that a very similar SP picture was obtained from the survey carried out at the end of the dry season but this did not show the lobe to the southeast. If this is a reliable feature, it presumably indicates a process occurring at shallow depth, which is active only during higher groundwater levels.

9.3.2 Electrical resistivity soundings

Resistivity field studies indicate very high resistivities to the northwest for the Kombolgie Sandstone, medium resistivities for the Cahill Formation weathered zone and high resistivity bedrock at depth. The indicated and inferred resistivities were generally in accord with those determined in the laboratory. The data indicated the presence of high resistivity zones to the northwest through the Kombolgie Sandstone. The Cahill Formation at shallow depths is weathered and has relatively high electrical conductivity; below the weathered zone it is a banded but generally high resistivity unit. Low resistivity zones trend to the south from the southwest tip of the orebody, suggesting a shear or fracture zone, and this gravity delineated flexure can be seen quite clearly in the deep resistivity data.

9.3.3 Electromagnetic traverses

These contours reflect information down to about 30 m and their pattern suggests higher resistivities to the east and southeast, indicating the possible influence of Cahill schist bedrock in these data. The edge of the Kombolgie Sandstone appears as a high resistivity feature to the northwest. Elsewhere to the south relatively low resistivities trend in a belt that correlates quite well with the BTV (Borehole TV) and SP data and the gradient array resistivity interpretation (see below). The low resistivity electromagnetic data are interpreted as reflecting a continuation or preservation of a bedrock fracture zone into the weathered zone, where it is manifest as a porous wet channel.

9.3.4 Geophysical interpretation

A qualitative interpretation of the geophysical data was obtained by considering the data together. Information on the basic structure and lithological units at Koongarra was obtained and is presented as a composite plan in Figure 9.3. This clearly shows the main drainage, lithological and structural features of the site. Fluid channelling was interpreted to arise mainly from the southeast part of the orebody and flow occurs to the south. Orebody drainage in the weathered zone is thought to have occurred mainly through the microfractured matrix and not through major fractures. This is in contrast to the unweathered zone hydrogeology, which is fracture-controlled. Very shallow movement of dispersed radionuclides in the surface unconsolidated sands was indicated by radiometric (gamma ray) results.

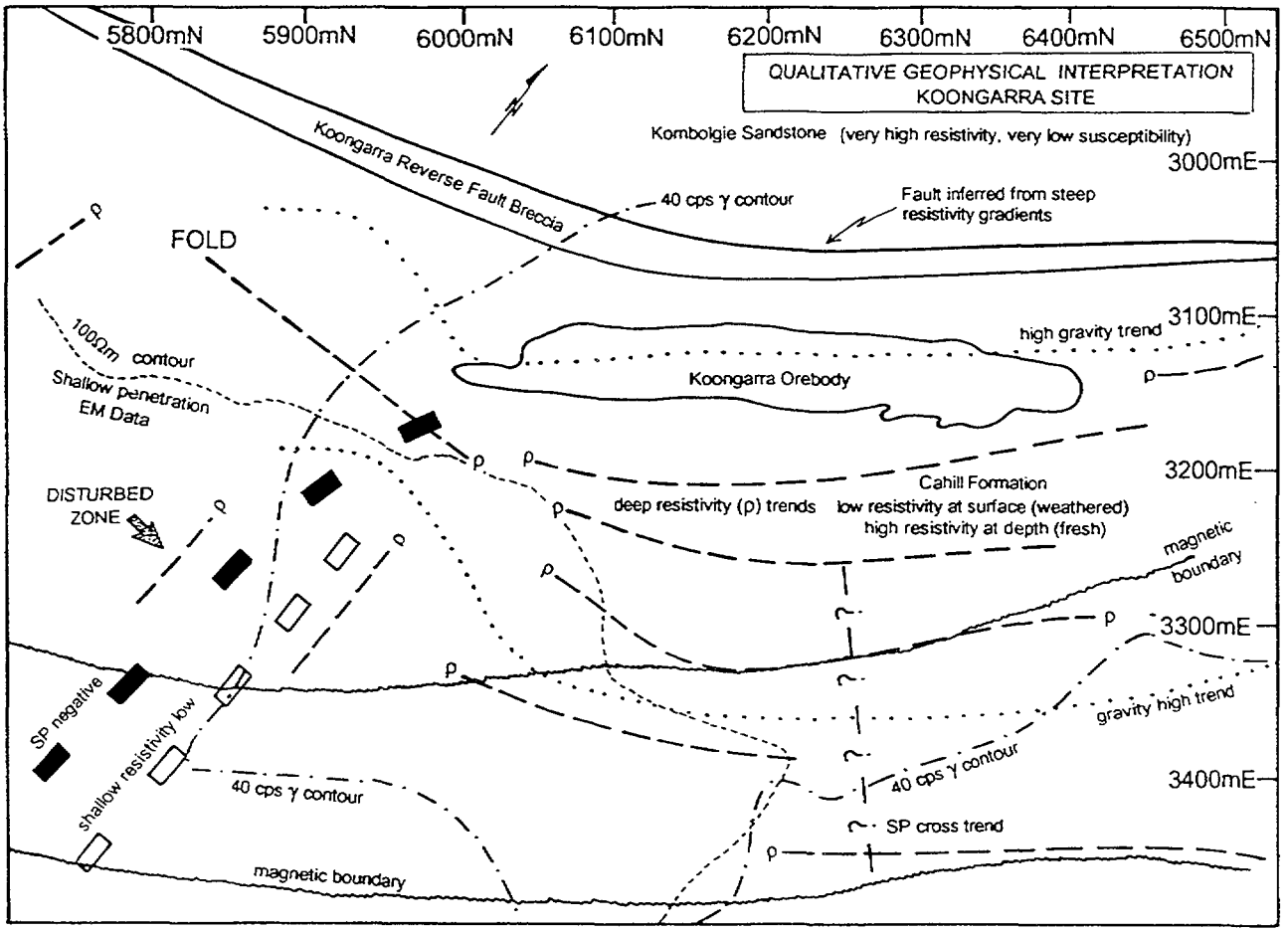

FIGURE 9.3 Composite interpretational plan of the Koongarra site – the interpretations are integrated, qualitative assessments of the various geophysical responses.

9.4 Borehole TV Mapping

The field structural studies were integrated with a borehole television (BTV) mapping program of a total length of 469 m carried out in 20 boreholes to identify geological features such as the orientations of the schistosity, fracture densities (*in situ*) aperture widths and orientations. The BTV technique demonstrated great potential for the investigation of the *in situ* orientation of structural features in drill holes. Figures 9.4 and 9.5 provide examples of the BTV measurements with the 360° images of the surrounding walls showing planar structural features in boreholes M3, M4 and PH58; structural features down to 0.5 mm thick could be resolved. The drilling logs were used to assist the lithological interpretation, but the orientation and width of visible structural features could be determined using the BTV accurately and with confidence.

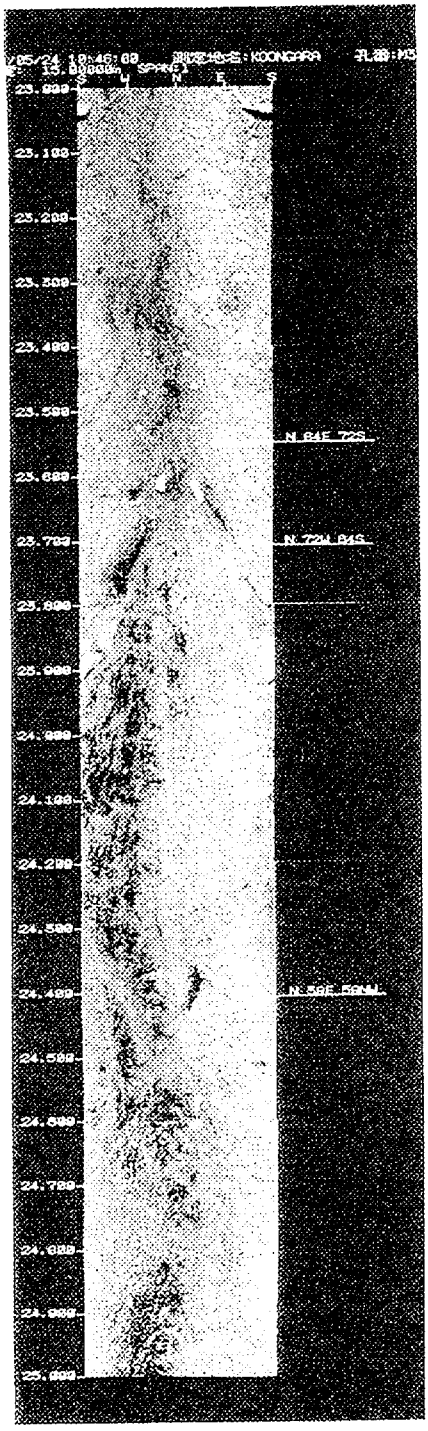

FIGURE 9.4 This figure shows a short section of the 360° BTV image spanning the boundary between the weathered zone and the transition zone over the depth range 23.0-25.0 m in borehole M3. In the weathered zone the aluminiosilicate components of the clay are converted to clay, and iron occurs in the ferric state, causing the rusty colour of the clay zone. Structures and textures inherited from the original rock may be traced as ghost features in the weathered zone. The boundary between the weathered and transition zones, at about 23.7 m, is well defined within an interval of 100-200 mm. Cracks and open fissures in the transition zone show signs of advanced oxidation and clayey alteration, but the rock between these fissures may be preserved more or less intact and may show the various mineralogical, structural and textural features of the unweathered rock.

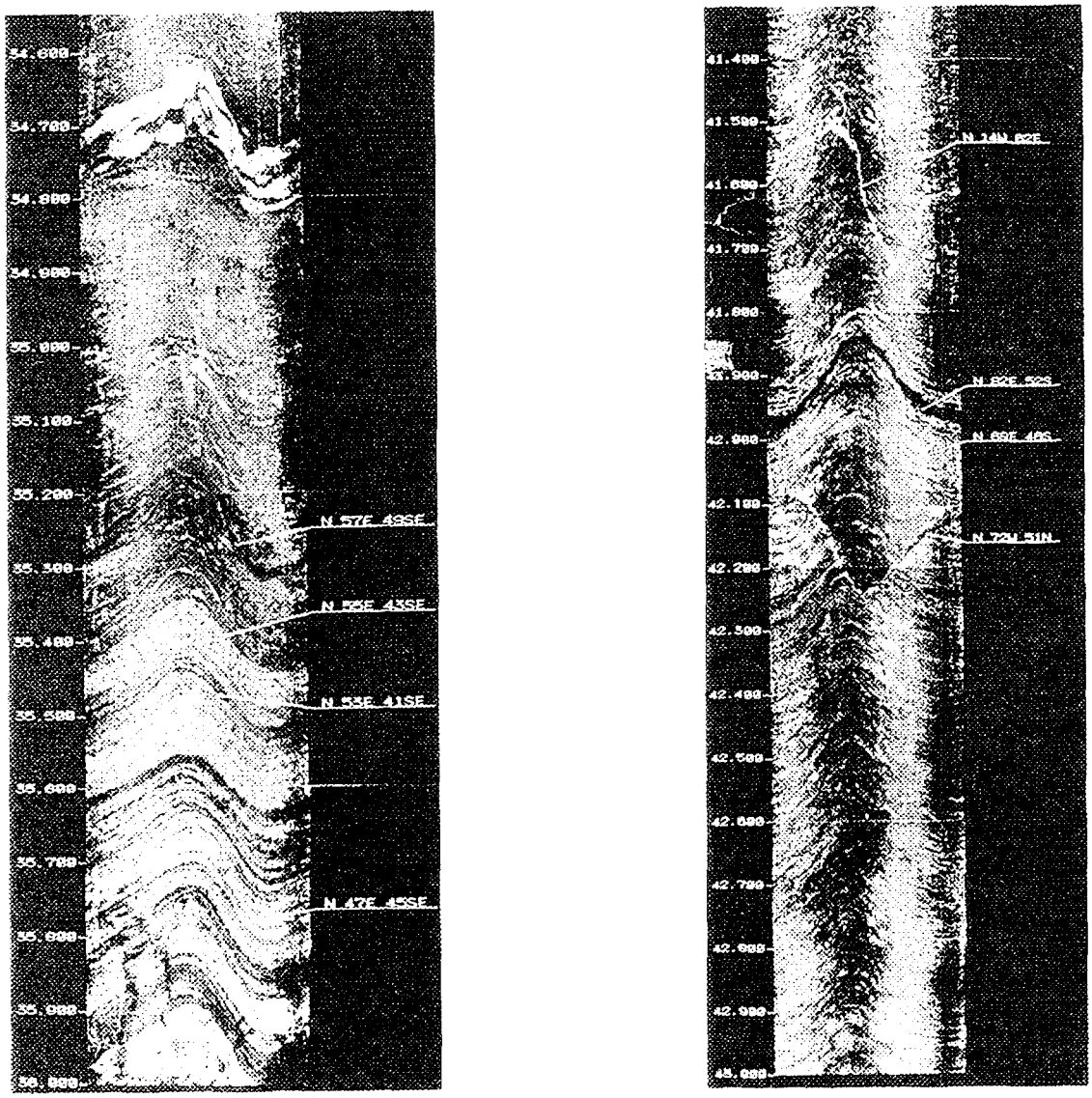

FIGURE 9.5 Segments of 360° BTV image illustrating planar structural features.

(a) Section from 34.6-36.0 m in borehole M4. This section shows striking visual contrasts between schistocity parallel lithological laminations and layering striking NE and dipping SE at about 45°. The upper part of the section consists of muscovite-chlorite schist containing a schistocity parallel quartz vein. The lower part of the section consists of well-laminated quartz-muscovite-chlorite schist.

(b) Section from 41.3-43.0 m in borehole PH58. The dominant schistocity in this section of quartz-chlorite schist dips at a moderate angle to the south. Two thin quartz veinlets are shown, the upper one dipping steep east and the lower one dipping moderately north. Structural features down to 0.5 mm thick can be resolved in the BTV images.

Locally, the BTV measurements showed directional trends in the schistosity (Figure 9.6) similar to the geophysical trends and to the directions of the axes of the aquifer test drawdown cones (discussed below). This probably indicates that the aquifertests were dominated by fractures in the deeper unweathered zone. A major drainage feature to the south of the orezone was identified. Regionally, BTV measurements identified the dominant schistosity and fracturing that can account forthe main southeast dispersion fan. It was also observed in both the geotechnical and core studies and in the BTV program that overall, the site is moderately fractured with the graphitic schist lithologies exhibiting the highest fracture intensities.

9.5 Conclusion

The petrophysics study of the Cahill Formation established that the weathered zone is heterogeneous and has a high porosity, an erratically distributed but overall moderate matrix permeability in the lower part; the anisotropic bedrock has a low porosity and low matrix permeability. Significant fluid movement in the unweathered Cahill can only be by fracture flow; fluid movement in the weathered zone operates mainly through the matrix permeability - there being no direct evidence of effective fracturing except in the lower weathered transitional zone.

Consideration of the geotechnical and BTV data and the field observations indicates fracturing over the entire site with the graphitic units having the most abundant fractures. Fracturing tends to be discontinuous at the macro- and micro-scales but some zones in the unweathered bedrock exhibit continuity and enhanced permeability.

The geophysical and geological fieldwork (including borehole core logging) showed that the site itself is a folded, faulted, variably fractured Precambrian psammitic and pelitic schist sequence with a quasi-horizontal weathered zone superimposed on the steeply dipping rock fabric. Gravity, magnetic and electrical laboratory and field studies confirmed a broad folded fractured sequence of dipping layered host rocks, weathered in their upper parts and trending in a southwest-northeast direction. Qualitatively interpreted anomalies indicated the trend of the main groundwater movement to the south where dolomites are thought to act as a sink. The roles of the Kombolgie Sandstone as a source of water and the Koongarra Fault as a barrier or otherwise were not established owing to the difficulty of geophysical access over the site's escarpment.

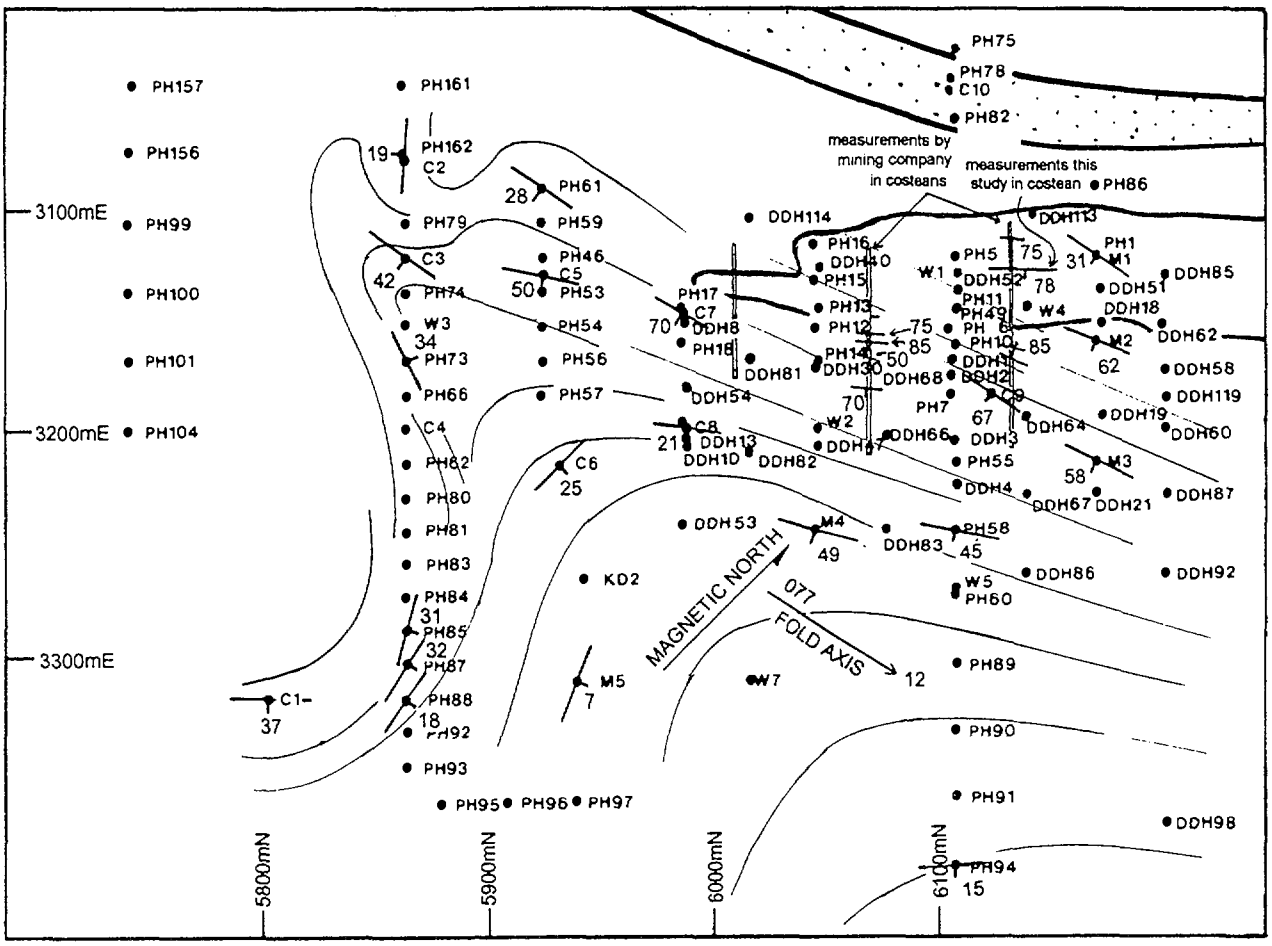

FIGURE 9.6 Plan view of folds in BTV-interpreted schistocity.

10 HYDROGEOLOGICAL FIELD STUDIES

The hydrogeology of the Koongarra site has been interpreted primarily from long-term hydrographs, water level maps, water injection (slug) tests, aquifer pumping tests, logs of bore holes, and chemical analyses of groundwater samples. Data have been collected over a 21-year period, starting with test drilling in 1970. The first intensive period of hydrogeological investigations was from 1978 to 1981 and was related to anticipated exploitation of uranium ore at Koongarra (AGC, 1980). The second period was from 1986 through 1991 and was related to the ARAP. Hydrogeological field studies are discussed in detail in Volume 5 of this series.

10.1 Water Levels

Long-term hydrographs of water levels in observation wells show seasonal fluctuations that range from about 2 m to a maximum of about 16 m. Highest water levels in the observation wells are reached about two months after the period of maximum rainfall, which is normally in January and February. This delayed reaction probably relates to the length of time that is needed for the near-surface sediments and rocks to reach field capacity with respect to moisture. Water overflows the tops of casings on a number of observation wells at the end of the rainy season. This suggests that the groundwater is partly confined in much of the area investigated.

Water-level maps show that groundwater generally flows from the base of the uplands in the northwest to Koongarra Creek in the southeast. The orientation and spacing of lines of equal hydraulic head vary locally in response to areas of recharge and discharge as well as to lateral variations in aquifer properties. Natural hydraulic gradients in the schist vary from a minimum of roughly 0.005 to a maximum of about 0.05. A groundwater mound with an elevation of about 6 m above adjacent areas is present along the Koongarra fault in the northeastern part of the study area; this is particularly evident during the wet season (Figure 10.1). This mound may reflect a zone of maximum recharge, which is near a known area of surface seepage of water that persists even during the dry season.

Water levels were monitored on a regular basis to establish baseline conditions for the correction of drawdown data. Daily water level fluctuations were monitored in several bores that did not respond to pumping, and these were plotted against tidal strain and barometric pressures. Natural cyclic fluctuations of groundwater levels, which have one or two maxima and minima per 24 hours, can be produced by earth tides, changes in barometric pressure, and transpiration. Records of earth tides are best seen in boreholes that tap rigid and confined aquifers with very low porosity. Thus, bore holes PH78, PH15, and KD2, which exhibit pronounced twice-daily tidal fluctuations, tap the fractured but only slightly weathered Cahill Formation. Bores PH84, PH61, and C8 also show some less pronounced tidal effects, suggesting that the rigidity is less and the porosity greater in the water-bearing zones at these localities

Atmospheric pressure will have a maximum effect on groundwater levels in bore holes which are connected with rigid and confined aquifers with relatively high porosity. Under ideal conditions, some bore holes could theoretically act as water barometers. Local effects of transpiration are not seen clearly in the hydrographs, hence the steady decline measured in water levels over the entire area in the dry season (Figures 10.2a and b), must be caused by transpiration. Koongarra Creek is dry during the late dry season, and no other logical explanation for the decline during this period exists. One explanation for the lack of direct transpiration effects is the possibility that tree roots near most of the boreholes do not penetrate deeply enough to remove water from the saturated zone. Another more likely explanation is that trees and shrubs take water from the surficial deposits but the highly weathered Cahill forms a semipermeable barrier to water moving into the more permeable underlying schist. This type of barrier might smooth out the daily fluctuations caused by transpiration

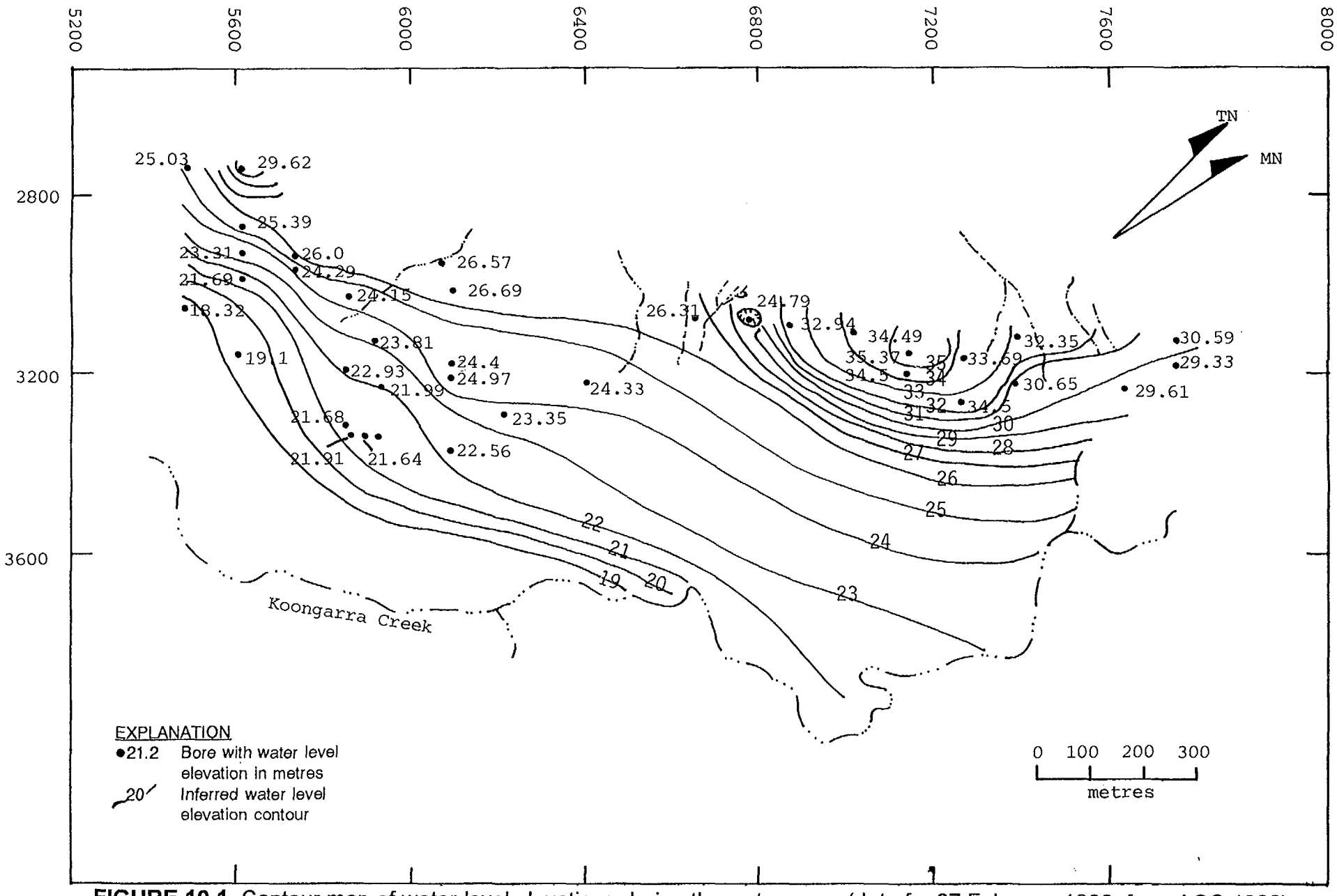

FIGURE 10.1 Contour map of water-level elevations during the wet season (data for 27 February 1980, from AGC 1980)

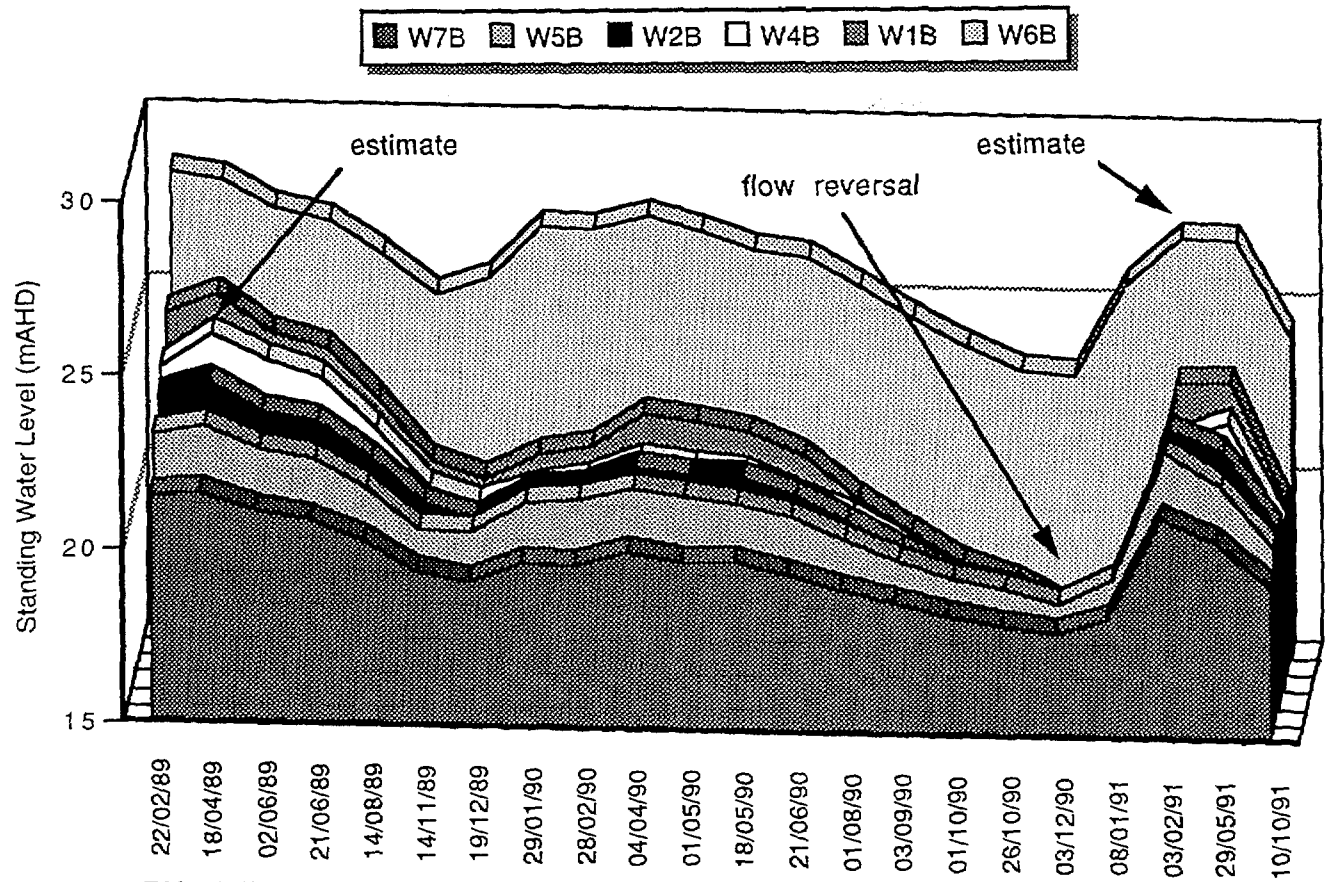

FIGURE 10.2a Time series of standing water levels at W series of bores

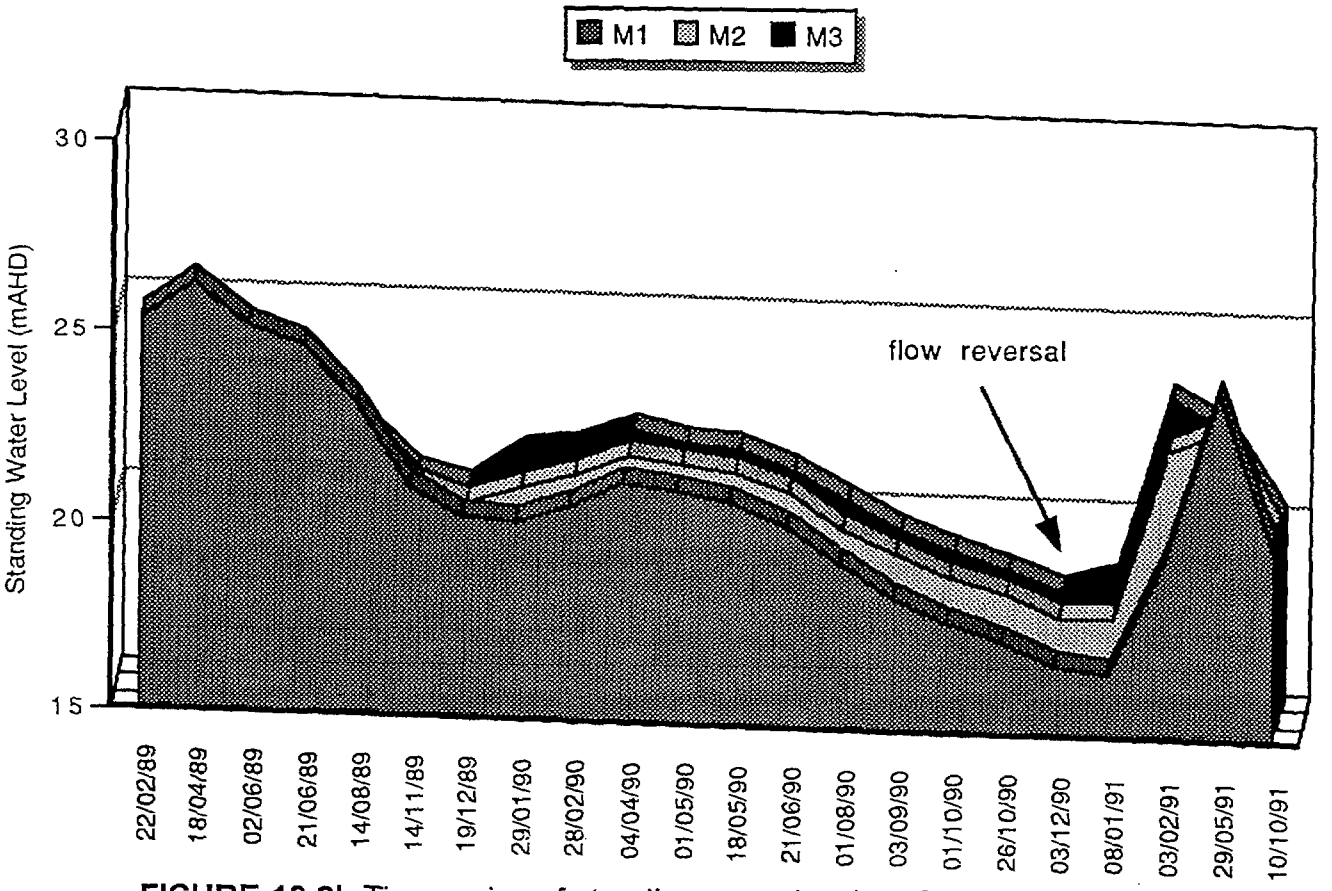

FIGURE 10.2b Time series of standing water levels at M series of bores

10.2 Injection Tests

Various types of water injection tests were made on numerous boreholes. These short-term tests measured hydraulic properties of rocks close to the boreholes. The results indicated a wide variation in conductivities of the subsurface materials. A total of 45 slug tests of water-bearing zones were made in 1989 and suggested transmissivity values which varied from 3×10^{-5} m^2/day to 43.07 m^2/day, with a median value of 2.07 m^2/day. The depth intervals tested varied, but generally involved about 5 m of hole. Hydraulic conductivities were inferred to be of the order of 0.4 m/day for the water-bearing zones which were tested. In another set of 50 water-pressure tests made in 1979, hydraulic conductivities measured varied between 7.5×10^{-4} and 0.47 m/day and had a geometric mean of 1.3×10^{-2} m/day. This significant difference is due to the fact that the 45 slug tests were made in zones of known permeability and the earlier 50 water-pressure tests were made in the more weathered schist, which did not generally transmit much water.

10.3 Aquifer Tests

Long-term aquifer tests were carried out during 1980, 1987, 1988 and 1989 using 13 different test holes for the well which was pumped. Most of the holes were pumped for more than 1,000 minutes and the hydraulic response of the aquifer was measured in 3 to 10 different observation holes. Each test resulted in a unique response to the pumping stress. The resulting drawdown cones were in general elongated in northeast-southwest to north-south directions. Three of the aquifer tests showed highly localised drawdowns in a narrow band, suggesting strongly that most of the groundwater flowing into the pumped well was transmitted through well-defined fractures (see Figure 10.3).

Drawdown data from the constant discharge aquifer tests were analysed using equivalent porous media equations designed for isotropic homogeneous and anisotropic homogeneous conditions. The log-log plots of drawdown versus time were used to identify dominating flow regimes through "type curve" matching. Early, middle and late time data are known to reflect near-bore conditions, the behaviour of an effectively infinite aquifer, and the effects of outer boundary conditions, respectively (Gringarten, 1982).

Values of transmissivities and aquifer storage coefficients were also calculated from recovery data to verify drawdown calculations. Complete recovery of water levels after each pumping test indicated that the aquifer has active circulation. However, during the PH49 test the water levels continued to decline for nearly three hours in bores M1 and M2 before commencing recovery. This suggested a poor connection with the pumped bore and may also indicate the limited extent of the aquifer near the Koongarra Fault. Transmissivities determined by the tests varied from 0.22 to 66.8 m^2/day with a median value of 26 m^2/day. Most water was pumped from the partly weathered Cahill schist. If the thickness of the water-bearing zone is assumed to be 40 m, then an average hydraulic conductivity of 0.65 m/day is implied.

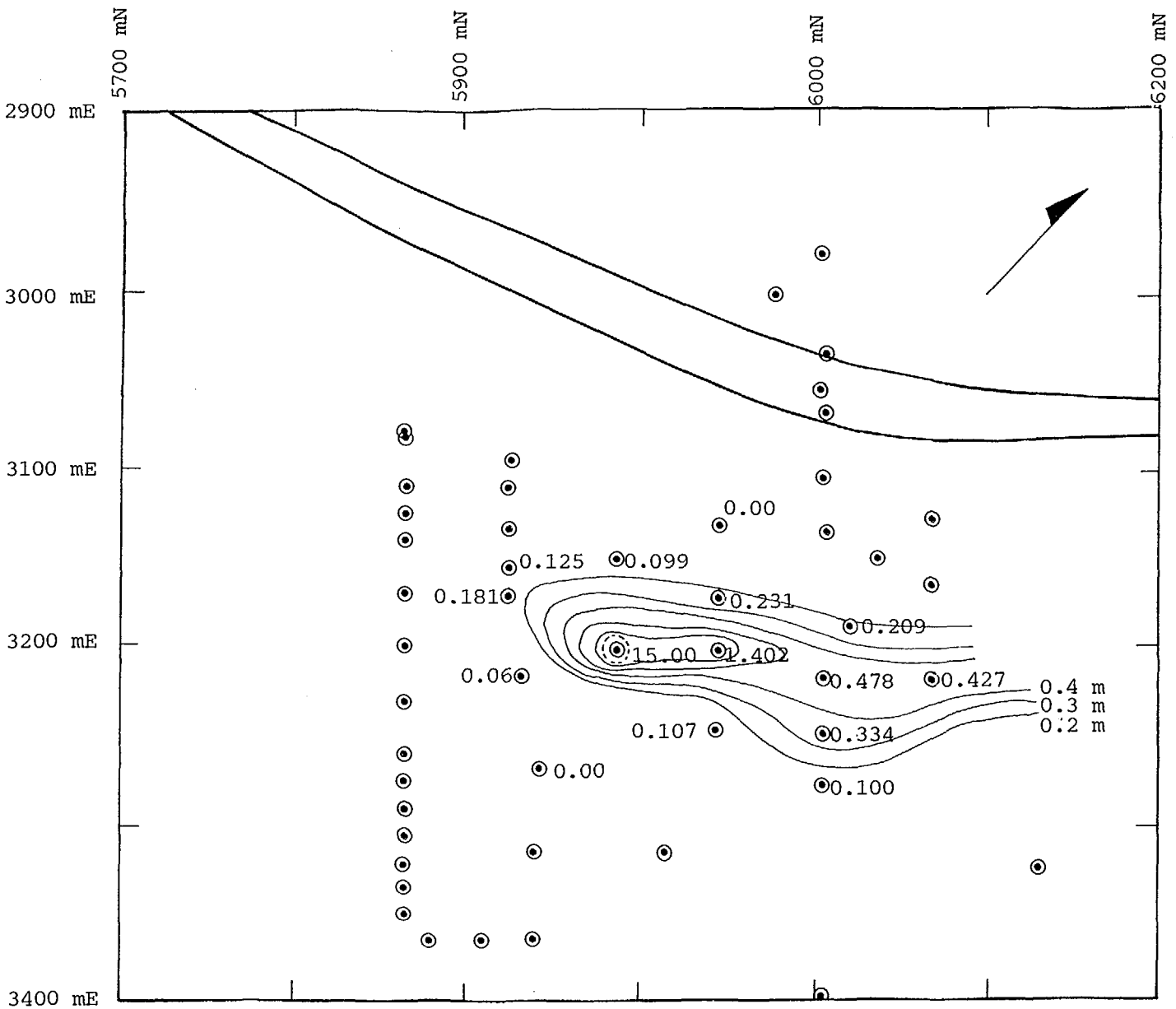

FIGURE 10.3 Contour map of final measured drawdowns in Aquifer test C8, dry season, 1989.

10.4 Summary of Findings

A large number of hydrogeological observations were considered in building a conceptual model of the present-day hydrogeological system of the Koongarra uranium deposit. The observations included not only water level measurements, discharge from test holes during aquifer tests, and similar physical and geophysical measurements, but also numerous chemical analyses of water samples (see below). The physical and chemical systems are not independent, and both must be compatible with a unified conceptual model. The single most difficult question is the apparent conflict between so-called groundwater ages, some of which are measured in thousands of years and the results of aquifer tests, which suggest a rapid movement of water in the saturated zone.

From a hydrologic viewpoint, the geologic materials at Koongarra can be divided into five groups, which are described below.

- Kombolgie Formation, a late Precambrian sandstone with low to moderate porosity and low hydraulic conductivity

  Some zones of greater conductivity are probably present along fractures that traverse the sandstone. This unit borders the site to the northwest and underlies the Mount Brockman uplands to the north.

- Surficial sands, silts, and clays, which cover most of the site and extend from the present-day land surface to depths of 0.5 m to 9 m

  The sands of the surficial sediments are probably the most permeable of the geologic materials. The thickness and nature of the surficial sediments were determined in 234 backhoe pits and 73 auger holes. During the dry part of the year, most of the surficial materials are not saturated.

- Residual clay which grades downward into moderately weathered Cahill schists

  The clay has a thickness which varies from about 2 m to 20 m. It is porous but has, in general, a very low hydraulic conductivity.

- Partly weathered and fractured Cahill schist

  Under present climatic conditions, this zone is saturated throughout the year and constitutes an aquifer, which is from 10 to more than 30 m thick, depending on the location considered. The aquifer, however, is extremely heterogeneous and in many locations is dominated by fracture flow, which imparts an apparent anisotropy to the flow field.

- Unweathered Cahill schist in which water is generally semistatic owing to very low porosity and permeability

  Although some fracture flow certainly occurs at depths in excess of 1.0 km, the bulk of the groundwater flow in the Cahill schist is probably at depths of less than 100 m. Thus, somewhat arbitrarily, the dense unweathered and nonpermeable schist is assumed to start at depths of about 100 m below the base of the residual clay.

Recharge of the groundwater appears to occur primarily by infiltration of seasonal surface runoff from Mount Brockman, together with some direct infiltration of rainfall. Discharge of groundwater takes place in three distinct ways. During times of high water levels, groundwater seeps directly into Koongarra Creek or into riparian seasonal wetlands. Direct soil evaporation accounts for a large part of the groundwater loss at these times. Transpiration from vegetation is significant during the entire year and is the dominant avenue of discharge during the late part of the dry season after Koongarra Creek has ceased to flow. The slow recession of groundwater levels during this season reflects use of water by plants.

During the wet season, when groundwater saturates the surficial sands, the water tends to flow through the zones of maximum sand thicknesses. Thus, the direction of the maximum hydraulic gradient will not in itself determine the direction of the maximum groundwater velocity. During the dry season, some of the thicker sands will still be saturated, but a greater portion of the groundwater flow will be through the partly weathered and fractured Cahill schist. The apparent anisotropy in these rocks should bend the groundwater flowlines in a more-or-less north-south direction, which would not correspond with the direction of the maximum groundwater gradient.

Most groundwater is undoubtedly discharged through the surficial sands during the wet season. The total groundwater moving below the residual clay in the upper part of the weathered schist may only be a small fraction of the wet-weather flow through the sand.

11 GROUNDWATER COMPOSITION AND COLLOID CHARACTERISATION

An extensive field measurement program to sample and measure the chemical parameters of groundwater at various locations and depths in the vicinity of the Koongarra No. 1 orebody was undertaken during the ARAP. Seven sampling programs were carried out at the end of the wet season, when water levels were high and at the end of the dry season, when water levels were at their lowest, in order to determine the extent of seasonal variations in water quality. Samples were normally obtained using submersible pumps located between packers to restrict the depth being sampled, or, in a few cases, using balers. A number of specially installed wells provided groundwater sampled from a depth of 13-15 m in the weathered zone and at 23-25 m in the unweathered rock. Figure 11.1 shows the location of boreholes used for the water sampling program.

Appropriate filtration, chemical treatment, and storage conditions were selected for the various samples, which were then transported to the laboratory for analysis. Measurements of the pH, redox state, conductivity, and bicarbonate alkalinity provided a starting point for interpreting water chemistry. Values of these parameters that may vary with water storage were measured in the field. Colloids and particles were also collected and analysed to study the relative importance of colloids and migration in true solution. The distributions of isotopes such as deuterium, tritium, ^{13}C and ^{14}C enabled groundwater mixing and flow paths to be studied.

Full details of the investigations of water quality are presented in Volume 7 of this series. All chemical and isotopic data are included in the Appendices to that Volume.

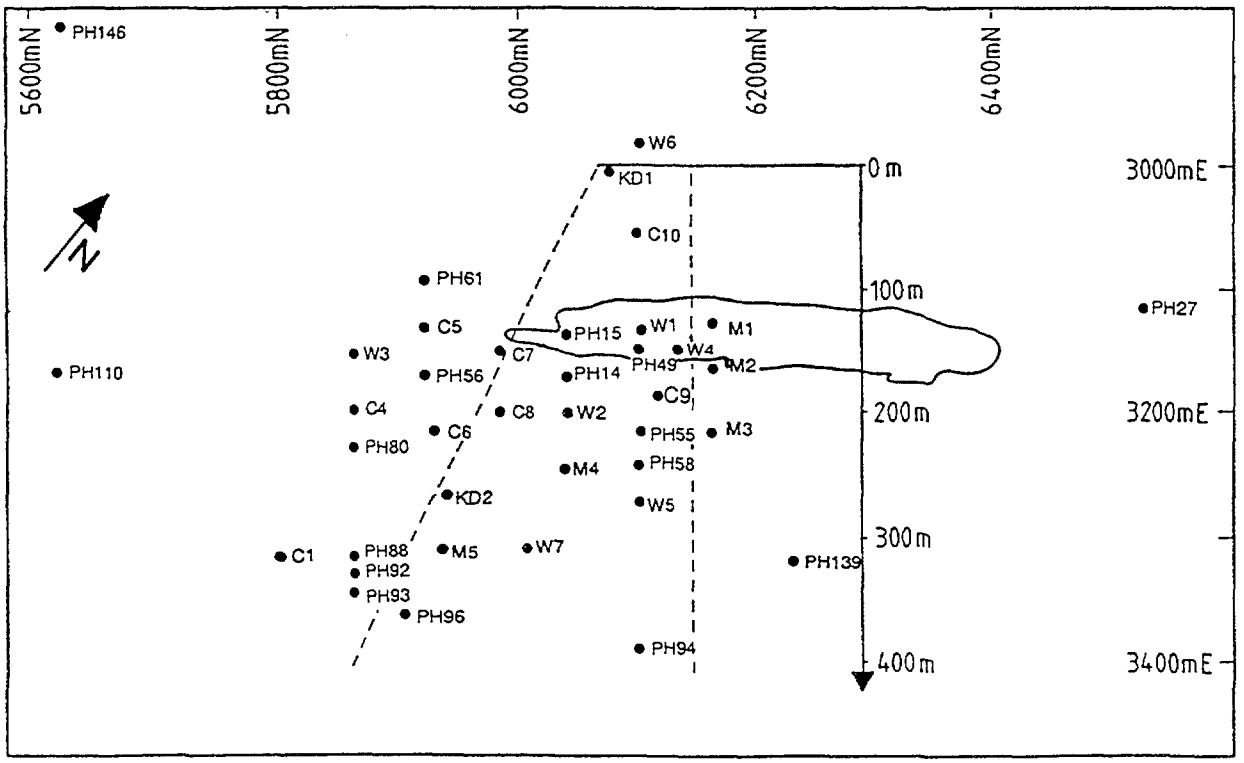

FIGURE 11.1 Koongarra plan showing the position of the primary orebody, boreholes sampled during the ARAP and the transect selected for projected cross-sections of groundwater chemistry (between dashed lines)

11.1 Groundwater Composition

Groundwaters exhibit characteristic compositions, depending on the location and depth of the sampling point. Selected parameters for a sample from near the centre of the orebody (borehole PH49), which shows the major features of water chemistry for a mineralised aquifer at Koongarra, are given in Table 11.1.

The main characteristics of this sample are:

- pH close to neutral
- low conductivity indicating a dilute groundwater with low levels of dissolved constituents
- magnesium as the dominant cation, reflecting the chlorite content of the host rock
- bicarbonate as the main anion

- elevated concentrations of uranium and radionuclides in its decay series
- low levels of total organic carbon
- slightly oxidising with respect to U^{4+}/U^{6+}, and
- significant levels of Si.

TABLE 11.1 CHEMICAL COMPOSITION OF A GROUNDWATER FROM THE NO. 1 OREBODY

Borehole	PH49
Depth	28-30 m
Date	May 1988
pH	6.74
Eh (mV)	+ 130
EC (µS/cm)	236
Mg^{2+}	26.4
Ca^{2+}	3.9
Fe^{2+}	0.8
K^{+}	0.7
Na^{+}	1.4
Si	8.9
HCO_3^{-}	154
Cl^{-}	3.7
F^{-}	0.2
PO_4^{3-}	0.310
SO_4^{2-}	2
U (µg/L)	274
TOC	1.5

Major components of Koongarra groundwaters, often measured at levels above 0.1 mg/L, include F, Na, Mg, Si, Cl, K, Ca, Mn, Fe, U, and HCO_3, SO_4 and PO_4. Measurable amounts of numerous other components present at trace levels (below 100 mg/L) included Ti, Br, Rb, I, W, V, Sr, Mo, Ba, and B.

The occurrence and distribution of major species at Koongarra are presented using both cross-sections and plan views in Volume 7 of this series. The contour plans consist of a map of the No.1 orebody showing the boreholes where groundwater samples from depths greater then 16 m were taken and a concentration contour of each parameter; an example for phosphate is shown in Figure 11.2. Cross-sectional views need to be considered in terms of the site geology (see Figure 6.1); an example of this presentation, again for phosphate, is shown in Figure 11.3.

In the centre of the No. 1 orebody, elevated levels of uranium and its decay products are present, with uranium concentrations in groundwaters up to four orders of magnitude higher than background levels. Groundwaters of the weathered zone are characterised by $^{234}U/^{238}U$ isotope ratios, which are often substantially below unity. These low isotope ratios are correlated to the ratios in accessible (readily leached) uranium of the solid phases. In the unweathered zone, where uranium is less mobile, the groundwater $^{234}U/^{238}U$ ratios generally exceed unity.

The chemistry of Koongarra groundwaters is a major factor influencing the mobility of uranium in the system. The pH and Eh conditions, together with the elemental composition of groundwater, determine the state of saturation with respect to the solid mineral phases that may potentially be present. In addition, the chemical speciation of uranium (which influences its adsorption behaviour) is a function of the concentrations of complexing ligands. Koongarra groundwaters are quite low in total organic carbon, therefore, inorganic species, such as carbonate and phosphate, are likely to be the main uranyl complexing agents (see below).

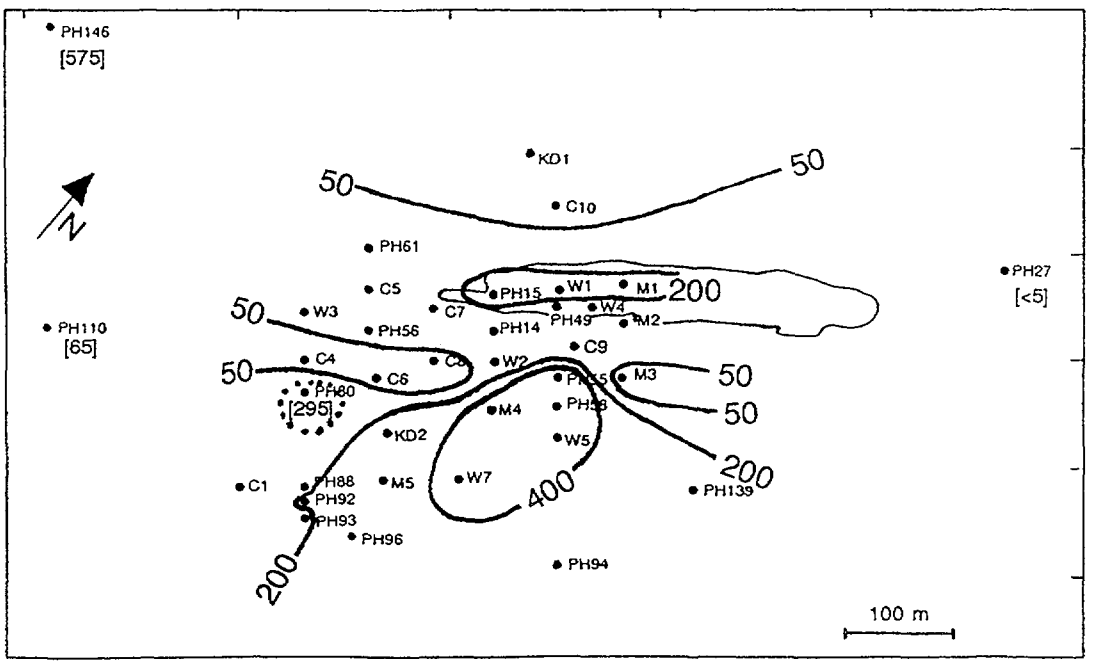

FIGURE 11.2 Phosphate in groundwater (µg/L) – contour plan. Contours in the vicinity of PH80 are uncertain.

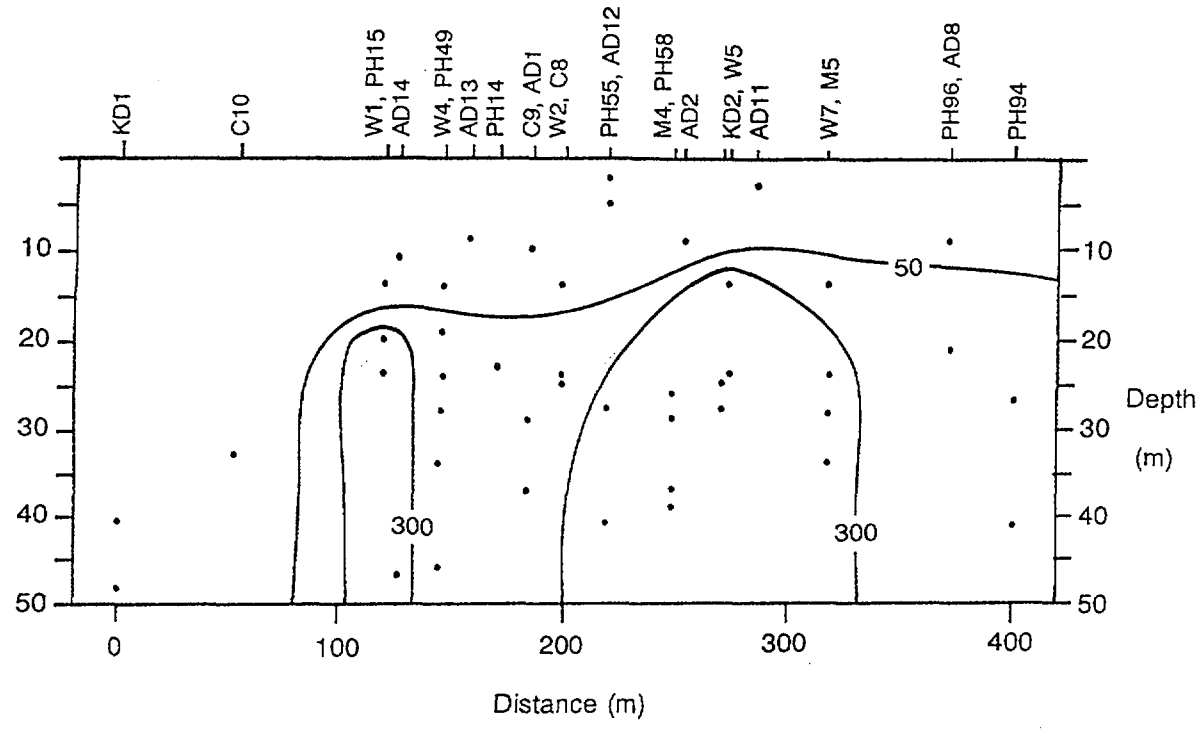

FIGURE 11.3 Phosphate in groundwater (μg/L) – projected cross-section

11.2 Depth Relationships and Seasonal Effects

It was found that the chemistry of the groundwater was being modified by water percolating downwards from the surface. This local recharge is seasonal, has low uranium content, pH and conductivity, and generally low levels of dissolved constituents such as phosphate; ie, is not greatly modified relative to rainwater. With the exception of changes occurring in shallow groundwaters from auger drillholes, there were no significant seasonal changes in groundwater chemistry; it was therefore decided that seasonal chemical changes did not need to be included in the modelling.

The data suggest that most uranium mobilisation occurs in the lower section of the weathered zone (or transition zone), where groundwater chemistry is characterised by high levels of bicarbonate, which complexes uranium. In this depth range, in the permanently saturated zone above the weathering front, $p(CO_2)$ is elevated relative to equilibrium with the atmosphere. Conductivity, Mg, and uranium levels are relatively high compared to shallow seasonal groundwaters, and the ^{14}C content of the dissolved inorganic carbon (DIC) is below 100% modern, although it rises gradually with distance away from the orebody. The pH is higher than the seasonal groundwaters (close to neutral), and the $^{234}U/^{238}U$ isotope ratio is generally substantially below unity.

In the unweathered zone, the groundwater chemistry is not strongly depth dependent, possibly because the layering dips very steeply. A major feature of this zone is $^{234}U/^{238}U$ exceeding unity, which is in contrast to the situation in the aquifer in the weathered zone.

11.3 Mineral/Groundwater Interactions

The groundwaters are all dilute waters with up to 150 mg/L total dissolved solids (TDS) dominated by Mg and HCO_3. Dissolved silica is a major constituent, reaching concentrations of 0.5 mM and often exceeding the concentration of the major cations. Bicarbonate ion dominates the anionic composition. Chloride concentrations are generally quite low and are slightly higher than the level expected in rainfall, suggesting only a slight degree of evaporation for the recharge waters. Magnesium, Ca and HCO_3 are enriched relative to chloride in the groundwaters and compared to their abundances in atmospheric deposition.

The release of alkaline earths and increased alkalinity results from mineral-solution reactions within the soil zone and within the aquifers themselves. The correlation between Mg and alkalinity (mostly HCO_3) indicates some common processes affecting Mg and the dissolved carbonate system. On the N-S transect along the line of inferred flow, both Mg and alkalinity are highest in the orezone but decrease down gradient of the orebody.

The types of mineral-solution reactions that most probably occur within the Koongarra groundwaters are induced by the action of CO_2 on carbonate or silicate minerals within the weathered zone or within the main aquifers. The source of the added CO_2 may be from degradation of plant material and root respiration within the soil zone, or CO_2 produced *in situ* within the aquifer from degradation of sedimentary organic matter by bacteria.

Closer to the orebody, the groundwater cation chemistry is dominated by Mg, and substantial levels of Si and HCO_3 are also present. Weathering dissolution of chlorite by CO_2-charged groundwaters would release Mg, and SiO_2, while increasing alkalinity by consuming protons to convert CO_2 to bicarbonate. Hence, the major ion chemistry of Koongarra groundwaters is consistent with the weathering of minerals such as chlorite to ultimately form kaolinite (see also Sections 13 and 16, and Volumes 9 and 12 of this series).

11.4 Colloid Characterisation

Two sampling systems were used to concentrate colloids from the groundwater. In the first, large volumes (1000 L) of prefiltered groundwater were processed using a hollow fibre ultrafiltration system to maximise the amount of colloidal material available for chemical and physical analysis. In the second approach, much smaller volumes (600 mL) were ultrafiltered through flat membranes in a stirred cell.

The total amount of ^{238}U and ^{230}Th carried by unfiltered groundwater and passing through successive filters is shown in Figure 11.4. The majority of uranium was present in true solution that passed through the ultrafilter, rather than as colloids, and is probably present as uranyl carbonate complexes. In contrast, thorium was almost entirely found in large particles > 1 mm that are normally immobile in the Koongarra system and result from pumping the boreholes. However, of the small amount of ^{230}Th that passes through a 1.0 mm filter, a significant proportion is associated with colloidal particles. These mostly consist of fine quartz grains, and iron oxides and clay minerals, particularly kaolinite and chlorite, which carry a small proportion of the uranium in the system.

In some fine particle and colloidal fractions, the $^{227}Th/^{230}Th$ activity ratio in the thorium alpha spectrum was unusually high, indicating the presence of substantial quantities of ^{227}Ac. This suggests that actinium could be present as a mobile colloid phase. Actinium appears to be slightly more mobile than thorium and is associated with colloids to a greater extent, although generally present in low concentrations. The results for Th(IV) and Ac(III) suggest possible colloidal transport of trivalent and tetravalent actinides in the vicinity of a nuclear waste repository.

11.5 Summary

The groundwater chemistry and isotopic composition suggests that a proportion of the groundwater which enters the region of the No.1 orebody originates from fractures in the Kombolgie sandstone and moves across the fault zone. However, downward infiltration in the fault zone, and in the region between the fault and the orebody, appears to be a major source of groundwater entering the flow system of the orebody. The groundwater that enters the orebody is characterised by low levels of ^{14}C, high $p(CO_2)$, low pH and is depleted in ^{2}H.

Groundwaters in the centre of the orebody have elevated levels of uranium and its decay products are present, with uranium concentrations in groundwaters up to four orders of magnitude higher than background levels. Groundwaters of the weathered zone are characterised by $^{234}U/^{238}U$ isotope ratios, which are often substantially below unity. These low isotope ratios are correlated to the ratios in accessible (readily leached) uranium of the solid phases. In the unweathered zone, the groundwater $^{234}U/^{238}U$ ratios generally exceed unity. Thorium is virtually immobile in the Koongarra system. The uranium in the groundwater occurs in true solution, rather than as colloids, and is probably present as uranyl carbonate complexes. Overall, colloidal transport of radionuclides is believed to be of minor importance, although there is some association of both actinium and thorium with colloids

After passing through the orebody, the groundwater chemistry and isotopic composition is further modified by mixing with local recharge, which permeates through the surficial sand and clay layers causing mixing and dilution. Hence, moving down-gradient, there is a gradually reducing $p(CO_2)$ and simultaneous increase in ^{14}C content, together with a change of $\delta^{2}H$ to less negative values.

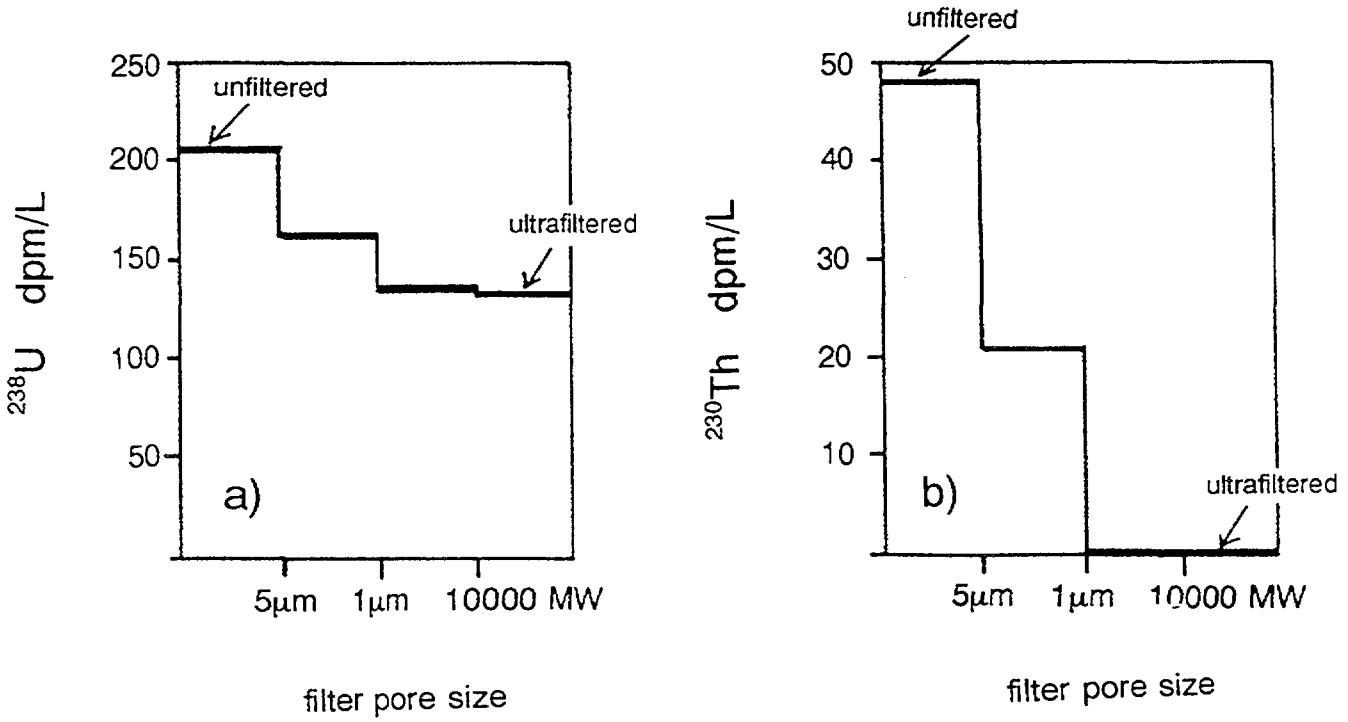

FIGURE 11.4 Effect of filtration on radionuclide levels in groundwater: (a) ^{238}U, (b) ^{230}Th

Down gradient, the groundwater chemistry directly south (towards PH88) closely resembles that in the orebody zone. This is reflected in factors such as its magnesium content, conductivity, bicarbonate concentration, and concentration of uranium (Figure 11.5) and in its decay products such as radium, radon and ^{210}Pb (Figure 11.6). These factors suggest that groundwater movement could occur in this direction. This is a slightly different direction to the main extent of the dispersion fan, which extends more towards the southeast. Thus, present groundwater flow paths may well include a component towards PH80 or PH88, which is at an angle to the flow inferred from the extent of the secondary uranium mineralisation, which extends more perpendicularly away from the fault.

The data suggest that most uranium mobilisation occurs in the lower section of the weathered zone (or transition zone). In this depth range, in the permanently saturated zone above the weathering front, the $p(CO_2)$ is elevated relative to equilibrium with the atmosphere. Conductivity, Mg, and uranium levels are relatively high compared to shallow seasonal groundwaters, and the ^{14}C content of the DIC is below 100% modern, although gradually rising, moving away from the orebody. The pH is higher than the seasonal groundwaters which are close to neutral, and the $^{234}U/^{238}U$ isotope ratio is generally substantially below unity.

In the unweathered zone, the groundwater flow could be through fractures. However, uranium transport is not as great in this zone and radium migration is more likely. In this zone the groundwater chemistry is not strongly depth dependent. A major feature is $^{234}U/^{238}U$ exceeding unity, in contrast to the aquifer in the weathered zone.

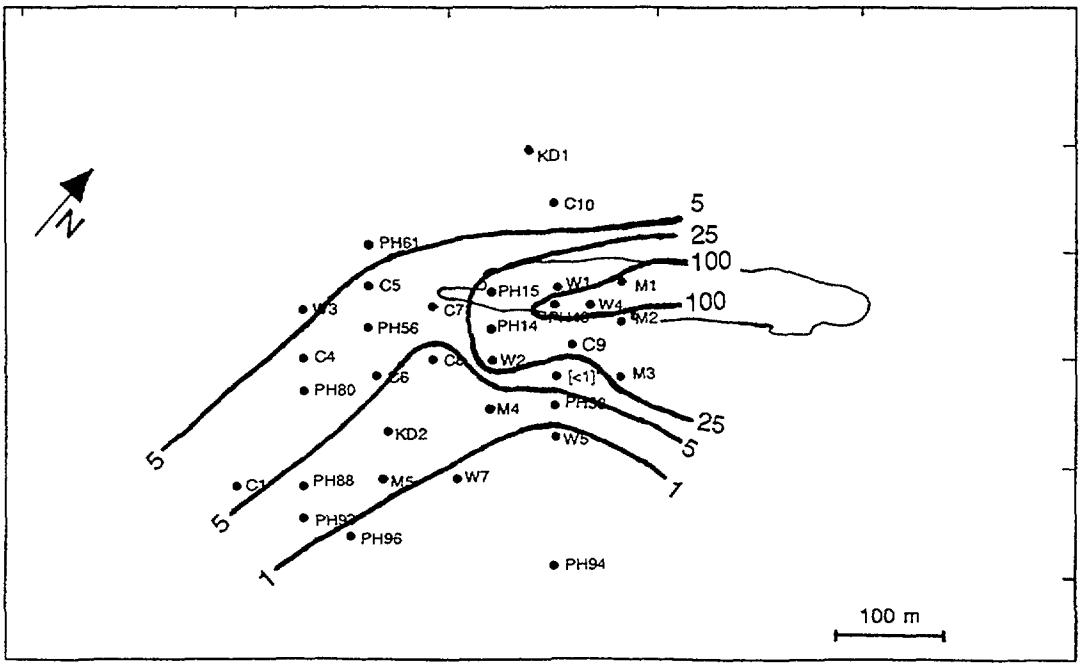

FIGURE 11.5 Contour plan of uranium concentrations in groundwater (μg/L). The anomalously low value for PH55 (< 1 μg/L) is shown. This point was excluded in drawing the contour lines.

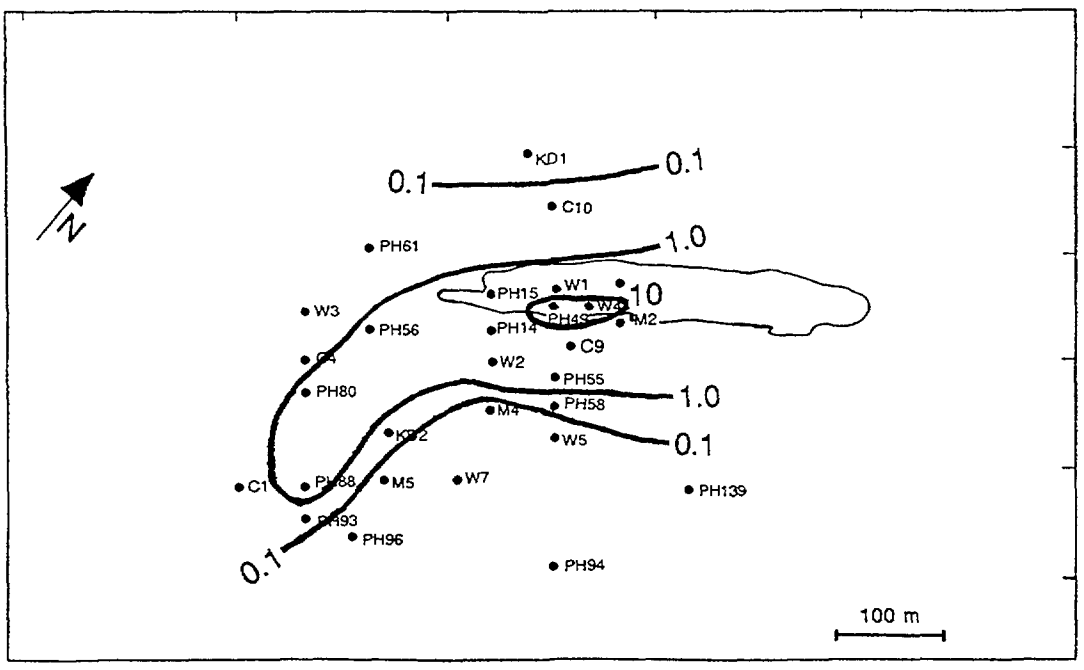

FIGURE 11.6 Pb-210 in groundwater (Bq/L) – contour plan

12 THE SOLID PHASE

An extensive study of the chemistry and mineralogy of the solid phase was carried out to review all available data from previous studies and, with a range of techniques, analyse a large selection of materials sampled during the ARAP. This has resulted in information relevant to the migration of radionuclides over long timescales, and particularly that of uranium in the vicinity of the Koongarra No. 1 orebody. In addition to site specific information, more universally applicable data have been collected on:

- the importance of the early stages of weathering in radionuclide transport
- the behaviour of uranium in weathered environments and the development of isotopic disequilibria under such conditions
- the behaviour of rare earth elements, and
- the associations of uranium with mineral phases.

These data, and those discussed already for groundwater, provide a geochemical framework of the Koongarra system that can be used to develop and test transport and geochemical models. The framework can also be used to realistically evaluate the transferability of the results to other systems.

Details of the chemistry and mineralogy of the solid phase are provided in Volume 8 of this series.

12.1 Mineralogy and Chemistry

12.1.1 Primary ore

The primary ore consists of uraninite (or pitchblende, i.e. uranium oxide) veins and veinlets (1 to 10 mm thick) that crosscut the foliation of the brecciated and hydrothermally altered host schist. Groups of uraninite veinlets are intimately intergrown with chlorite, which forms the matrix to the host breccias within the schist. Small (10-100 μm) euhedral uraninite grains are finely disseminated in the chloritic alteration adjacent to veins, but these grains may coalesce to form clusters, strings and massive uraninite. The Appendices of Volume 2 of this series list representative analyses of Koongarra chlorites, uraninites, sulfide minerals, bulk drill core assays, uranium-lead oxides, uranyl silicates and uranyl phosphates.

Associated with the ore are minor volumes (up to 5%) of sulfides; these include galena (PbS) and lesser chalcopyrite ($CuFeS_2$), bornite (Cu_5FeS_4) and pyrite (FeS_2), with rare grains of native gold, clausthalite (PbSe), gersdorffite-cobaltite ((Ni,Co,Fe)AsS) and mackinawite $((Fe,Ni)_{1.1}S)$. Galena is the most abundant, commonly occurring as cubes (5 to 10 μm wide) disseminated in uraninite or gangue, and as stringers and veinlets particularly filling thin fractures within uraninite. Galena may also overgrow clausthalite, and replace pyrite and chalcopyrite. Chalcopyrite occurs as irregular to rounded grains 10 to 100 μm in diameter, frequently with other sulfides, but occasionally as small inclusions within uraninite itself or in chlorite-filled fractures within uraninite. Pyrite is ubiquitous in the

host schist but occurs more sparsely in the primary ore, where small rounded grains are disseminated in the gangue in proximity to uraninite. Occasionally there are larger crystals, grains and masses.

Chlorite, predominantly magnesium-rich chlorite, is the principal gangue, and its intimate association with the uraninite indicates that the two minerals formed together. Rutile (TiO_2) may comprise up to 5% by volume of the ore. Hematite is not a common gangue phase, but may occur as a selvage (less than 2 mm thick) to some of the thicker (more than 3 mm) uraninite veins in the high grade ore zone immediately below the hanging wall graphitic unit. Hematite is also present in the breccia in the reverse fault at Koongarra, and in the schist immediately above.

12.1.2 Secondary mineralisation

One of the most important features of the uranium mineralisation at Koongarra is the occurrence of abundant secondary uranium minerals. These occur principally within the dispersion fan above the No. 1 orebody, but also to a lesser extent within the top of the primary ore zones just below the weathered zone, and at the bottom of the primary zones along and just above the fault.

Oxidation and alteration of uraninite within the primary ore zone have produced a variety of secondary uranium minerals, particularly the uranyl silicates kasolite ($Pb(UO_2)SiO_4.H_2O$), sklodowskite ($Mg(UO_2)_2\ Si_2O_7.6H_2O$) and uranophane ($Ca(UO_2)_2Si_2O_7.6H_2O$). Uraninite veins, even veins over 1 cm wide, have been completely altered *in situ*. Some uraninite veins are concentrically sheathed outwards by the uranium-lead oxides vandendriesscheite ($PbO.7UO_3.12H_2O$), fourmarierite ($PbO.4UO_3.4H_2O$), curite ($2PbO.5UO_3.4H_2O$), and sklodowskite. Other veins are partially or totally replaced by intergrown uranyl silicates. Uranophane and sklodowskite, remote from any parent uraninite, are also found as veins and stringers within fractures, between grain boundaries and within mica cleavage planes. Within fractures sklodowskite has also crystallised as aggregates of radiating acicular (needle-like) crystals, with chlorite as the infilling matrix. Within the primary ore zone this *in situ* replacement of uraninite is most pronounced immediately above the reverse fault breccia, and this alteration and oxidation diminish upwards toward the high grade ore beneath the hanging wall graphitic schist unit (Figure 6.1). Extensive *in situ* replacement of uraninite by uranyl silicates has also occurred where the high grade ore is intersected by the transitional zone to the weathered schists.

The secondary mineralisation of the dispersion fan in the weathered schists above the No.1 orebody is characterised by uranyl phosphates, particularly saleeite ($Mg(UO_2)_2(PO_4)_2.8H_2O$), metatorbernite ($Cu(UO_2)_2(PO_4)_2.8H_2O$) and renardite ($Pb(UO_2)(PO_4)_2(OH)_4.7H_20$), which is found exclusively in the tail of the fan. Much of this phosphate-bearing tail has been shown to be weathered and leached primary ore and was originally, before weathering, the up-dip continuation of the present primary ore lenses. Away from the tail of the dispersion fan uranium is dispersed in the weathered schists and apparently adsorbed onto the surfaces of clay and iron oxide minerals.

In the top of the No. 2 orebody, which has no secondary dispersion fan, only uranyl silicates have been found. This contrasts with the pattern in the No. 1 orebody, where uranyl phosphate minerals are found in the tail of the secondary dispersion fan, both in, and down gradient from, what was the upwards extension of the primary ore zone. Uranyl silicates are, however, found either in the primary ore zone below or at the interface between the two.

12.2 Distribution of Minerals and Uranium

An extensive database of uranium concentrations at Koongarra was compiled from the drilling logs (Noranda, unpublished) and an extensive measurement program undertaken by the ARAP. The data are reported in Appendix 4 of Volume 8 of this series. The scale of the redistribution of uranium from the primary ore body was visualised by drawing contour maps of the distribution of uranium concentrations in plan-view and cross-section. An example can be seen in Figure 12.1, where the 100 mg/g uranium contour line is shown in plan-view for three depths:

- 35-40 m (unweathered zone)
- 15-20 m (deep weathered zone), and
- 5-10 m (shallow weathered zone).

Concentrations in excess of 100 mg/g in the unweathered rock were only detected in the vicinity of the ore body. Leaching and deposition of uranium is strongly linked to the weathering process and uranium concentrations are increased in the weathered and transition zones for at least 300 m from the source. The spatial contours of uranium concentration in the weathered zone show that concentrations of high-grade uranium have migrated in the weathered schist from the primary zone towards the southeast direction. However, a more extensive dispersion fan of uranium (not ore grade but above background levels) is detected towards the south of the orebody, about 300 m from the primary source. This distribution is clearly similar to that identified from the groundwater chemistry and the geophysical measurements (see above), both of which also suggest a present-day southerly direction of flow from the orezone.

Figure 12.2 shows the uranium concentration contour for the Mine Grid Section 6109 mN, which has been used in many of the transport modelling studies discussed in Section 17. It can be seen that at the extremity of the uranium redistribution most of the enrichment occurs near the surface. Outside the zone of primary mineralisation there is an abrupt uranium concentration boundary between the weathered and unweathered zones. This is evidence that the uranium found in the weathered zone SW-SSW of the primary deposit was indeed deposited, and not simply inherited from the parent rock. The most important zones of enrichment appear to be near the base of weathering, and in the very shallow zone. The shallow component appears to be more widespread than the deeper component; however, it accounts for only a small proportion of the mobilised uranium detected.

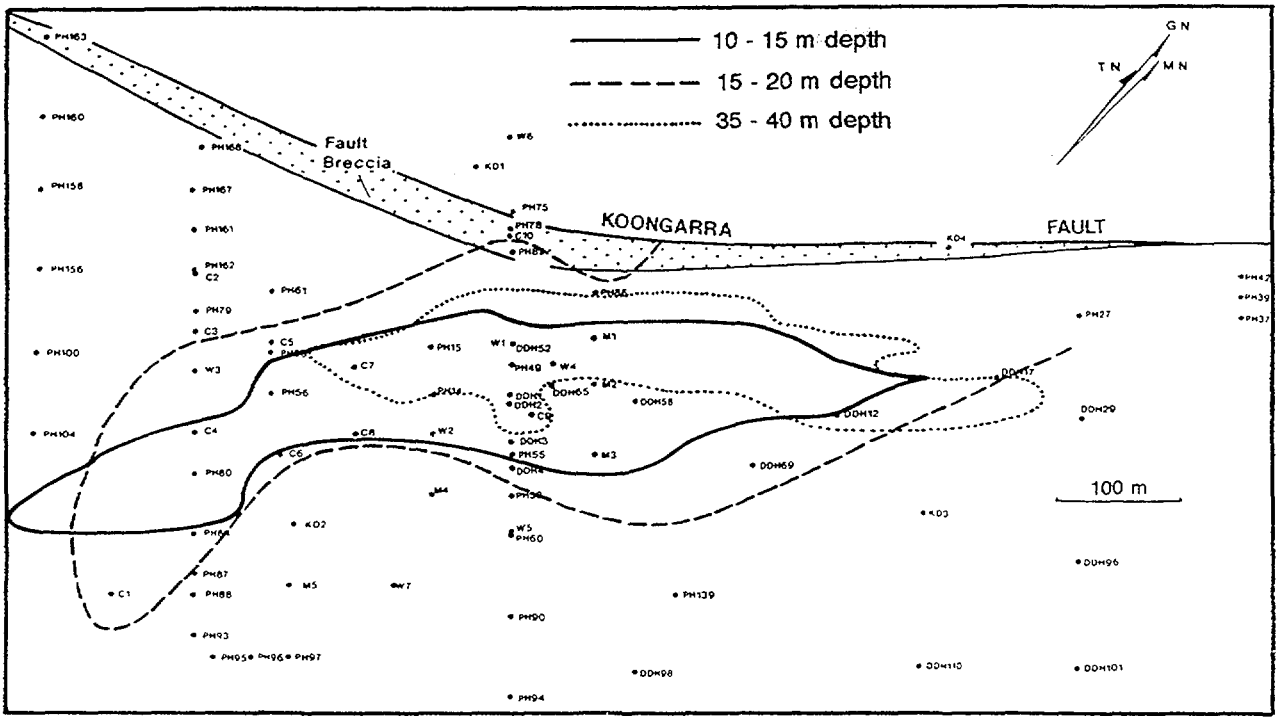

FIGURE 12.1 Contour lines of uranium concentration µg/g at three depths.

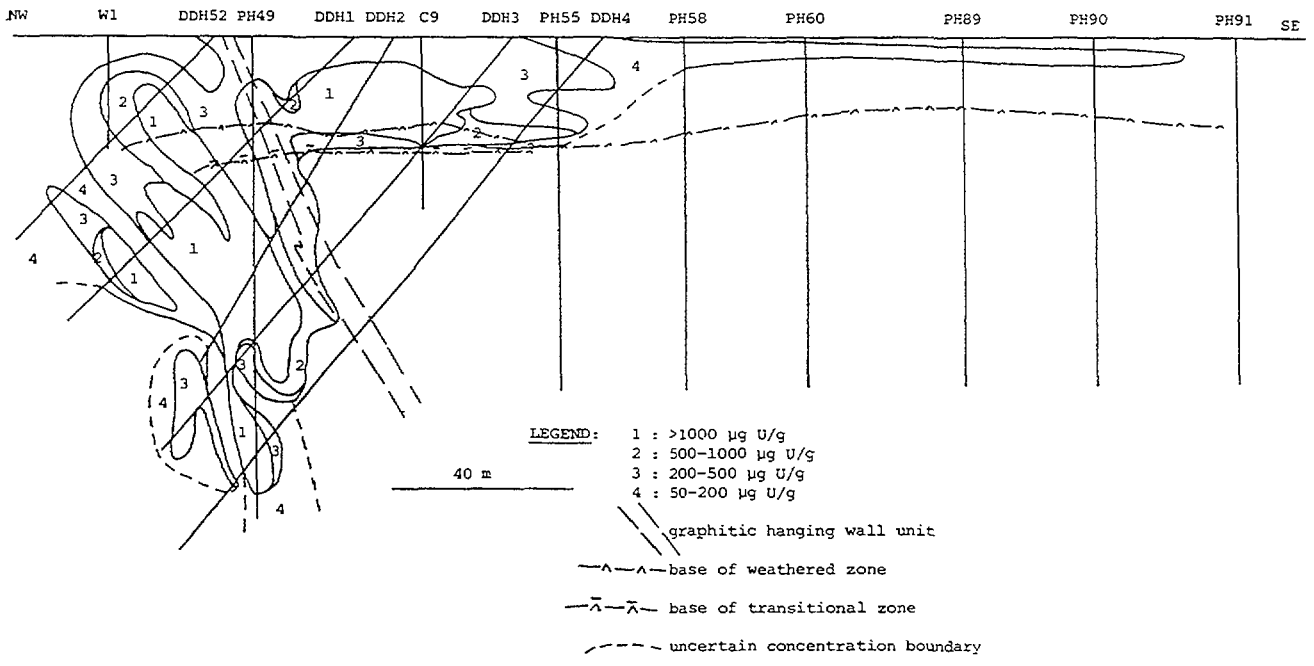

FIGURE 12.2 Contours of uranium concentration in Section 6109 mN

12.3 Rock and Soil Chemistry

In the weathered zone above the primary orebody, where quartz and chlorite dominate, kaolinite is the only significant clay mineral above a thin layer of vermiculite near the base of weathering. Down gradient, where the degree of chloritisation of the rock is less, smectite also becomes a significant weathered zone component. The iron oxides detected at Koongarra are goethite, haematite and ferrihydrite, and they occur as fissure and remnant schistosity coatings, dispersed clay coatings, and nodules. The different forms probably play different roles in the capture and storage of otherwise labile species (see below).

The abundance of iron oxides is very variable over a scale of centimetres, with occasional bands of bleached clay juxtaposed with iron rich bands. The greatest heterogeneity in the distribution of iron appears to be with the crystalline phases. The concentration of ferrihydrite, estimated by chemical extraction, was between 43 and 145 mg/g, making up 4-48 % of the total iron. Lithiophorite is the only manganese mineral identified in the weathered zone, and mainly occurs coating fissures and remnant schistosity. The material coating potential transport pathways is well placed for contact with migrating species.

12.4 Uranium-mineral Associations

In the unweathered zone, uranium appears to be associated with niobium, molybdenum, lead and nickel, but not with any major rock-forming element. In the weathered zone, uranium correlates with phosphorus in the uranyl phosphate zone, and with iron and other iron oxide associated elements further down gradient. The concentrations of phosphorus within the uranyl phosphate zone were not significantly greater than elsewhere, suggesting that a phosphorus concentration anomaly does not explain the distribution of uranyl phosphates. The main source of phosphorus at Koongarra is probably fluorapatite.

The area of primary mineralisation is characterised by strong relative enrichment of heavy rare earth elements, compared to the regional host rock. The heavy rare earth elements are also those most accessible to the groundwater, and may therefore be preferentially transported. On the basis of phase selective chemical extractions, cerium, in comparison to other rare earth elements, appears to be preferentially taken up into inaccessible phases, probably into oxides of iron and manganese.

Uranium-mineral associations were studied using various microscopic and chemical techniques. In the weathered zone, uranium appears to be associated with secondary oxides of iron and manganese. The relationship with the iron oxide appeared to be of a diffuse nature, suggesting that sorption was the initial mechanism for association. However, within the manganese phases, uranium is associated with hot spots containing mainly a cerium oxide or hydroxide phase (Figure 12.3). The mechanism for the cerium-uranium association is not entirely clear, but probably involves a redox interaction between manganese and cerium.

Measurements were also made on rock phases resulting from sequential extractions. The procedures used are summarised in Table 12.1 and a detailed description is given in Volume 8 of this series.

TABLE 12.1

SUMMARY OF SEQUENTIAL EXTRACTION PROCEDURE

Reagent	Minerals Dissolved	Extraction Conditions
1) Morgan's solution 1M NaOAc adjusted to pH 5.0 with HOAc	Carbonate minerals, adsorbed trace elements	40 mL/g sample, shaken for 4 hours
2) Tamm's acid oxalate (TAO) 10.9 g/L oxalic acid + 16.1 g/L ammonium oxalate pH 3.0	Adsorbed trace elements, amorphous minerals of Fe, Al and Si (e.g. ferrihydrite), secondary uranium minerals	40 mL/g sample, shaken in the dark for 4 hours
3) Citrate dithionite bicarbonate (CDB) 0.3M tri-sodium citrate, 0.2M sodium hydrogen carbonate, 1 g/g sample sodium dithionite, pH 8.5	Crystalline iron oxides, hydroxides and oxy-hydroxides	60 mL/g sample, stirred for 30 min. at 85°C, filtered and repeated
4) 6M HCl	Clay minerals (vermiculite, smectite, kaolinite), uranium oxides	Stirred for 2 hours at 85°C
5) Digestion (and fusion)	Remaining resistant minerals (quartz, muscovite)	HF/$HClO_4$ digestion, sodium carbonate/borax fusion

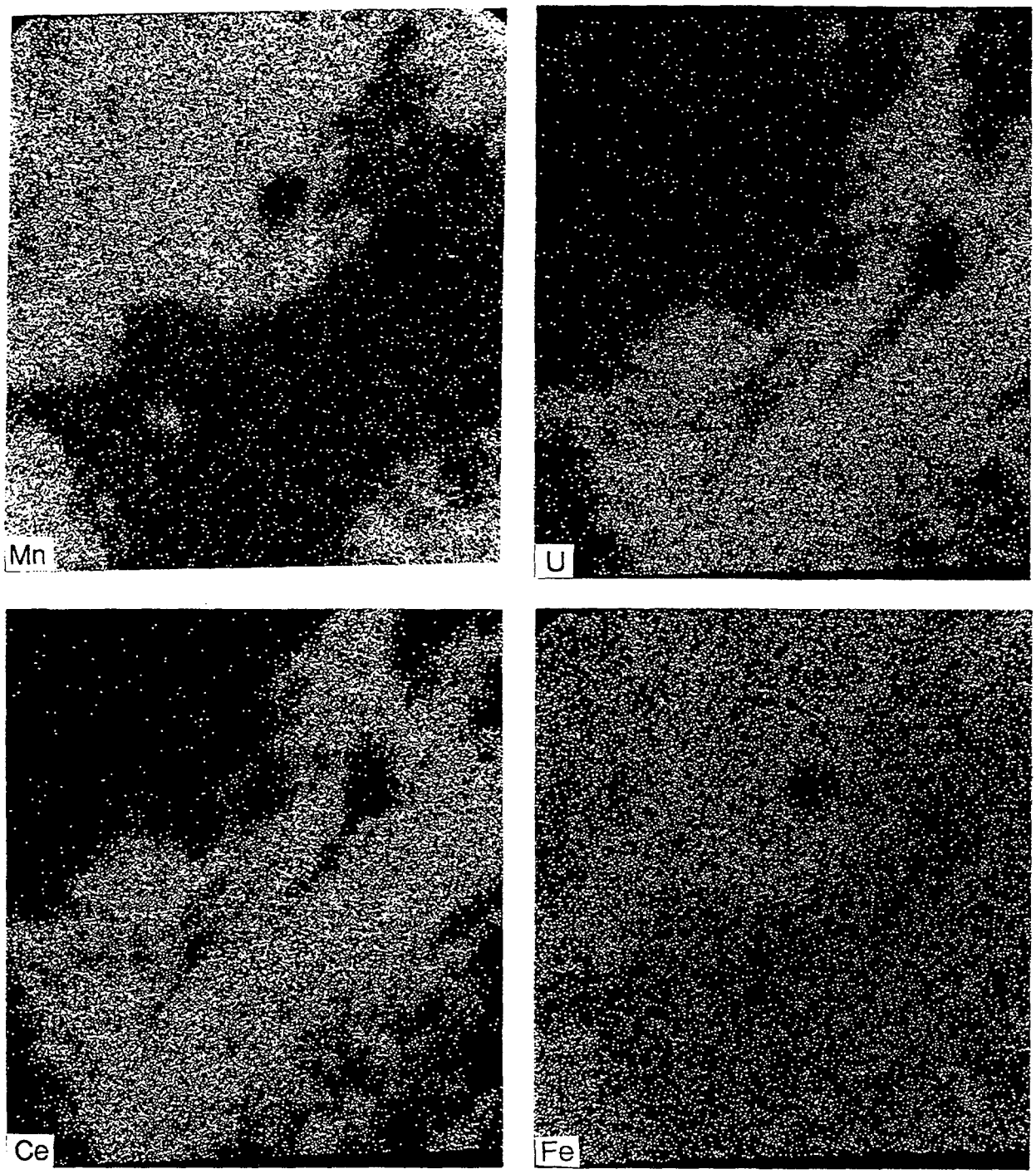

FIGURE 12.3 X-ray maps of Mn, U, Ce and Fe from a manganese-rich area from M2 at 17 m depth. The width of the micrograph area is 62.5 μm.

The phase selective extraction schemes showed that the uranium in the weathered zone is mainly accessible to the groundwater (adsorbed or associated with amorphous phases, 10-73 %), or entrapped within crystalline iron oxides (< 27-82%). The form of the uranium in the crystals is unknown.

The degree of uranium migration into the matrix from fissures was studied in rock showing various degrees of weathering, with changes in uranium concentration from fissures estimated on the basis of electron microprobe line scans, spot analyses, changes in α-track density, etc. Measurements on unweathered rock showed that there had been very little penetration of uranium into the quartz matrix and an apparent diffusivity of 10^{-24} m^2s^{-1} was estimated. This suggested that matrix diffusion is a minor factor in the retardation of uranium migration and would have been insignificant over the timescale of concern for repositories. In weathered rock samples, material adjacent to or infilling fissures generally contained much more uranium than the matrix. This suggested that associations of uranium with fissures were a result of redox properties at the fissure surfaces determining the distribution of sorbing phases.

12.5 Uranium Disequilibria

An extensive measurement program for uranium series disequilibria was also conducted on Koongarra core and pulp material, particularly from the weathered zone. The degree of disequilibria was determined for bulk whole rock, chemically defined phases resulting from extraction schemes, mineralogically distinct zones and secondary uranium minerals. The isotopes most frequently considered were ^{238}U, ^{234U} and ^{230}Th, with some analyses of ^{235}U, ^{226}Ra, ^{210}Pb and ^{232}Th. The resulting database was used to test radionuclide transport models discussed in Section 17.

In the unweathered zone, the ore material and the host rock were at approximate secular equilibrium, except for a small apparent depletion of ^{226}Ra. In the weathered rock above the primary mineralised zone, high $^{230}Th/^{234}U$ activity ratios indicate strong recent leaching of uranium. In these leached areas the $^{234}U/^{238}U$ activity ratios are high, above unity in the bulk rock and near unity in the accessible phases. The most intensely leached samples came from near the surface, near the up flow boundary above the primary ore.

The most intense recent accumulation of uranium appears to have occurred about 0-50 m from the down flow boundary of primary ore, particularly near the base of weathering. This highlights the importance of the early stages of weathering to the migration and retardation of uranium. At distances greater than about 100 m from the primary ore, uranium deposition occurs SSW of the deposit and is most pronounced near the surface.

It appears that the onset of weathering conditions caused the rapid dissolution of the primary uranium minerals, resulting in the congruent liberation of ^{238}U and ^{234}U. This was followed by preferential entrapment of ^{234}U from solution and accessible sites resulting in preferential mobility of ^{238}U which leads to high $^{234}U/^{238}U$ activity ratios in leached samples and low ratios in depositional samples, down gradient. Beyond

about 50 m down gradient, where the uranium content of groundwater and accessible phases is low, uranium mobilised from the primary ore makes a smaller contribution to the total accessible uranium. It is suggested that where the uranium content in accessible phases is high, then the accessible (or solution) $^{234}U/^{238}U$ activity ratio will tend to decrease with time or distance due to preferential retardation of ^{234}U. However, where the accessible phase uranium content is low, and a major source of the accessible uranium is resistant minerals, then the accessible $^{234}U/^{238}U$ activity ratio will tend to increase due to preferential leaching of ^{234}U.

The results of sequential extractions showed that most of the uranium in the dispersion fan is accessible or entrapped by crystalline iron oxides, with the crystalline phases containing higher $^{234}U/^{238}U$ activity ratios than accessible phases. This indicates an isotopic fractionation mechanism, which involves iron oxides. The high activity ratios in these essentially chemically inert phases suggest that α-recoil emplacement of ^{234}Th is a significant process occurring at Koongarra. Other mechanisms may also be operating to reduce the mobility of ^{234}U, however processes related to the chemistry of ^{234}Th need to be rapid.

12.6 Partitioning of Uranium and Thorium

The partition coefficient (P) for a radionuclide bound by a solid phase is defined as:

$$P = \frac{\text{amount of radionuclide bound by solid per unit mass}}{\text{amount of radionuclide in solution per unit volume}}$$

The distribution ratio K_d is defined similarly to P, except that it refers strictly to adsorbed species only. The distribution ratio R_d, defined similarly to K_d, is more appropriate in cases where equilibrium may not be achieved, such as in laboratory experiments.

In Volume 8 of this series, groundwater concentrations and $^{234}U/^{238}U$ activity ratios were compared to those in bulk rock near the groundwater sampling position and, when available, in accessible phases of the solid material. Comparisons between groundwater and entrained particles were also made. Some examples of the results are provided below.

12.6.1 Partitioning of ^{230}Th between groundwater and bulk rock

Table 12.2 shows a comparison of ^{230}Th concentrations in groundwaters and nearby core samples. Thorium concentrations for groundwaters, and reported values for solid-phase (crushed rock) samples from the vicinity of the water sampling location were compared. The resulting bulk partition values (P_B total rock/groundwater) were extremely high (2×10^5 to 2×10^8 mL/g), reflecting the levels of dissolved ^{230}Th in these groundwaters, which bordered on detection limits.

TABLE 12.2

COMPARISON OF ^{230}Th ACTIVITY IN GROUNDWATER AND ROCK (ASSUMING APPROXIMATE EQUILIBRIUM BETWEEN ^{238}U AND ^{230}Th IN THE ROCK)

Hole/Depth (m)	^{230}Th water (dpm/L)	[U] rock (µg/g)	^{230}Th rock (dpm/g)	P_B ^{230Th} (mL/g)
PH14 <26	0.0014 (.0011)	~500	~370	~2.6 10^8
PH14 <30	0.0034 (.0011)	~500	~370	~1.1 10^8
PH49 28-30	0.050 (.005)	~6000	~4450	~8.9 10^7
PH49 44-46	0.036 (.006)	~810	~600	~1.7 10^7
PH55 40-42	0.001 (.005)	3	2.2	2.2 10^6
PH56 26-28	<0.0017	32	24	>1.4 10^7
PH61 43-45	0.0024 (.0022)	8	6	2.5 10^6
PH88 38-40	0.0055 (.0017)	4	3	5.5 10^5
PH94 40-42	0.0052 (.0012)	3	2.2	4.2 10^5
PH96 <26	0.0114 (.0025)	2	1.5	1.7 10^5

Data is also available for the partitioning of ^{230}Th and ^{238}U between groundwater and entrained particles, and of ^{238}U partitioning on < 10 µm size particles.

12.6.2 Partitioning of uranium between groundwater and bulk rock

Averaged bulk rock ^{238}U contents compared with groundwater from the same borehole/depth are shown in Table 12.3. The bulk partition coefficients (P_B) were estimated only for points where the occurrence of uranium minerals was unlikely. This was done to minimise the inclusion of very large amounts of uranium not accessible to the groundwater. The range of P_B values for this data set is from 1.0×10^3 to 4.5×10^4 mL/g.

The W-holes were constructed for the purpose of obtaining water and core samples from the same location within the dispersion fan. Hence, these data probably provide the best distribution data so far obtained at Koongarra.

12.6.3 Partitioning of ^{238}U between groundwater and rock accessible phases

It was also possible to compare the groundwater with different chemically defined phases of the solid substrate to see if the ^{234}U/^{238}U activity of a particular component of the solid material reflects an interaction with the groundwater. Table 12.4 shows this comparison. The amount of uranium accessible for interactions with the groundwater was estimated using a Tamms acid oxalate extraction. The

comparisons could only be made where the rock sample was weathered and contained no uranium minerals.

TABLE 12.3

BULK PARTITION COEFFICIENT (P_B) BASED ON TOTAL ROCK URANIUM CONCENTRATIONS

Hole	Depth (m)	[U] Rock	[U] Water	P_B (mL/g)
PH56	43-45	7	7	$1.0\ 10^3$
W2	14	46	43.4	$1.1\ 10^3$
W2	24	100	85	$1.2\ 10^3$
PH61	43-45	6	3.47	$1.7\ 10^3$
PH58	25-27	4	1.82	$2.2\ 10^3$
W5	24	3	1.3	$2.3\ 10^3$
PH61	26-28	8	3.44	$2.3\ 10^3$
PH88	38-40	8	3.14	$2.5\ 10^3$
W4	14	1418	441	$3.2\ 10^3$
PH56	26-28	32	9.69	$3.3\ 10^3$
PH55	40-42	4	1.02	$3.9\ 10^3$
PH58	38-40	3	0.76	$3.9\ 10^3$
PH49	44-46	809	199	$4.1\ 10^3$
W1	24	250	60.4	$4.1\ 10^3$
W3	24	9.2	1.6	$5.8\ 10^3$
W7	13	7.1	1	$7.1\ 10^3$
PH96	26	2	0.28	$7.1\ 10^3$
W7	24	3	0.42	$7.1\ 10^3$
PH94	40-42	3	0.38	$7.9\ 10^3$
PH88	28-30	22	2.52	$8.7\ 10^3$
W5	13	3.5	0.4	$8.8\ 10^3$
PH55	26-28	5	0.5	$1.0\ 10^4$
PH94	26-28	2	0.2	$1.0\ 10^4$
PH14	21	670	65	$1.0\ 10^4$
W3	14	60	5.5	$1.1\ 10^4$
PH80	20	89	7.8	$1.1\ 10^4$
W4	24	5441	348	$1.6\ 10^4$
PH14	26	548	31	$1.8\ 10^4$
W1	13	278	6.2	$4.5\ 10^4$

While only five data points are available, there does appear to be a strong linearity between uranium concentrations in the groundwater and accessible phases of the rock. The accessible phase partition coefficient (P_A) was almost constant over a large range of uranium concentrations, mineral components, and groundwater chemistries. This, along with the similar $^{234}U/^{238}U$ activity ratios in groundwater and accessible phases, suggests exchange between the two phases.

TABLE 12.4

COMPARISON OF URANIUM CONCENTRATION AND ACTIVITY RATIO BETWEEN BULK ROCK, ACCESSIBLE PHASES (TAO-EXTRACTABLE) AND GROUNDWATER

Hole	Depth	Total rock		TAO-extractable		Water		P_A
	(m)	[U] (µg/g)	$^{234}U/^{238}U$	[U] (µg/g)	$^{234}U/^{238}U$	[U] (µg/L)	$^{234}U/^{238}U$	(mL/g)
W1	24	250	1.0	28	0.86	60	0.78	460
W2	14	46	0.86	21	0.67	43	0.65	480
W4	14	1418	0.91	239	0.80	441	0.81	540
W5	13	3.5	0.94	0.3	1.4	0.4	0.88	800
W7	13	7.1	0.98	1.0	0.86	1.0	0.88	1000

12.6.4 Conclusions on partitioning

A large number of measurements have become available in the course of the ARAP and this has allowed several different approaches to the description of partitioning of uranium between solid and solute phases. The various P values are summarised in Table 12.5. The choice of appropriate values is left to individual modellers, bearing in mind that bulk rock data or data for more sorptive fine particles or accessible phases could lead to different results. The use of bulk rock data unambiguously overestimates the partitioning of material onto the solid phases, so a more realistic value may be obtained using chemical extractions. However the specificity of these schemes for the target phases is uncertain. Nonetheless, the data tend to indicate that the variations from one sampling point to another are the major cause of the variability in "P" values obtained.

TABLE 12.5

SUMMARY TABLE OF PARTITION COEFFICIENTS

Partition Coefficient (P)	Range of observed values (mL/g)	
	^{238}U	^{230Th}
Bulk rock	$1 \times 10^3 - 5 \times 10^4$	$2 \times 10^5 - 3 \times 10^8$
Bulk rock accessible phases	$5 \times 10^2 - 1 \times 10^3$	
Particles < 10 μm, bulk	$5 \times 10^3 - 1 \times 10^5$	
Particles < 10 μm, accessible	$3 \times 10^3 - 5 \times 10^4$	
Particles in groundwater, bulk	$4 \times 10^4 - 7 \times 10^4$	$7 \times 10^7 - 2 \times 10^9$
Particles in groundwater, accessible	$2 \times 10^4 - 7 \times 10^4$	$2 \times 10^6 - 1 \times 10^9$

If the data as a whole are considered, a reasonable average P value for ^{238}U might be in the range 5×10^3 to 2×10^4 mL/g. Comparing accessible (TAO-extractable) phase data with groundwater suggests a much lower partition ratio, with values lying in the range 4×10^2 to 1×10^3 mL/g.

13 WEATHERING

The processes, mechanisms, and kinetics of chlorite weathering and uranium concentrations in associated minerals were the subject of a detailed investigation, which is described in Volume 9 of this series. The aim was to understand the effect of chlorite weathering on the redistribution of uranium in the vicinity of the ore deposit. X-ray diffraction (XRD) analysis, scanning electron microscopy, electron microprobe analysis, transmission electron microscopy, autoradiography, visible spectroscopy, and alpha and gamma spectrometry techniques were used.

If radionuclide migration is to be considered over long geologic timescales, the changes in host rocks which are structurally and chemically altered by water rock interactions, such as weathering or alteration, should also be considered (see Section 16). At Koongarra, the host rock, quartz chlorite schist, has been subjected to weathering. Although quartz is resistant to weathering, chlorite has been altered to clays and iron minerals. Two other minerals, biotite and muscovite, are also subjected to weathering. Biotite has the same weathering process as that of chlorite; ie, conversion to vermiculite and then to kaolinite. On the other hand, muscovite, which is more resistant to weathering than chlorite or biotite, is converted to illite and then probably to kaolinite.

The conversion sequence of chlorite to kaolinite by weathering was found to be (1) chlorite, (2) chlorite/vermiculite intergrade, (3) regularly interstratified chlorite/vermiculite intergrade and vermiculite, (4) vermiculite and (5) kaolinite (+ smectite). On the basis of XRD results, the presence of major clay minerals were described as a function of depth. Chlorite is not weathered at depths greater than

25 m. It rapidly decreases between 25 and 24 m and disappears at 24 m. Vermiculite appears at a depth of 25 m and kaolinite begins to persist at a depth of 24 m. Vermiculite disappears at 20 m where kaolinite is predominant, as it is in the shallower zone.

If we use average compositions of chlorite and vermiculite, we can express the weathering in chemical formulae as follows:

$(Mg_{2.24}Fe^{2+}_{2.61}Al_{1.14})(Si_{2.89}Al_{1.11})O_{10}(OH)_8$ (chlorite) $\Rightarrow$
$(Mg_{1.36}Fe^{3+}_{0.95}Al_{0.55})(Si_{2.80}Al_{1.20})O_{10}(OH)_2$ (vermiculite) $\Rightarrow$
$Al_2Si_2O_5(OH)_4$ (ideal kaolinite).

Iron and magnesium are released in all stages of the weathering; ie, during the transformation of chlorite to vermiculite and the decomposition of vermiculite to kaolinite. Iron minerals that are closely related to the uranium association are located between chlorite and vermiculite slabs at first (a few microns in size), and then accumulated between grain boundaries occasionally forming veins.

Fractures and schistosities are preferential pathways of water macroscopically whereas the domains of chlorite (hundreds of nm in size), which are attached by low angle grain boundaries with layer terminations, are microscopic pathways of water molecules. The weathering finally changes chlorite into sub micron to micron sized weathered products, iron minerals and kaolinite. Calculations of the changes in mineral compositions with time, assuming a first-order reaction, suggested that the weathering rate was not constant but rather time-dependent.

The chlorite weathering appears to have affected the uranium redistribution both microscopically and macroscopically. The relative mineral compositions were compared to uranium concentrations (mg/g) along the DDH3 drillhole from near the end of the secondary ore deposit (see Figures 6.4 and 13.1).

On the metre scale, the abundances of chlorite, vermiculite, and kaolinite correspond well to uranium concentrations. The chlorite dominant zone corresponds with the zone of lower uranium concentration, the vermiculite predominant zone corresponds to the zone of intermediate uranium concentration, and the kaolinite predominant zone corresponds to the zone of highest uranium concentration. On a millimetre scale, uranium concentrations are qualitatively proportional to the extent of the weathering; weathered chlorite grains have a higher uranium concentration.

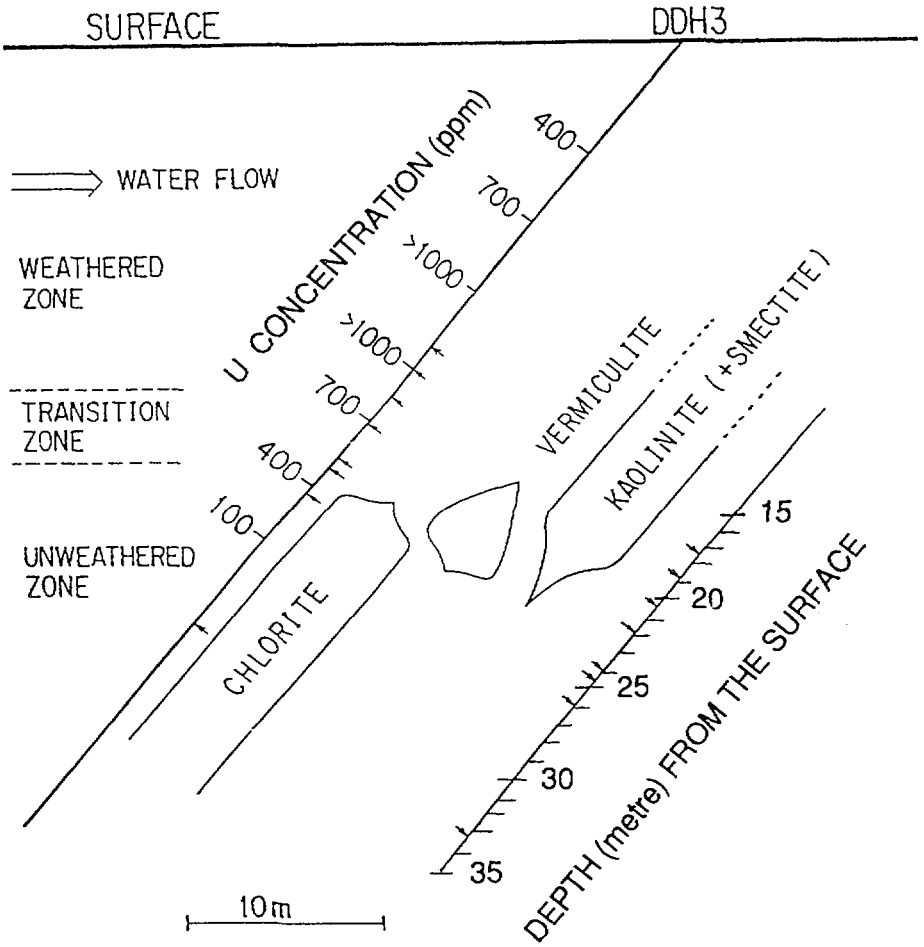

FIGURE 13.1 Comparison of U concentrations and mineral abundances. The arrows indicate the sampling locations for the XRD measurements

Of the weathered products, uranium is mainly associated with CDB extractable phases (see Table 12.1), probably goethite and hematite, containing a 40-60% fraction of uranium. Electron microprobe analysis and visible microspectroscopy confirmed this result. Uranium occurs with iron, and sub micron size saleeite, a uranyl phosphate, is the most probable uranyl phase associated with iron minerals. Possible uranium fixation mechanisms are saleeite microcrystal coprecipitation and sorption to the iron minerals released during the chlorite weathering.

The results suggest that the interaction of the uranyl solution with chlorite causes the weathering of chlorite and the precipitation and sorption of uranium in the weathered products from the solution and, thus, the uranium migration is retarded at Koongarra.

As a consequence of this work, a one-dimensional, advection-dispersion-sorption model was developed to study the effect of chlorite weathering on uranium migration. This is discussed in Section 17.

14 GEOCHEMISTRY OF PLUTONIUM-239, IODINE-129, TECHNETIUM-99 AND CHLORINE-36

Among the most persistent radioactive constituents of high-level wastes from nuclear fission power reactors are ^{239}Pu, ^{129}I, and ^{99}Tc, with half-lives of 24,100 y, 1.6×10^7 y and 2.1×10^5 y, respectively. Natural analogues, particularly uranium ore deposits, offer a means to evaluate the geochemical transport and retention properties of these radionuclides in analogous natural materials. In these natural environments, ^{239}Pu and fission-product elements are produced by nuclear processes in minerals and have a unique geochemical history. Under certain hydrogeochemical conditions, they may be released from their host minerals, transported from their site of production, and retained at another location. However, the feasibility of using uranium minerals as analogues to characterise the behaviour of these nuclear reaction products (NRP) in spent fuel relies upon a capability to characterise NRP concentrations in the host minerals.

Volume 15 of this series documents a study to evaluate the accuracy and precision with which NRP production rates can be estimated, and the degree of retention of these radionuclides by the source uranium ore. Measured abundances of natural ^{239}Pu, ^{99}Tc and ^{129}I in uranium ores are compared below to calculated abundances. The comparison is formalised by calculating the fractionation factor:

$$\alpha = (NRP/U)_M / (NRP/U)_{SE}$$

where subscript M refers to measured element ratios, and subscript SE refers to element ratios calculated under the assumption of secular equilibrium, the condition in which the rates of production and decay of a radioactive species exactly balance one another. If the uncertainty in the production rate estimate is small, then α is a measure of the extent of any change in NRP concentration relative to uranium over several NRP half-lives; eg, a period of about 1×10^5 years for ^{239}Pu. An α-value of 1

indicates no fractionation between the two elements. Values less than 1 suggest preferential loss of the NRP relative to U, and values greater than 1 suggest preferential gain of the NRP relative to U. This approach is being used to provide information useful to the development and verification of source-term models used in the performance assessment of high-level waste repositories.

14.1 Sample Descriptions and Analyses

The study focussed on samples from unweathered and unaltered zones in several different primary ore deposits; ie, samples believed to represent systems that are closed with respect to retention of nuclear reaction products. A wide range of uranium contents and ore mineralogies was selected in order to test our understanding of factors controlling nuclide production rates and degrees of nuclide retention. The deposits investigated include Koongarra (Australia); Key Lake, Cigar Lake, and Beaverlodge (Canada); Oklo (Gabon); and Shinkolobwe (Zaire). These ores can be considered as natural analogues of spent fuel and of its alteration products as well as source terms for radionuclide migration in groundwater. A few analyses of NRP concentrations were also made in samples from dynamic open systems, and specifically in ores from the altered and weathered zones of the Koongarra deposit, and in groundwaters from Koongarra.

Sample preparation methods are documented in Volume 15. Iodine-129 and ^{36}Cl measurements were obtained by accelerator mass spectrometry (AMS) at the Nuclear Structure Research Laboratory of the University of Rochester. Tc and Pu isotopic abundances were measured by thermal ionisation mass spectrometry. Measured NRP concentrations are reported below in Table 14.1.

14.2 Source-term Modelling

In order to assess NRP mobility, measured NRP concentrations were compared to those expected if the ores had behaved as closed systems with respect to uranium and its products. Under conditions of secular equilibrium in closed systems, NRP concentrations are solely a function of neutron flux, uranium content, and NRP decay rates. Fission products ^{99}Tc and ^{129}I are produced by three mechanisms: spontaneous fission of ^{238}U, which is a function of the uranium concentration, and neutron-induced fission of ^{235}U and ^{238}U. For ^{239}Pu, the only production mechanism is neutron-capture by ^{238}U; ^{36}Cl is produced by neutron-capture by ^{35}Cl and is of interest as a possible *in situ* monitor of the neutron flux and as an indigenous water tracer. The physical and chemical properties that affect the *in situ* neutron flux were measured in each sample, including abundances of major elements, selected minor and trace elements, and neutron production rates. Using these data as inputs, a

Monte Carlo Neutron and Photon transport code, MCNP (Briesmeister, 1986), was used to calculate neutron fluxes and neutron-capture reaction rates for the ore samples .

TABLE 14.1

MEASURED NRP/U RATIOS (X 10^{12}) IN PRIMARY URANIUM ORES

SAMPLE	DEPOSIT	% U	$^{239}Pu/U$	$^{129}I/U$	$^{99}Tc/U$
G4674	Koongarra	11.5	1.4	1.0	n.m.
G2698	Koongarra	19.1	2.6	1.3	≤ 1.8
KL756	Key Lake	22.4	2.6	0.75	n.m.
KL785	Key Lake	9.0	1.3	n.m.	n.m.
CS235L	Cigar Lake	54.6	1.9	2.1	n.m.
W83A	Cigar Lake	40.8	3.0	1.8	≤ 1.8
W83C	Cigar Lake	46.8	2.8	2.8	n.m.
Z9-005	Oklo Zone 9	62.8	0.8	n.m.	n.m.
Z9-028	Oklo Zone 9	62.2	3.0	2.7	n.m.
NBL-6	Skinkolobwe	45.4	5.2	7.2	1.6*
BL-5	Beaverlodge	7.1	3.1	n.m.	n.m.

n.m. not measured

* Kenna B.T., and P.K. Kuroda (1964) J. Inorg. Nucl. Chem., 26:493-499.

Modelling was conducted for two geometries:

(a) The "infinite model" was used to estimate NRP abundances by modelling the sample as homogeneous material with the elemental composition of the sample and infinite dimensions. In cases where the material surrounding the sample has a lower uranium concentration, which is true for nearly all of the samples in this study, the infinite model results should generally serve as upper limits for the true NRP abundances. This approach nearly always led to a substantial over estimate of the NRP production rates.

(b) The "geometry model" was used to obtain more realistic estimates of NRP abundances. In these cases, each sample was modelled as high-grade material bordered by material with different, generally lower, uranium concentrations.

14.3 Comparison of Measurements with Model Predictions

14.3.1 Iodine-129

Measured $^{129}I/U$ ratios in unweathered primary ores investigated in this study (Table 14.1) exceed minimum ratios predicted from spontaneous fission of ^{238}U ($^{129}I/U = 6 \times 10^{-13}$). However, concentrations are variably less than amounts predicted by the source-term model under a wide variety of assumptions (Figure 14.1). Although production of ^{129}I by neutron-induced fission of ^{235}U and ^{238}U is difficult to estimate with any accuracy, the measurements suggest that ^{129}I may be depleted to a larger extent in samples from Koongarra (G2698 and G4674) than in samples from Cigar Lake (CS235L, W83A and C). Samples from weathered primary

ore from Koongarra contain quantities of ^{129}I that are well below the minimum abundance expected for spontaneous fission, an unambiguous indicator of loss of this fission product from its site of production. The mobility of radioiodine is also apparent from its high concentrations in groundwaters flowing through the Koongarra deposit.

14.3.2 Technetium-99

Predictions of the source term model indicate that ^{99}Tc production in uranium ores is dominated by spontaneous fission of ^{238}U. Production of ^{99}Tc by induced fission of ^{235}U is 5-25 % of the total for the samples studied, and that by neutron-induced fission of ^{238}U, is generally $\leq$4%. The dominance of the spontaneous fission component simplifies interpretation of measured ^{99}Tc concentrations in uranium minerals. The validity of the source-term model prediction is borne out by three preliminary analyses of ^{99}Tc in primary ores, which suggested ^{99}Tc abundances about the levels predicted by the model, and no more than 10% above that expected for spontaneous fission alone ($^{99}Tc/U = 1.6 \times 10^{-12}$).

14.3.3 Plutonium-239

Source term models predicting ^{239}Pu abundances in uranium minerals lead to ambiguous conclusions. Measured abundances are generally, but not always, within the range of predicted values (Figure 14.2). In very heterogeneous media, such as those typical of uranium ore deposits, chemical parameters critical for the determination of ^{239}Pu production rates are difficult to characterise with sufficient accuracy to use the results for evaluating the degree of retention or loss of ^{239}Pu from the orebody.

14.4 Conclusions about Modelling Capability

The source term model is most useful as a predictive tool in cases where the sample represents a volume of material that is large relative to the mean path length of a neutron (eg, NBL-6 and BL-5, which have been distributed as certified reference ores for uranium assays) or where the sample is derived from relatively homogeneous material. The model also provides useful predictions, although with greater uncertainties, of NRP abundances in samples taken from well-specified locations in geometrically well-defined environments. In the latter case, realistic results are only obtained when the model incorporates additional information about the sample environs. The largest uncertainties attend calculations of NRP abundances in small samples taken from heterogeneous geologic systems. For these samples, even with detailed composition information, the source-term model is not able to predict absolute NRP abundances with the accuracy needed to calculate NRP retention or losses, unless the fractionation between uranium and its reaction products is substantial; ie, $\alpha > 0.1$ or $\alpha < -0.1$.

Uncertainties associated with the source-term model range from low (~10%) for ^{99}Tc to moderate (~20-50 %) for ^{129}I and ^{239}Pu. These uncertainties are almost certainly

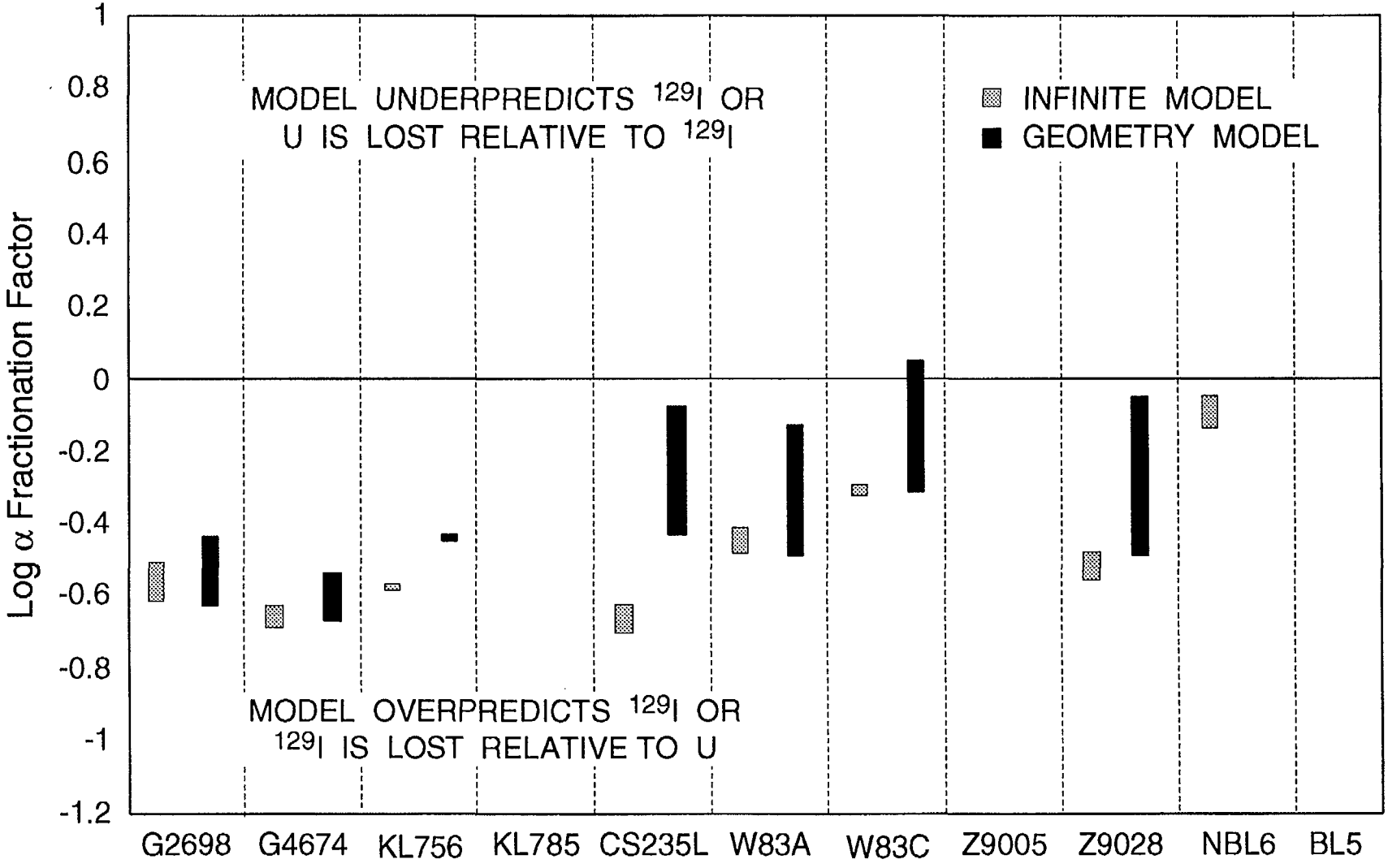

FIGURE 14.1 Comparison of measured and predicted ^{129}I concentrations for primary uranium ores. The definition of α is given above.

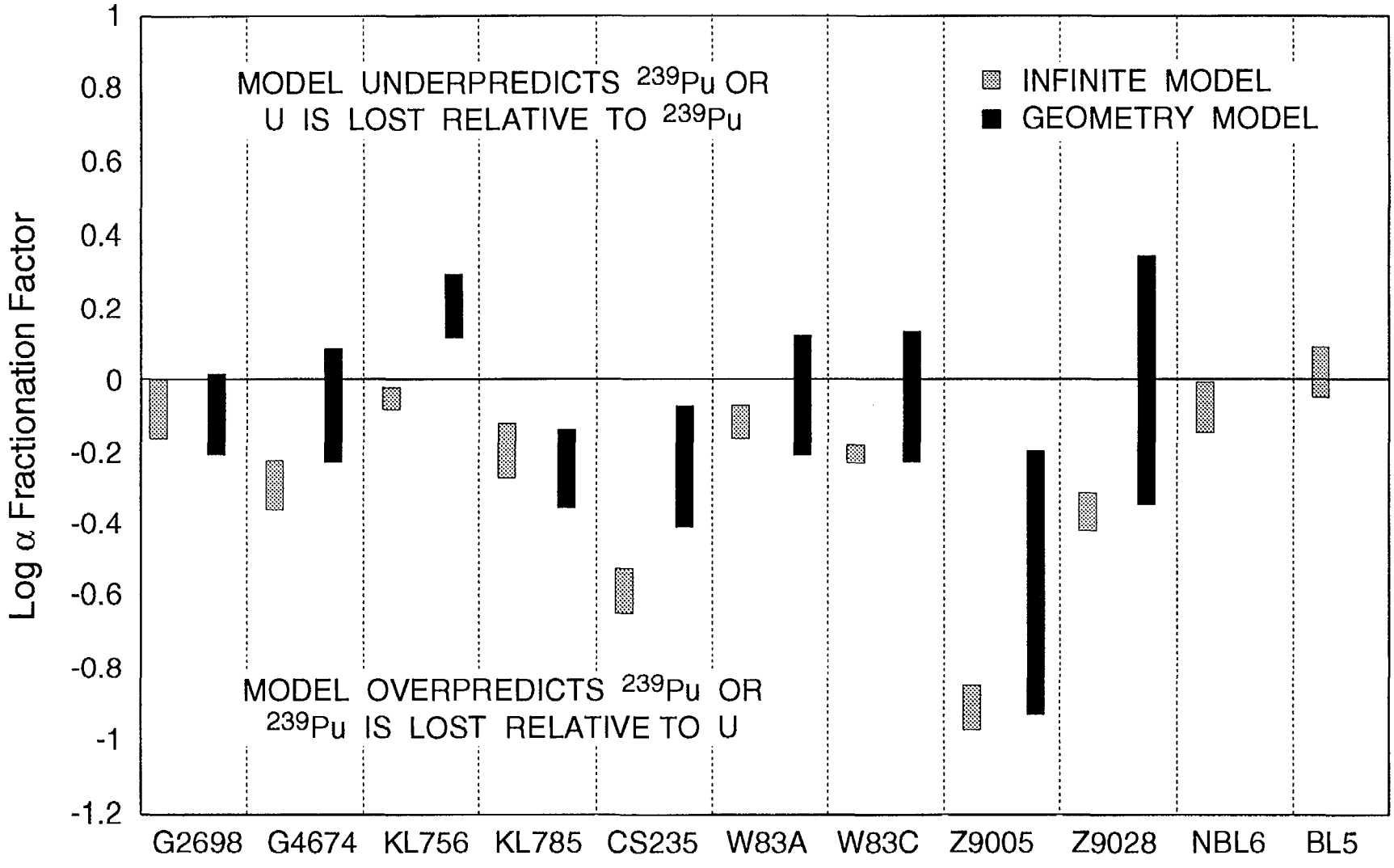

FIGURE 14.2 *Comparison of measured and predicted ^{239}Pu concentrations for primary uranium ores. The definition of α is given above.*

underestimated. For example, H/U and Gd/U ratios are shown by the model results in Volume 15 to be critical parameters in controlling ^{235}U fission rates. But varying Gd/U ratios within the ranges used in that study (80-120% of measured values) may not sufficiently reflect the true uncertainty in their concentrations. The effects of varying other elemental concentrations, such as B, F or Fe, which might also have a major influence on the neutron flux in some of the ores, have not been investigated. For the geometry model, an infinite number of cases could be proposed to model the lateral extent, thickness, and elemental heterogeneities in stratigraphic intervals; eg, with barren high-porosity seams cutting through dense high-grade material, or vice versa.

Even where the source term model has not been able to provide precise estimates of the true NRP production rates, it has been invaluable for identifying the critical elemental parameters controlling these rates and establishing the conditions under which various NRP production rates should correlate with or constrain one another. For example, under most conditions, ^{36}Cl ($t_{1/2}$, 3.0 x 10^5y), another long-lived neutron-capture product found in uranium ores, is shown to be an ideal *in situ* monitor of the ^{235}U fission rate, which is the dominant source term for ^{129}I and possibly a significant one for ^{99}Tc. Similarly, $^{239}Pu/U$ ratios can be used to establish limits on the ^{238}U neutron-induced fission rate. The ratios measured in this study suggest that ^{238}U induced fission comprises <4% of the total fissions in most of the ore samples studied and hence can be neglected as a source of ^{129}I and ^{99}Tc, as was assumed in the preparation of Figure 14.1.

15 HYDROGEOLOGICAL MODELLING

The secondary dispersion fan of the No. 1 orebody at Koongarra is believed to be the result of groundwater transport and chemical processes over long periods of time. Understanding the hydrogeology of the site was therefore a major objective of the ARAP, both directly, through hydrogeological field studies, and indirectly, through the use of geophysics, petrophysics, water chemistry and rock chemistry, which provided indicators of past and present hydrogeological processes. At the same time, there was a major effort to use existing hydrogeological flow models to interpret available data and to predict rates and directions of groundwater flow. Details of the geohydrological modelling are provided in Volume 6 of this series.

A number of attempts were made to predict groundwater movement near the orebody. The goal was to use available data, both physical and chemical, quantitative and qualitative, to predict rates and directions of movement under present-day hydrogeological and climatic conditions. Paleohydrology was specifically excluded, mainly because it was perceived that there would not be enough data to make significant progress in that direction. Section 17 focuses on radionuclide transport, thus coupled flow and transport modelling is also specifically excluded here. Any use of chemical data in the development and calibration of hydrological models was only qualitative, in the sense that spatial distributions of dissolved or sorbed species provide evidence for past or present directions of flow.

The hydrogeology of the Koongarra site is complex and difficult to model because:

- region subsurface flow is a minuscule component of the overall water balance of the region
- significant flow occurs as fracture flow rather than as porous media flow
- the region is extremely heterogeneous, with a wide range of material types and fracturing on several scales
- many of the available hydrogeological measurements were collected from open exploration holes, which were constructed to determine the extent of uranium orebodies rather than specifically to understand groundwater flow, and
- observations are concentrated near the No.1 orebody, hence there is limited knowledge about the regional geology and about boundary conditions for regional groundwater flow.

A hierarchy of models was applied by a number of individuals and modelling teams working independently of each other (see Volume 6 of this series). All but one of the models are porous media models, which assume that the fractured medium acts as a continuum and that flow is governed by Darcy's Law with some effective or average hydraulic conductivity. One model is a fracture flow model, based on generating a finite number of discrete fractures with random orientations. Another model is an inverse model, which attempts to utilise data from aquifer tests to estimate heterogeneous transmissivities and aquifer storativities in a number of zones. The hierarchy of models includes models with varying dimensionality and models which are both steady and transient. Each type of model is able to describe at least some features of the Koongarra site.

15.1 Two-dimensional Models in Vertical Section

These were the first models actually applied. They showed that if a water table exists beneath the Mount Brockman Massif, flow from Mount Brockman can indeed occur towards the Cahill Schist with flows moving generally upwards from the Koongarra Fault through the primary orebody towards the land surface. Details of the flow pattern and velocities near the orebody are quite sensitive to the assumed hydraulic conductivity of the fault zone.

The earliest cross-sectional model, using NAMMU (Atkinson et al., 1986), assumed that a groundwater divide exists beneath Mount Brockman and that there is also a no-flow boundary beneath Koongarra Creek, which acts as the final discharge point for the flow system. The purpose was not to perform a detailed analysis of the groundwater flow, but rather to obtain a broad understanding of the nature of the local-scale groundwater flow at Koongarra. Variations in the hydrogeological properties of the important rock units and in the position of the various boundary conditions were all considered. Assuming that the Koongarra Fault is highly permeable, and that the weathered Cahill Formation acts as an aquifer compared to the unweathered layer below, the fault acts to "channel" flow towards the surface, with a significant "leakage" into the aquifer weathered layer (Figure 15.1).

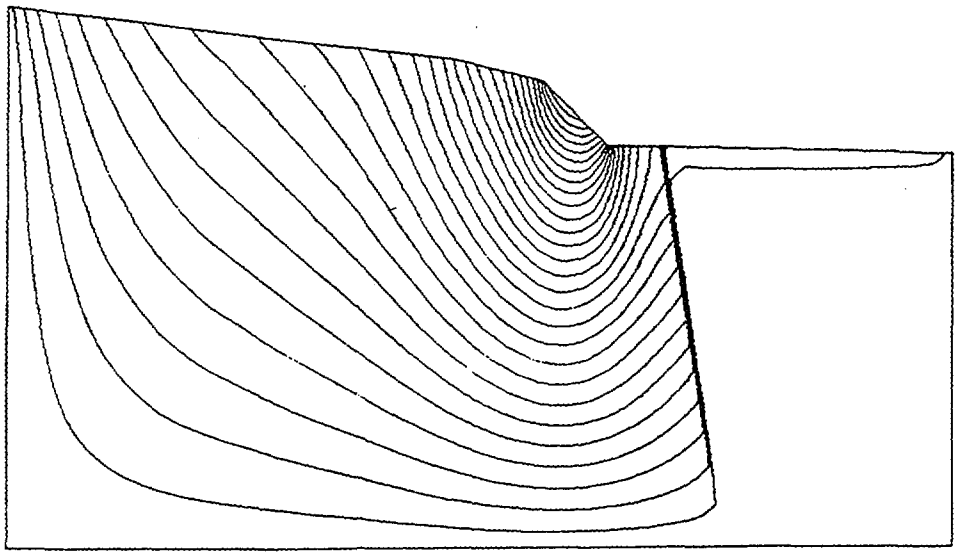

FIGURE 15.1 Streamlines for the case with a highly permeable fault and an aquifer weathered layer

A second, similar model assumed that hydraulic conductivities were anisotropic, with the principal direction of anisotropy in most materials roughly aligned with the plane of the Fault. Figure 15.2 shows contours of hydraulic heads and streamfunction, as well as vectors indicating the direction and magnitude of flow, for the case of a highly conductive fault.

In order to check the boundary conditions assumed by these earlier models, another two-dimensional cross-sectional model was set up on a regional scale, using AQUIFEM-N (Townley, 1987). The latter model assumed boundaries on the Arnhem Land Plateau and on the far side of Mount Brockman, and included the Sawcut Fault as another major fault system. Sensitivity studies showed that it is indeed very likely that a local flow system exists, as originally hypothesised. In other words, it is extremely unlikely that a significant groundwater flow, taking water from Mount Brockman beyond Koongarra Creek, could occur.

15.2 Three-dimensional Models

Two separate three-dimensional models were created for a region 3 km square. Their purpose was to demonstrate, with similar assumptions to those used in two-dimensional vertical sections, that flow directions could deviate significantly from a plane. By including a highly conductive zone to represent Koongarra Fault, it was found that significant flows could occur horizontally along the Fault. Figure 15.3 shows three-dimensional views of the model domain, showing the curved structure of the Koongarra Fault and a streamtube containing water which carries recharge to the water table within Mount Brockman through the No.1 orebody. The model was useful to study the sensitivity of groundwater flow to a wide range of hydrogeological assumptions.

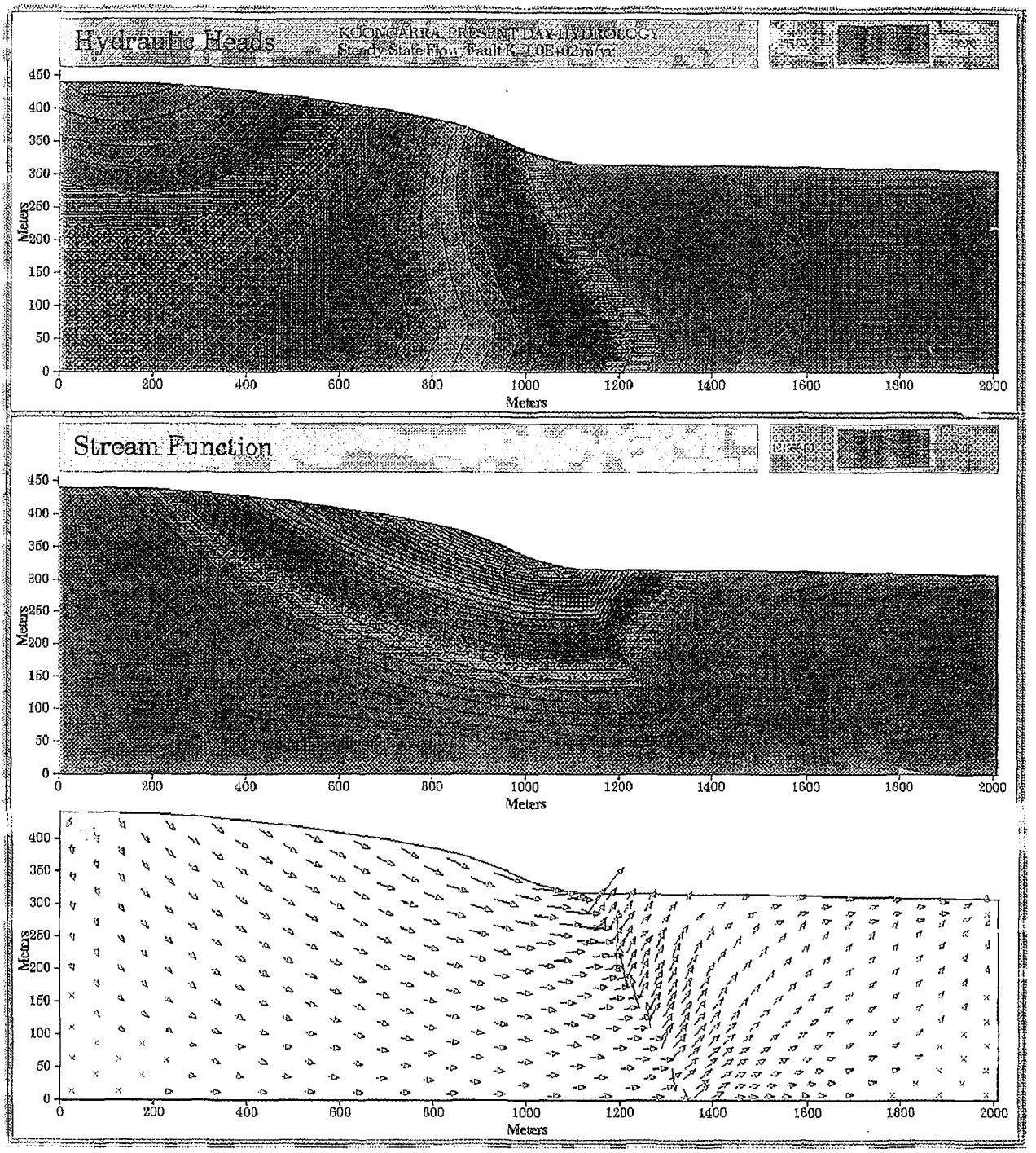

FIGURE 15.2 Simulation with fault conductivity equal to 10^2 my^{-1}

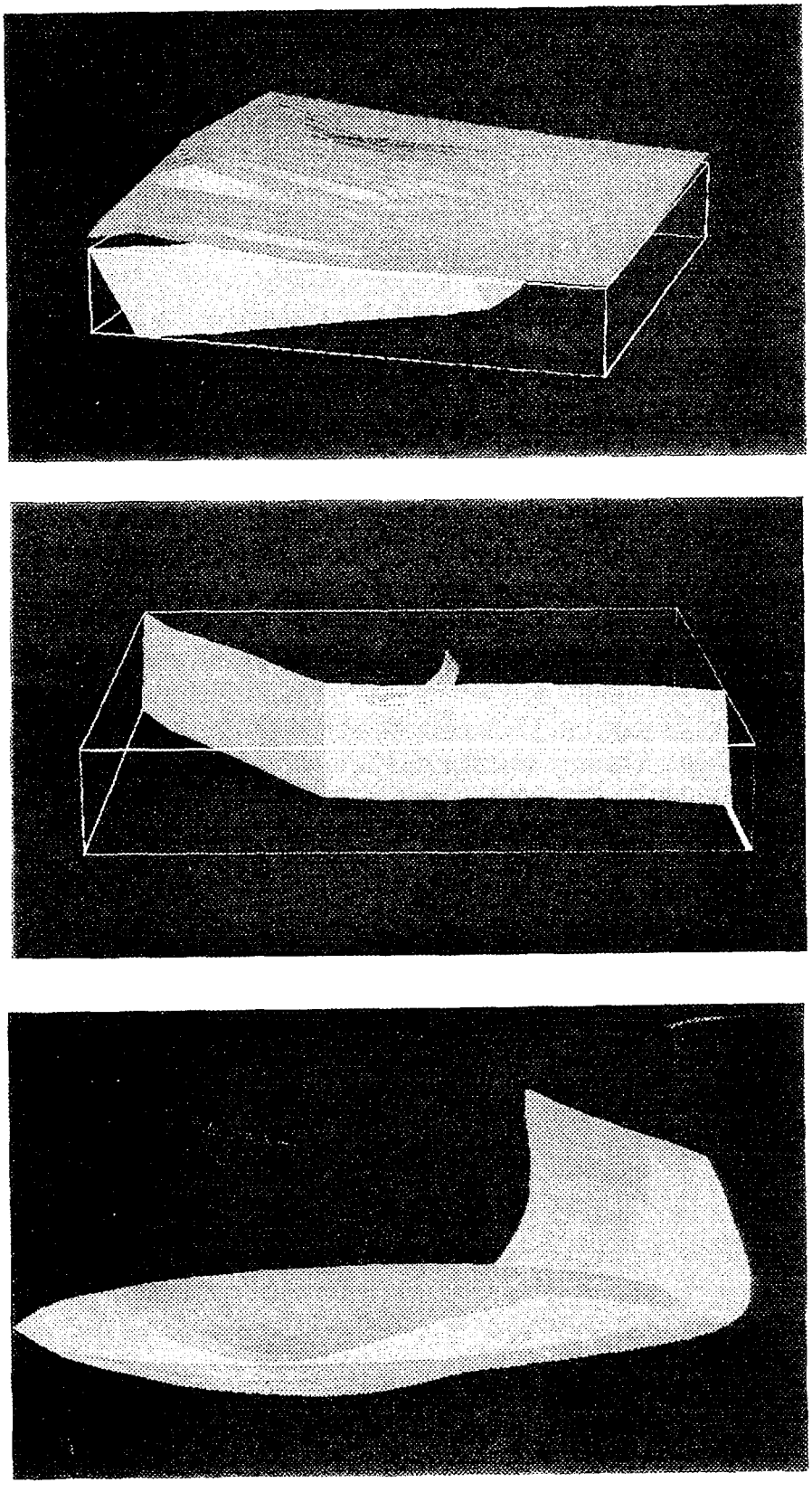

FIGURE 15.3 Three-dimensional views of the model domain, showing the curved structure of the Koongarra Fault and a streamtube containing water which carries recharge to the water table within Mount Brockman through the No.1 orebody.

A third three-dimensional model was developed independently at a much more local scale. The purpose of this model was to demonstrate the significant effect of anisotropy (see Figure 9.5), which was determined based on Borehole TV measurements of the orientations of planes of schistosity.

15.3 Aquifer Modelling

Aquifer testing described in Section 10 uses the concept of transmissivity in its interpretation of aquifer response to pumping. The concept of an aquifer, a layer transmitting significant quantities of water in a mainly horizontal direction, seems hard to accept in an environment as heterogeneous as that at Koongarra. But modelling of aquifers both in one dimension and two-dimensionally in plan contributed significantly to our understanding of the site.

A one-dimensional model with three layers (often described as a quasi two-dimensional model – Figure 15.4) was applied to flow between the Fault and Koongarra Creek. Being a transient model, it was able to show that reverse flows can indeed occur back towards the Fault, but only if there is distributed recharge over the orebody as well as a mechanism for the Fault, or a region near the Fault, to remove water from the simulated cross-section. The model also showed clearly that the response of the three-layered system, consisting of a highly weathered zone, a fractured transmissive zone and a less conductive lower schist zone, is governed mainly by the transmissivity and storage coefficient of the middle layer. The storage coefficient of the upper layer has little effect.

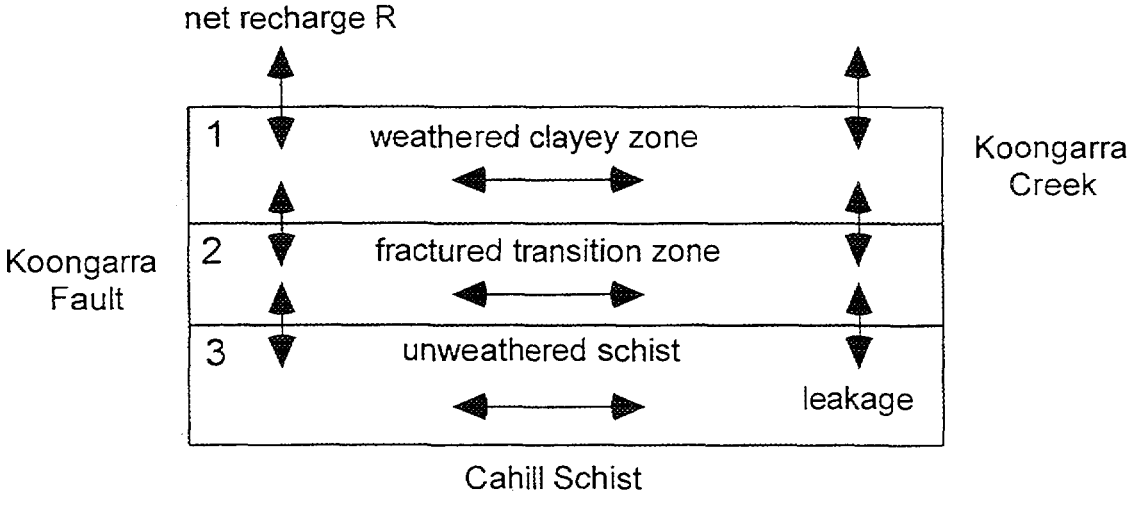

FIGURE 15.4 Conceptualisation for a three-layered one-dimensional model

A two-dimensional model in plan assumed an unusual description of anisotropy, with the principal directions of anisotropy varying in space throughout the domain (in some sense an idealisation of Figure 9.6), to show that reverse flows can also occur even without a conducting Fault. Throughout this modelling, the Koongarra Fault was assumed to act as a no-flow boundary. Koongarra Creek and part of the length of small tributaries were assumed to act as mixed (3rd type) boundaries, with water levels in the streams varying both spatially and seasonally. Recharge to the water

table was represented as the sum of steady and periodic (sinusoidal) components, to represent the strong seasonal cycle of rainfall/recharge and evapotranspiration.

Figure 15.5 shows the results of one simulation with strong anisotropy. The magnitudes and directions of groundwater flow change substantially throughout the year, and a local reversal of flow is seen to occur between Mine Grid 3150 and 3300 mE.

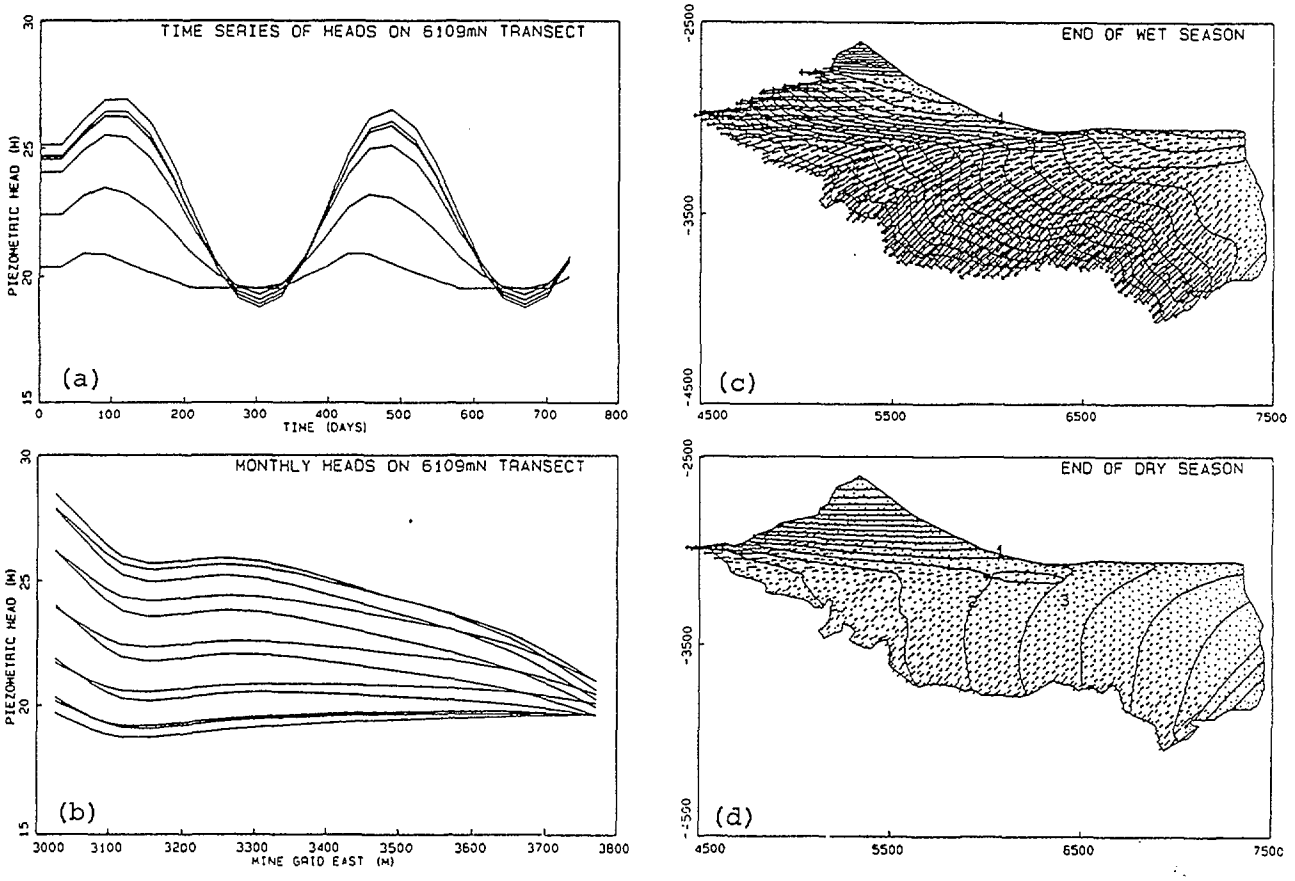

FIGURE 15.5 Results of transient modelling of aquifer flow, showing (a) temporal variations in water table elevations at a number of locations on a transect at 6109 mN, (b) spatial variations of water table elevations along that transect at monthly intervals, (c,d) contours of the water table at the end of the wet and dry seasons.

15.4 Fracture Flow and Inverse Modelling

Modelling of a three-dimensional region using discrete fractures showed that it is certainly possible to simulate systems like that observed at Koongarra, but that large amounts of data are probably needed to obtain realistic descriptions of the fracture networks. The hydraulic head distribution through the fracture network is shown in plan view in Figure 15.6 (flow is from left to right); the distribution of fractures near the top of the cube can also be seen. The fracture density across the network is

relatively sparse at 0.2 m^2/m^3, but it allows for sufficient hydraulic connection for flow across the 180 m block. A change in colour scale across a fracture describes the change in hydraulic head across the fracture. Relatively small hydraulic gradients are generally observed across individual fractures. Such a response would be expected, given good hydraulic connection in a parallel plate representation of a fracture with reasonably high transmissivity.

Inverse modelling of the data from nine multi-well pumping tests, selected because they represent an exceptional amount of transient data over a relatively small area; approximately 4,000 time-drawdown data over a 1200 m by 800 m area, was also tested. The results have shown that inverse procedures may have some advantages over fitting of analytical type curves, especially in highly heterogeneous environments. Inverse modelling may also be useful in the estimation of spatially varying (heterogeneous) aquifer parameters and/or allow for the joint interpretation of multiple sets of pumping test data.

15.5 Conclusions

The objective of determining rates and directions of groundwater movement has not been achieved with any degree of confidence. The most that can be said is there are many combinations of hydrogeological and climatic variables that could produce groundwater velocities in the range apparently needed by coupled flow and transport models. In the final analysis, hydrogeological data do not contain as much information as the chemical data, thus fitting of coupled models is more likely in the long term to be capable of identifying the best combination of model parameters.

On the other hand, in order to interpret present-day spatial distributions of dissolved chemical species it is, in principle, necessary to run models for millions of years. Since it is yet not possible to run three-dimensional models for these time scales, there may be results that can be achieved from three-dimensional hydrogeological modelling alone that can not yet be achieved from coupled modelling. There is clearly a role for hydrogeological modelling, but modelling is not a substitute for careful design of field experiments and careful analysis of data.

During the study, it became apparent that the objective of developing hydraulic models in isolation from transport models was somewhat artificial, if not ill conceived. This conceptual segregation between flow and transport processes has led to Volume 6 of this series attempting to offer conclusions about flow patterns etc., for use in other Volumes, but without taking full advantage of observed spatial distributions of dissolved species in groundwater. A more modern approach would encourage consideration of coupled flow and transport processes from the start.

16 GEOCHEMICAL MODELLING

A number of groups carried out modelling studies to further understand geochemical phenomena considered to be important at the Koongarra site, including:

- formation of the primary uranium deposit
- formation of the uranyl silicate zone

- formation of the uranyl phosphate zone
- fixation of uranium in the dispersion fan "downstream" of the uranyl phosphate zone, and
- weathering.

In modelling these processes the groups adopted a range of approaches based on their individual conceptualisations of the site and the likely controlling factors. The majority of approaches were based on the premise of thermodynamic equilibrium and relied on fundamental thermodynamic data for the included chemical species. In specific cases the models were extended to include chemical kinetics.

The modelling attempted to unravel the nature, properties and interactions between groundwaters and their host rocks. Given the chemical composition of a groundwater, one of the initial steps in geochemical modelling is to calculate the distribution of aqueous species in the water, based on the assumptions of thermodynamic equilibrium. The subsequent indication of which species are likely to be important may then allow identification of the specific mass transfer processes that have occurred between the aqueous phase and the host rock mineralogy.

A common step towards understanding such fluid-rock interactions is to calculate the saturation state of the minerals present in the rock with respect to the composition and speciation of the groundwater. For these calculations the theoretical solubilities of the minerals in the groundwater are calculated from knowledge of their thermodynamic stabilities. Several computer codes were used to make speciation solubility calculations, including EQ3/6 (Wolery, 1983), PHREEQE (Parkhurst et al., 1980) and MINTEQA2 (Russo, 1987). The results of these calculations allowed predictions to be made as to which minerals may be dissolving, precipitating or otherwise controlling the groundwater chemistry.

Other geochemical factors which are likely to be important in controlling the distribution of chemical species between the solid and aqueous phases include "sorption" in its various manifestations, α-recoil, co-precipitation, recrystallisation, and the presence of colloids and natural organics. Details of the work carried out during the ARAP on sorption are provided in Volume 13 of this series. Reviews of thermodynamic data for uranium and thorium bearing species are provided in Volumes 11 and 12, as these are of particular relevance to Koongarra and its status as a natural analogue for radionuclide transport from a radioactive waste repository. Methods for extending the thermodynamic chemical models to non-standard state conditions, including the effects of temperature, pressure and salinity, are reviewed in Volume 10.

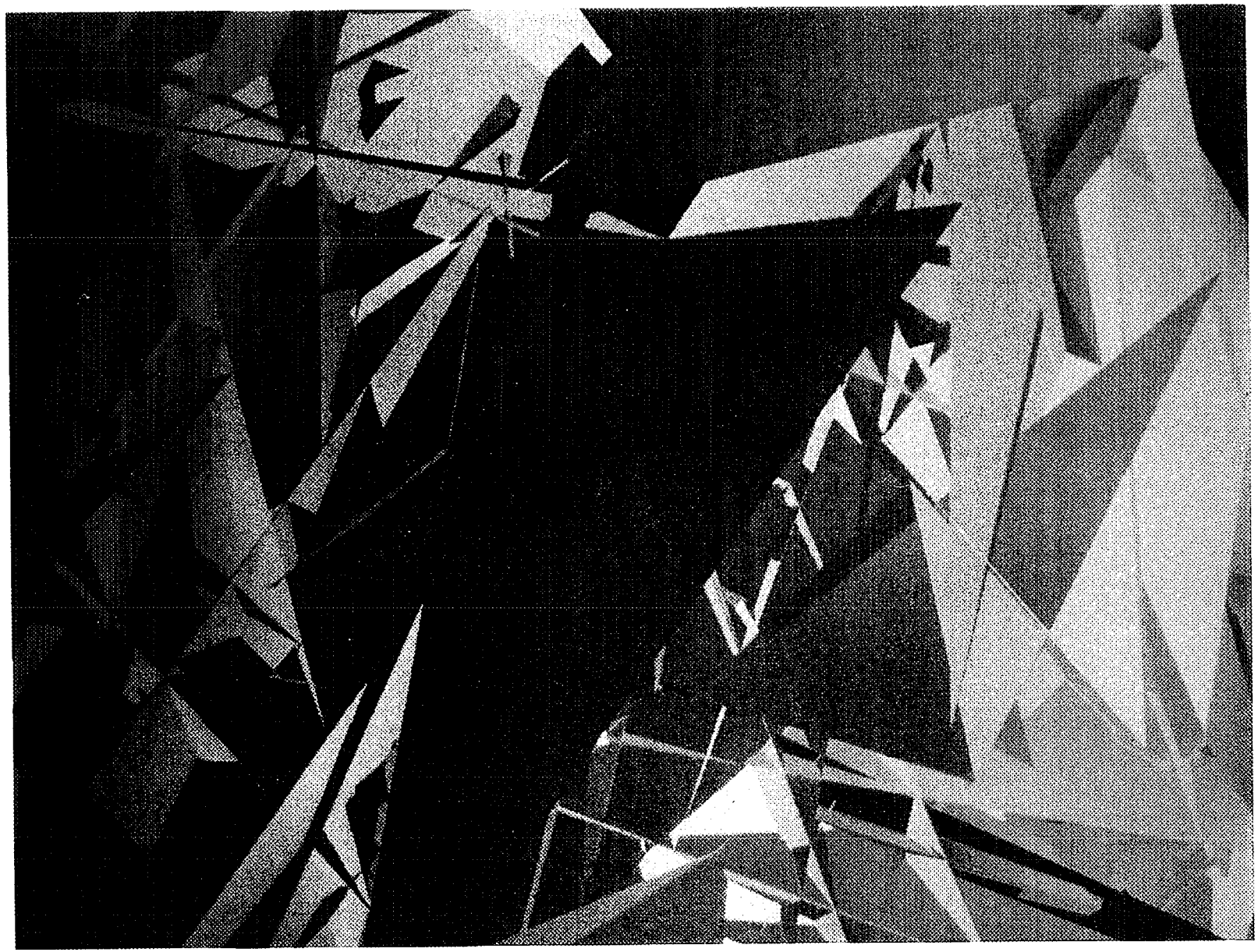

FIGURE 15.6 Plan view of discrete fracture flow field showing distribution of hydraulic head

16.1 Status of Thermodynamic Databases used in the ARAP

The results of the modelling and of any interpretations made cannot be compared unless the differences in the data used are clearly understood. Hence, the thermodynamic database employed in geochemical modelling is of primary importance. Ideally, the database should be complete in terms of the species it contains. At the very least it must contain all of the species thought to be relevant to the problem of interest. In reality, the continual acquisition of data means that any database necessarily contains a number of best estimates based on current knowledge. As such it must be fully referenced to the sources of data used in its compilation. Another criterion for a rigorous thermodynamic database is that of

internal consistency. It is not appropriate to "mix-and-match" equilibrium constants to achieve completeness without expending effort to achieve internal consistency amongst the data.

Brief summaries of the uranium and thorium databases employed in the ARAP are given here. Complete descriptions can be found in Appendices I and II of Volume 10 of this series.

The Johns Hopkins University database

This thermodynamic database was developed at the Johns Hopkins University, Baltimore, USA. The database is still evolving and changed significantly during the course of the project in response to earlier findings. The most recent version of the database (1992) contains 27 elements, 189 aqueous species, 139 minerals, 8 gases and 15 solid-solutions. The data originate from the comprehensive, although largely unreferenced, thermodynamic data file supplied with the EQ3/6 package (Wolery, 1983).

CHEMVAL database

The international CHEMVAL project was established in 1987 and the Stage 4 database was released in March 1992. The procedures adopted for its compilation and source review were based on CODATA recommendations (CODATA, 1978). The CHEMVAL 4 database is internally consistent and contains 563 aqueous species and 332 solid phases for 27 elements. All data are fully referenced to source and are quoted at 25°C, having been extrapolated to infinite dilution using a truncated form of the Davies equation (Read, 1990).

Thermodynamic data employed at ANSTO

Three computer codes were used at ANSTO: MINTEQA1 (Brown and Allison, 1987), HYDRAQL (Papelis et al., 1988) and MICROQL (Westall 1979). The thermodynamic data used for the major elements were those supplied with the codes. These were augmented with data for U(VI) bearing species using values from Grenthe et al., (1989). The data issued with the computer codes are generally unreferenced and have not been critically reviewed.

16.1.1 Thermodynamic data for uranium and thorium

Aqueous species

Potentially the most important differences in thermodynamic data for aqueous species used in modelling the Koongarra system relate to the U(VI) phosphates. The quality of these data is of prime importance for accurate modelling of the uranyl phosphate zone.

Data for certain U(VI) species containing the HPO_4^{2-} ligand (e.g. $UO_2(HPO_4)_2^{2-}$ and $UO_2(HPO_4)^0$) originate from a study by Moskvin et al., 1967. These data were later included in a well-known review of uranium solution-mineral equilibria by Langmuir (1978) and have consequently found their way into many "standard" geochemical databases since that time. Langmuir (1978) specifically noted the "remarkable stability" of $UO_2(HPO_4)_2^{2-}$.

Grenthe et al. (1989), critically reviewed the literature on the U(VI) phosphates and agreed with Tripathi (1984) that there was in fact no evidence for the formation of those U(VI) complexes in the data of Moskvin et al. (1967). The effect of including or omitting those species in geochemical calculations is large. If included, the U(VI) phosphates will often dominate over U(VI) carbonate species even where the phosphate:carbonate ratio is around 1:1000. Consequently, it is recommended that data for $UO_2(HPO_4)_2^{2-}$ and $UO_2(HPO_4)^0$ derived from these sources be excluded from calculations made for the Koongarra site.

Minerals

In contrast to thermodynamic data for aqueous species that are accessed in every speciation/solubility calculation, thermodynamic data for minerals are usually only utilised when specified by the user. Exceptions do occur; for example the EQ3/6 code accesses its thermodynamic database and "selects" minerals to precipitate (Wolery, 1983). In such cases the user must "restrain" the calculations, using geochemical experience, to maintain a level of reality in the simulation.

Differences in thermodynamic data for a given mineral would lead to different predicted solubilities. However, differences found for the minerals reviewed were less crucial since the minerals of importance in modelling the Koongarra system, uraninite, the uranyl silicates and the uranyl phosphates, were found in each listing. The high consistency found for uraninite should result in a well-defined source-term for uranium migration. Data for uranyl silicates were generally sparse, though there was a fair degree of consistency for coffinite and uranophane. In contrast, significant differences were found for the autunite minerals.

16.1.2 Recommendations

On the basis of the review, the following recommendations were made concerning thermodynamic data relevant to geochemical modelling of Koongarra:

- thermodynamic databases should contain entries which are traceable to their source measurements
- a database should be internally consistent and should be employed in a consistent manner; for example, if the data have been referenced to infinite dilution using one method of ionic strength correction, then it is necessary to use the same method in modelling calculations
- it is desirable that a confidence level is assigned to each database entry so that an assessment of the total uncertainty associated with any calculation can be made
- where further data are required to facilitate a calculation, any values added to the standard database being used should be clearly stated
- erroneous data for aqueous species $UO_2(HPO_4)_2^{2-}$ and $UO_2(HPO_4)^{\circ}$ present in the literature should be excluded from calculations made for the Koongarra site
- thermodynamic data for mineral species which exhibit a range in degrees of crystallinity should be given with an appropriate description of the state of the material used in the experimental work from which the data were derived, and
- probably the best reported experimental data for the solubility of the autunite group minerals in the published literature are those of Magalhaes et al. (1985); however, thermodynamic data for these minerals should be recalculated taking into account new findings concerning the stability of aqueous uranyl phosphate species and their degrees of hydration.

16.1.3 Conclusions

The underlying geochemical concepts behind the computer programs used to perform equilibrium calculations are essentially identical from one code to another. Detailed comparison of the codes themselves by means of cross verification tests showed that relatively little uncertainty results from the use of alternative programs.

The greatest differences in the predictions made by the ARAP participants were likely to arise from a combination of:

- the uncertainty in the thermodynamic data (including data used to parameterise the chosen sorption models)
- gaps in the standard thermodynamic databases; this is especially important for Koongarra regarding secondary uranium minerals
- the use of geochemical models outside their strict range of applicability (e.g. at high ionic strengths), and
- perhaps most significantly, differences in the conceptual models of the Koongarra site itself; conceptual models used as the basis for the calculations should be soundly based on field and experimental data for the Koongarra site;

similarly, the reasons for the choice of a particular geochemical model (e.g. Triple Layer Model or Diffuse Double Layer Model) to approximate the adopted conceptual model should also be given.

16.2 Modelling of Present-Day Groundwaters

The objectives of the study were to carry out geochemical modelling of Koongarra waters and interpret the water speciation and saturation states in order to establish the factors controlling the groundwater compositions and chemical evolution and their present state. The results of the calculations established the dominant species thought to be present in these groundwaters and the apparent states of saturation of the waters with respect to minerals and mineral assemblages through which the groundwaters might have migrated. The results were then used to infer possible rock-water interactions influencing or controlling aspects of the compositions of the groundwaters. All such inferences were tested and evaluated through reaction path calculations oriented towards studying the chemical evolution of the waters sampled at the present-day.

Aqueous speciation, saturation state and chemical mass transfer calculations were carried out using EQ3NR and EQ6 and a thermodynamic database generated at the Johns Hopkins University in 1984-92. In assembling these data, considerable effort was made to avoid inconsistencies that could introduce significant errors into the modelling calculations.

16.2.1 Speciation calculations for Koongarra waters

Initially, aqueous speciation models were used to calculate the composition of representative Koongarra waters. The groundwaters selected were from three depths: shallow, at 13 m depth in the weathered zone; intermediate, at 23 m depth in the transition zone; and deep at $\geq$ 37 m depth in the unweathered zone.

The shallow waters have acidic pH, high CO_2 and SiO_2 contents and low cation and anion contents. In contrast, the deepest groundwaters have slightly alkaline pH, low CO_2 and high HCO_3^- and magnesium contents. In the main No. 1 orezone containing uranyl oxide and silicate minerals, the deep groundwaters contain uranium up to about 0.1 mg/L. Waters from intermediate depths have characteristics intermediate between the shallow and deeper depths but have the highest values of SiO_2 (up to 43 mg/L) and PO_4 (up to 0.6 mg/L) at the site. In contrast to even the shallowest groundwater, rain water has a distinctively acid pH (about 4.4) and low levels of all other constituents.

The waters from the three depth intervals were thought to be representative of parts of a continuum of compositions, speciations and saturation states that extend from present-day rain water to deep (45 m) groundwaters in the primary orebody. In terms of chemical speciation, the three groundwaters showed systematic changes as a function of depth. This can be seen in Table 16.1, which depicts the predominant aqueous species calculated. It must be noted that these results were dependent on the species included in the model.

TABLE 16.1

PREDOMINANT SPECIES CALCULATED FOR EACH ELEMENT IN SELECTED GROUNDWATERS

Element	Shallow Groundwater	Intermediate Groundwater	Deep Groundwater
	W4A, 13m (Oct. 1989)	W4A, 23m (Oct. 1989)	PH49, 45m (Oct. 1989)
Na	Na^{+}	Na^{+}	Na^{+}
K	K^{+}	K^{+}	K^{+}
Ca	Ca^{++}	Ca^{++}	Ca^{++}
Mg	Mg^{++}	Mg^{++}	Mg^{++}
Al	AlF^{++}	$Al(OH)4^{-}$	$Al(OH)4^{-}$
Si	SiO_2	SiO_2	SiO_2
Zn	Zn^{++}	Zn^{++}	Zn^{++}
Pb	Pb^{++}, $Pb(HCO_3)^{+}$	$Pb(CO_3)$	$Pb(CO_3)$
Ba	Ba^{++}	Ba^{++}	Ba^{++}
C (total)	CO_2	HCO_3^{-}, CO_2	HCO_3^{-}
Cl	Cl^{-}	Cl^{-}	Cl^{-}
S	$SO4^{--}$	$SO4^{--}$	$SO4^{--}$
F	F^{-}	F^{-}	F^{-}
Mn	Mn^{++}	Mn^{++}	Mn^{++}
Fe	Fe^{++}	Fe^{++}	Fe^{++}
Cu	$Cu(OH)3^{-}$	$Cu(OH)3^{-}$	$Cu(OH)3^{-}$
U	$UO_2(CO_3)$, $UO_2(CO_3)2^{--}$	$UO_2(CO_3)2^{--}$	$UO_2(CO_3)2^{--}$
P	H_2PO4^{-}	H_2PO4^{-}, H_2PO4^{--}	H_2PO4^{-}, H_2PO4^{--}

The strong dependence of uranium speciation on depth is a direct consequence of the changes of pH and oxidation state of the groundwaters with depth. In the secondary orezone which contains uranyl phosphate minerals, the shallow groundwaters contain uranium predominantly as the species $UO_2CO_3(aq)$ and PO_4 predominantly as the species $H_2PO_4^-(aq)$. In the main orezone which contains uranyl oxide and silicate minerals, the deep groundwaters contain uranium predominantly as the species $UO_2(CO_3)_2^{--}$ (aq) and PO_4 (about 0.1 mg/L) predominantly as the species $H_2PO_4^-(aq)$, HPO_4^{--} (aq) and $MgHPO_4(aq)$.

These trends in water speciation can be seen in Figure 16.1, which shows the speciation of uranium calculated as a function of the oxidation state of the system, represented by $\log f_{O2}$, and the pH. It can be seen that the uranium speciation of the shallow and deep groundwaters refers to the $\log f_{O2}$ and pH fields corresponding to $UO_2CO_3(aq)$ and $UO_2(CO_3)_2^{--}$, respectively.

The trends can also be shown on ionic activity diagrams where the influence of rock-water interactions involving dissolution or precipitation of minerals can be displayed. They show a simple trend in $\log(a_{K+}/a_{H+})$ versus $\log(a_{Mg++}/(a_{H+})^2)$ that approaches the kaolinite/Mg-chlorite boundary (Figure 16.2). The diagrams include stability fields for kaolinite, muscovite, clinochore and phlogopite in equilibrium with quartz and water at 25°C and 1 bar. The trend from rain water activity ratios through to the kaolinite-chlorite-quartz boundary also corresponds to progressively increasing depth over the whole site (see Figure 16.3) indicating that the relatively unreacted waters are the shallowest and that the most reacted waters are at greatest depth.

The trends shown in Figures 16.2 and 16.3 are consistent with shallow waters from within the weathered zone undergoing progressive reaction with Mg-rich chlorite schist to evolve to the compositions of the deepest waters. These are possibly close to equilibrium with fresh (unweathered) chlorite schist. The trend of activity ratio could also be extrapolated back to rain water values. Hence, it was concluded that the waters have evolved through reactions such as:

chlorite kaolinite

$$Mg_5Al_2Si_3O_{10}(OH)_8 + 10CO_2 + 3H_2O = Al_2Si_2O_5(OH)_4 + 5Mg^{++} + 10HCO_3^- + SiO_2$$

which suggests that the initial water charged with CO_2 will react with chlorite to produce waters containing $Mg:HCO_3^-$: SiO_2 in the ratio 5:10:1. This is a good approximation to the compositions of the deepest, extensively reacted, Koongarra groundwaters.

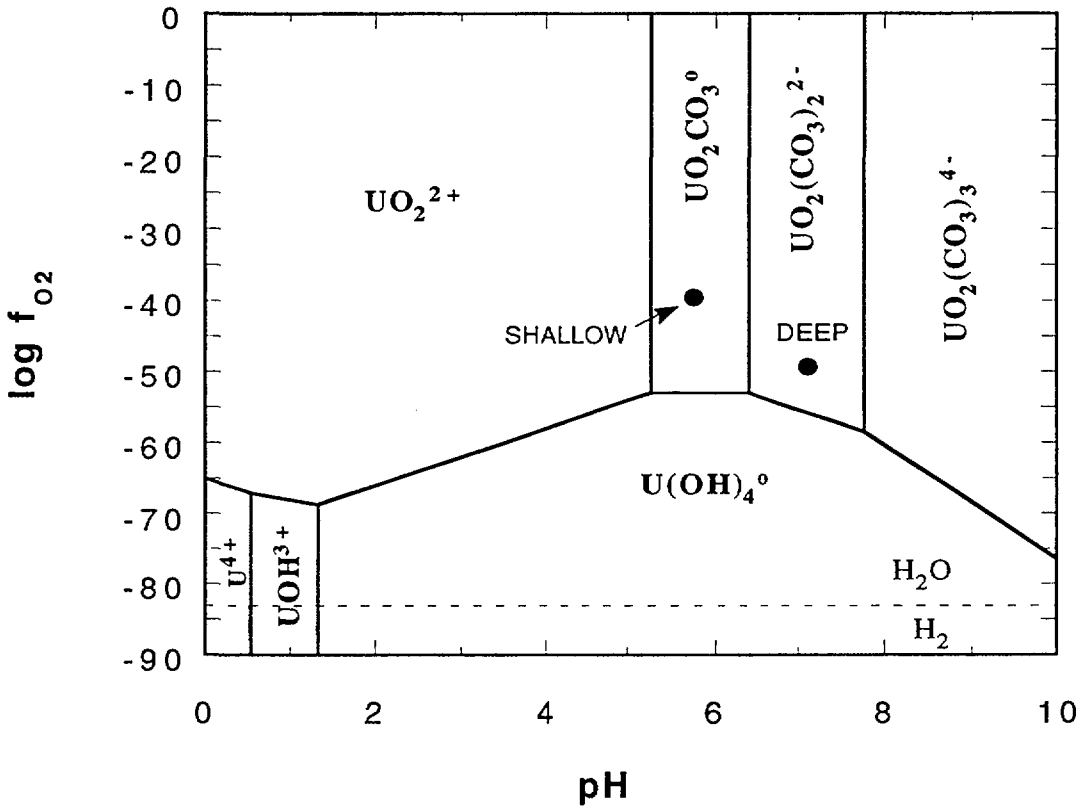

FIGURE 16.1 Calculated speciation of uranium as a function of the oxidation state of the system ($logf_{O2}$) and pH (based on data from Grenthe et al., 1989) at a partial pressure of CO_2 of 0.01 bars. The two points plotted represent shallow and deep groundwaters from Table 16.1

16.2.2 Modelling of the chemical evolution of present-day groundwaters

The weathering of chlorite-rich rocks also has important implications for the transport of uranium in the present-day groundwaters. In the shallow groundwaters, which are acidic and CO_2-rich, uranium is soluble only because these waters are also sufficiently oxidising. In the deep groundwaters, which are more reducing, uranium is nevertheless still soluble because the pH values of these waters are so much higher. This is a direct consequence of the conversion of CO_2 to HCO_3^- during weathering and the flow of the waters to greater depth, associated with addition of Mg and the alteration of chlorite to kaolinite.

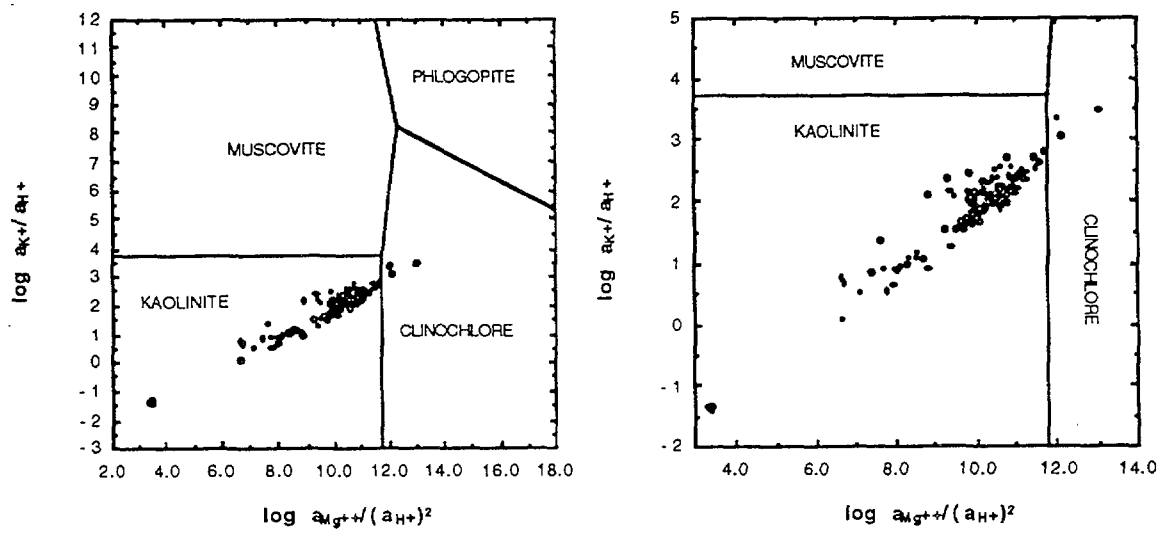

FIGURE 16.2 Partial log (a_K^+/a_H^+) versus $\log(a_{Mg}^{++}/(a_H^+)^2)$ diagram including the minerals kaolinite, muscovite, clinochlore and phlogopite in equilibrium with quartz at 25°C and 1 bar.

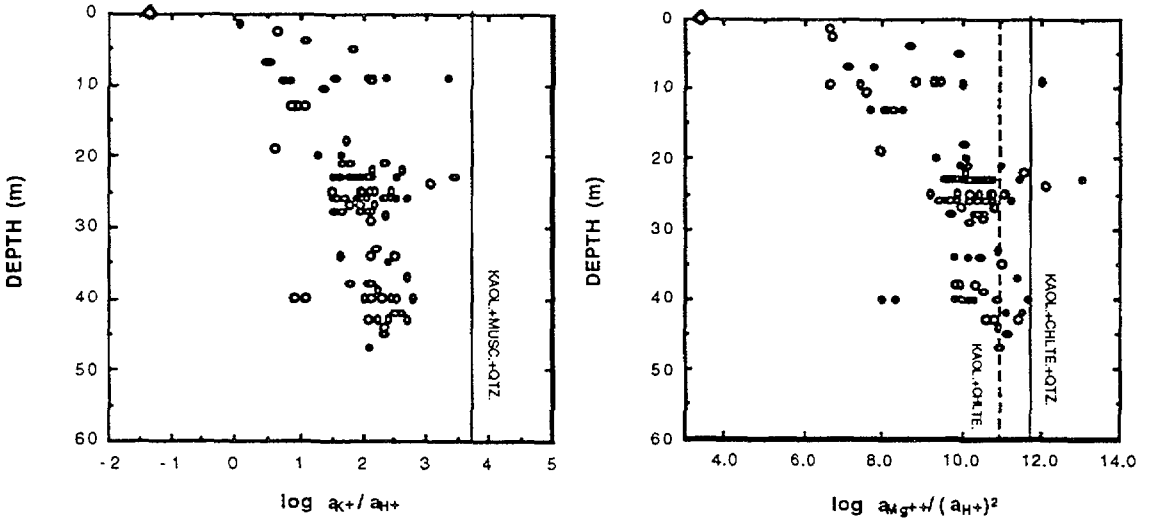

FIGURE 16.3 Depth dependence of the log (a_K^+/a_H^+) versus $\log(a_{Mg}^{++}/(a_H^+)^2)$ ratios of Koongarra waters compared to equilibrium boundaries at 25°C and 1 bar. The diamond at the top left of each diagram represents rainwater (Table 16.1).

Reaction path calculations were also used to confirm the hypothesis of acid attack on chlorite-rich rocks by CO_2 as the major driving force controlling the chemical evolution of the present-day groundwaters. It was shown that a typical shallow acidic groundwater from within the weathered zone followed a reaction path evolving

to a state typical of deep alkaline groundwater in equilibrium with kaolinite and chlorite. The resulting reaction path for chlorite schist can be seen in Figure 16.4, where the solid line represents calculated values and matches the natural waters closely. Table 16.2 lists the calculated final water and actual groundwater.

Similar calculations carried out with the same initial groundwater but with different initial (chlorite-free) rock types, such as garnet schist or feldspar schist, produced waters with significantly different chemistry. The reaction path on the activity diagrams also diverged from the natural waters.

16.2.3 Implications for the migration of radionuclides in natural analogues

The most important implication of the study for the migration of radionuclides is the strong role played by water-rock interactions, both above and below the water table. These influenced the overall chemical evolution of the groundwaters from rain water to deep groundwater. The first stage of the evolution is the interaction of rainfall and runoff with vegetation and near surface sands and soil, and evaporation. It is suggested that these processes explain the differences between precipitation and the shallowest groundwaters sampled in the ARAP. During these processes, the groundwaters are charged with CO_2 and can then undergo substantial chemical evolution.

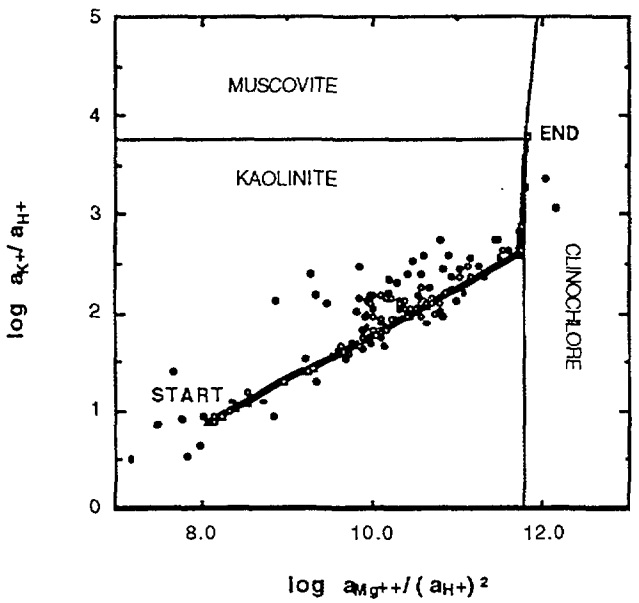

FIGURE 16.4 Computed reaction path for the predicted weathering of chlorite schist by shallow groundwater (Table 16.2). The solid line represents calculated values of log (a_K^+/a_H^+) and log($a_{Mg}^{++}/(a_H^+)^2$) activity ratios and matches the natural waters closely.

TABLE 16.2

PREDICTED WEATHERING OF CHLORITE SCHIST BY SHALLOW GROUNDWATER

Element or Species	Shallow Present-Day Groundwater[1]	Final Water after Reaction with Chlorite Schist[2]	Actual Deep Groundwater[3]
Na	1.70	1.70	1.28
K	0.53	0.90	0.75
Ca	2.19	2.19	8.15
Mg	10.7	47.0	26.9
Al	0.19E-09	4.4E-06	
Si	9.4	10.0	8.6
Zn	0.029	4.7E-08	0.0094
Pb	0.0009	1.4E-09	0.0012
Ba	0.024	0.0030	0.0073
C (total)	52.8	52.0	36.0
Cl	6.4	6.4	3.1
S	0.27	0.25	0.34
F	0.11	0.11	0.39
Mn	0.54	0.54	0.043
Fe	0.78E-09	4.7E-06	
Cu	0.0011	1.3E-12	0.002
U	0.44	9.9E-05	0.13
P	0.011	0.011	0.040
HCO_3^-	54.3	232.5	154.2
CO_3^{--}		0.25	
Other			
pH	5.75	7.26	7.10
$Logf_{O2}$	~39.5	-71.08	-49.3
$Logf_{CO2}$	-1.00	-1.98	-1.91
$Loga_{Mg}^{++}/a_H^{+2}$	8.06	11.65	11.11
$Loga_K^{+}/a_H^{+}$	0.86	2.59	2.35
$Loga_{Ca}^{++}/a_H^{+2}$	7.16	10.01	10.38
T (°C)	25.0	25.0	25.0

1 Groundwater from W4 (Oct.1989). Note that Al and Fe values given in the Table are calculated assuming equilibrium with kaolinite and hematite, not the analytical values.

2 After reaction of the water in Column 1 and the first appearance of chlorite in the reaction path calculation

3 As listed above.

The chemical evolution of waters in the system is strongly controlled by the initial availability of CO_2 and the rock types (mineral assemblages) encountered, which together determine the major element evolution of the waters by controlling the pH. The evolution of the pH of the moving groundwaters, in turn, reflects changing carbonate speciation in the waters. Because radionuclides such as uranium form complexes with carbonate in groundwaters, the acquisition of uranium by groundwaters from uranium-bearing solid phases is strongly influenced by the rate of

evolution of the pH of the groundwaters.The relative rates of evolution of the pH and the oxidation state of the groundwaters are also critical to the mobility of uranium. As emphasised above, the shallow Koongarra groundwaters are sufficiently oxidising that they can dissolve and transport uranium even under acidic conditions. Under the more reducing conditions of the deep groundwaters, uranium can still be dissolved and transported because of the evolution of the pH to levels permitting strong carbonate complexing. If, however, the oxidation state of the groundwaters with respect to uranium were to evolve much lower, more reducing levels, it would be expected that uranium would become immobile.

16.3 Modelling of Secondary Uranium Ore Formation

The major objective of this work was to unravel geochemical processes involved in the formation of the secondary mineralisation zones at Koongarra and delineate the optimum chemical conditions for the formation of a major part of the secondary mineralisation. The overall approach employed theoretical mass transfer calculations to reconstruct the reactions that were associated with the formation of the uranyl phosphate zone at Koongarra.

Studies of the Koongarra site prior to the ARAP suggested two possible scenarios for the development of the phosphate zone (see above). According to one scenario, groundwater originating in the Kombolgie sandstone crossed the fault and weathered the primary ore to produce the dispersion. Alternatively, groundwater from vertical recharge above the primary orebody was associated with the weathering of the primary ore.

Consequently, in this study, two present-day waters were used as starting solutions for chemical mass transfer calculations simulating the weathering process over geologic time. One water was assumed to be similar to the deep groundwater sampled from the Kombolgie sandstone (KD1, see Volume 2 of this series). This water represents samples from across the fault away from the orebody as a possible source of water to weather the primary ore (see also Volume 7 of this series). The other water was assumed to be similar to the shallow groundwater presently near the unsaturated zone over the primary orebody (W4A). This water represents one of the most oxidising waters sampled at the present-day. This is, however, a relative term, as the water is certainly not in equilibrium with the atmosphere.

The uranium and phosphorous contents of these waters at the present day reflect their passage in the present-day Koongarra system.

16.3.1 Chemical mass transfer calculations

Two reference calculations were carried out for the same initial reactant assemblage and the same initial water composition, but under two different conditions.

In the first reference run, the unbuffered calculation, the initial partial pressures of CO_2 and O_2 used for the groundwater were typical of shallow Koongarra groundwaters. These reflect chemical conditions significantly different from rainwater that is "equilibrated" with atmospheric CO_2 and O_2. In the second

reference run, the buffered calculation, the partial pressures of CO_2 and O_2 of the shallow groundwater were fixed throughout the calculation at the partial pressures of CO_2 and O_2 in the atmosphere in order to approximate chemical reactions in the unsaturated zone.

The reference mineral reactant assemblage was an approximation of the primary ore. The accessory phases in the primary ore that are critical to the formation of the secondary uranyl phosphates are graphite, pyrite, apatite and pitchblende. Of these, apatite and pitchblende exhibit the greatest mineralogical and thermodynamic complexity. Apatite in and near the primary ore varies in composition but is mostly F-rich (see Volume 8 of this series). Pitchblende is a complex phase that has been approximated in the present study by the well-characterised phase U_3O_8.

The mineralogical results of the reference runs are shown in Table 16.3 and Figures 16.5 and 16.6. It can be seen that the unbuffered calculation resulted in the final equilibration of the groundwater with the reactants chlorite and muscovite, and the formation of the product minerals cristobalite, kaolinite, chalcocite, and uraninite. In contrast, the buffered calculation resulted in the final equilibration of the groundwater with the reactants chlorite and muscovite, and the formation of the product minerals cristobalite, kaolinite, hematite, and saleeite.

The unbuffered calculations did not produce the kind of assemblages presently found in the weathering zone at Koongarra. Instead, the fluid became overwhelmed by the reactions with the highly reducing initial assemblage and eventually equilibrated with that assemblage. Rather than corresponding to groundwater reactions in the formation of the weathered zone, these unbuffered calculations instead probably correspond more closely to present groundwaters deep in the Koongarra section. Without buffering by the atmosphere, the groundwater rapidly loses its dissolved O_2 content by reactions with Fe^{2+}-bearing minerals.

The buffering of the O_2 and CO_2 in the first set of calculations shown in Table 16.3 is apparently highly advantageous for the formation of the uranyl phosphate zone at Koongarra. Under these conditions, the oxidation state of the reacting system is forced to remain defined by the atmospheric partial pressure of oxygen. This keeps the dissolved uranium that is acquired by reaction with pitchblende in the U(VI) oxidation state throughout the calculations and the whole weathering sequence. Under these circumstances the fluid can accumulate uranium by progressive reaction with the pitchblende until it reaches saturation with respect to saleeite.

TABLE 16.3

MINERALOGY OF BUFFERED VERSUS UNBUFFERED REFERENCE CALCULATIONS

	Initial reactant mineral assemblage	Final equilibrium mineral assemblage
Unbuffered	Chlorite, Muscovite, Quartz, Pyrite, Graphite, Apatite U_3O_8	Chlorite, Muscovite, Quartz, Pyrite, Graphite Apatite **Kaolinite** **Chalcocite** **Uraninite**
Buffered	Chlorite, Muscovite, Quartz, Pyrite, Graphite, Apatite U_3O_8	Chlorite, Muscovite, Quartz, **Kaolinite** **Hematite** **Saleeite**

16.3.2 Formation of the phosphate zone

It is clear that there are a number of parameters and conditions which strongly favour the formation of a saleeite-rich secondary ore. Despite the uncertainties and inadequacies of the thermodynamic characterisation of saleeite (see above), the present study strongly suggests the formation of saleeite is favoured by the following conditions:

- the formation of the assemblage kaolinite + hematite + saleeite could proceed by the weathering of primary ore containing the hydrothermal alteration assemblage chlorite + muscovite + quartz + pyrite + graphite + apatite + pitchblende under conditions buffered by atmospheric CO_2 and O_2
- the initial source of uranium, i.e. its form in minerals, does not seem to be important to the overall formation of a saleeite-rich secondary orezone
- pyrite appears to be crucial under such circumstances because it keeps the pH of the fluid from rising to values consistent with saturation with respect to apatite or to silicates not found in the uranyl phosphate zone at Koongarra
- buffering by atmospheric O_2 is important to maintain Fe and particularly U in their oxidised states while sufficient saleeite and hematite form; if the atmospheric partial pressure of O_2 is not maintained and if the rate of reduction of U(VI) aqueous complexes to U(IV) aqueous complexes is relatively fast, the uranium contents of the groundwaters will be extremely low because of the formation of secondary pitchblende
- buffering by atmospheric CO_2 is important because it results in a relatively low-CO_2 solution in which the activities of HCO_3^- and $CO_3^=$ are too low to complex much of the uranium in solution; under these conditions the dominant complexes of uranium are hydroxy complexes, and saleeite is significantly less soluble, which strongly favours the precipitation of saleeite, and
- buffering by atmospheric CO_2 is also important because it leads to relatively low total dissolved carbon values that do not result in the predicted formation of magnesite ($MgCO_3$), a phase that does not occur at the Koongarra deposit.

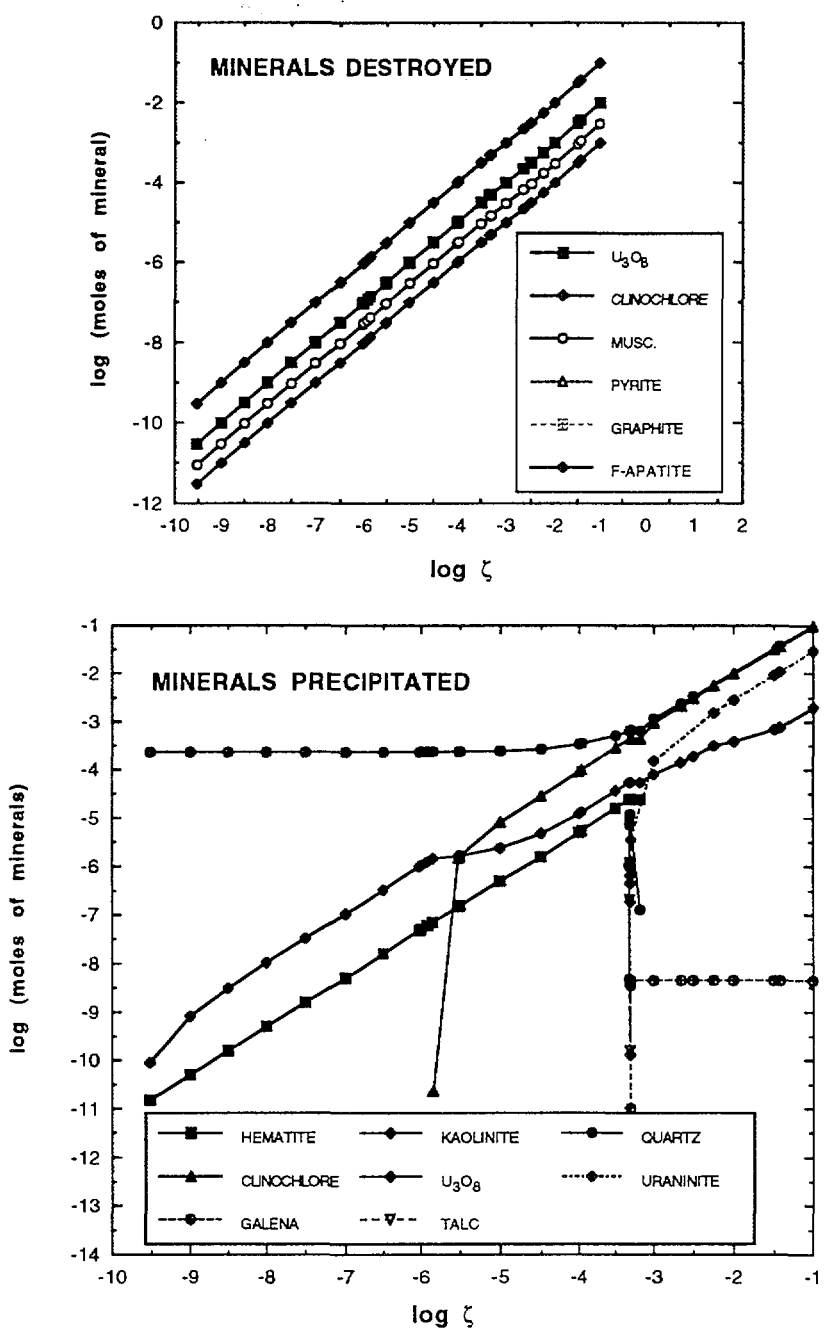

FIGURE 16.5 Results from unbuffered reaction path calculation: Evolution of the mineral phases

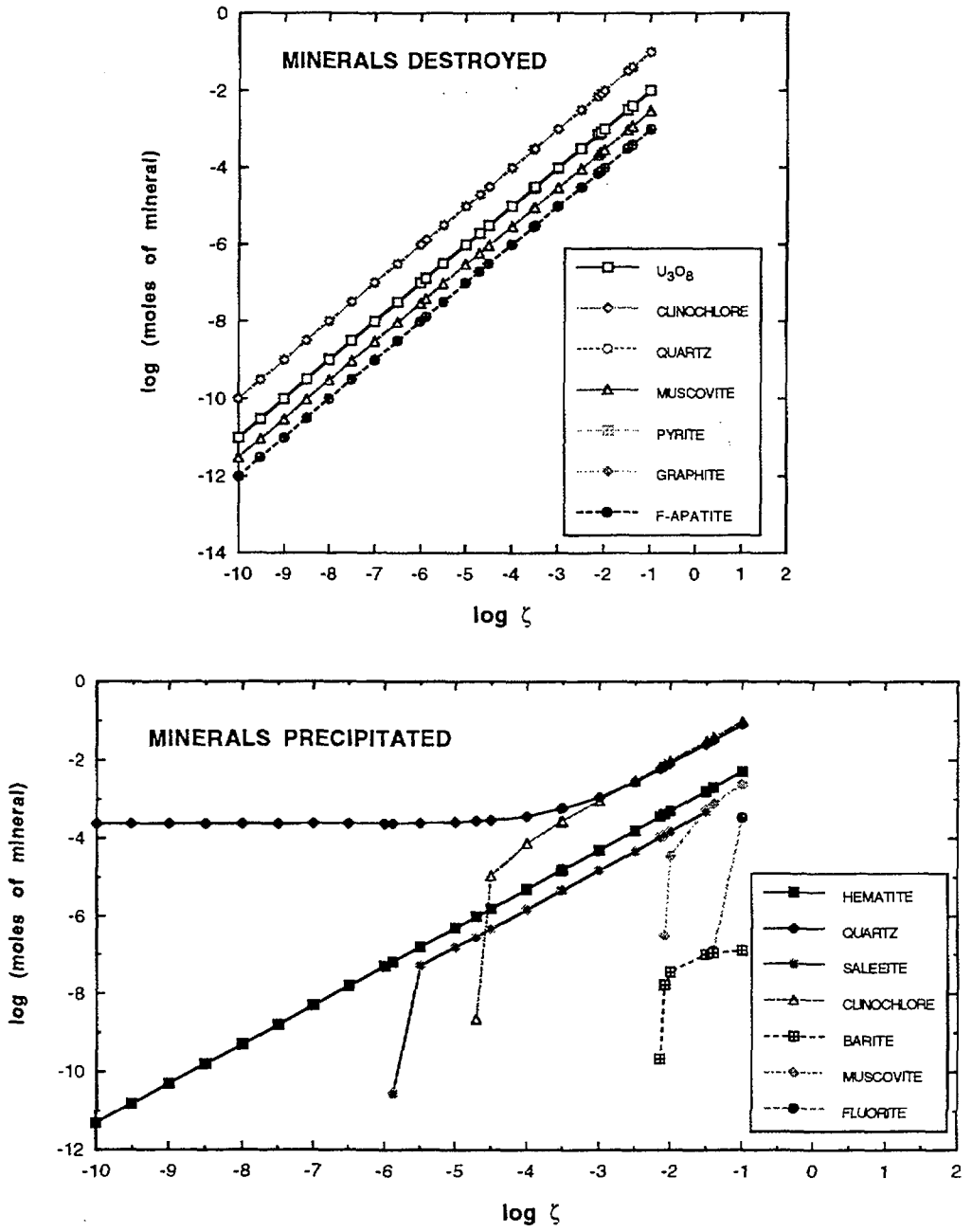

FIGURE 16.6 Results from buffered reaction path calculation: Evolution of the mineral phases

16.3.3 Formulation of a paleo-analogue model

The results concerning the formation of saleeite from water that was buffered by atmospheric CO_2 and O_2 strongly suggest that the formation of the uranyl phosphate zone took place in an unsaturated zone in which the pore spaces were partly filled with gases connected with the atmosphere. If we assume further that this unsaturated zone extended much deeper than at the present day, its base would be marked by the absence of any saleeite.

Therefore, the present base of the uranyl phosphate zone may represent (approximately) a paleo-water table. The base of the uranyl phosphate zone is at about the same level as the base of megascopically visible weathering, i.e. approx. 30 metres depth. Hence, it is suggested that the present-day secondary phosphate zone represents a paleoweathering profile that has subsequently been drowned by recent climatic changes and rises in the water table.

This suggests that the uranyl phosphate zone may have formed in a more arid climate that would have been associated with a much lower water table than at present. Such a climate may have prevailed prior to the relatively recent monsoonal climate initiated about 12,000 years ago. Although it is likely that a favourable arid climate in the geologic past would have alternated with a climate associated with a high water table and concurrent dissolution of the saleeite zone, the model suggested above would only require that the arid periods prevail. The present extent of the uranyl phosphate zone in cross section coincides with the maximum lateral extent of graphite-bearing hydrothermal alteration assemblages. This may possibly reflect a difference in the weathering and availability of PO_4.

16.3.4 Implications for the evolution of the phosphate zone

The formation of saleeite *in situ* must have proceeded from chemical weathering of primary ore because that was the ultimate source of the uranium in the weathered zone.

When the primary ore was essentially completely weathered and converted to an *in situ* uranyl phosphate zone, paleo-groundwater might have continued to enter the profile and started to dissolve the uranyl phosphates until it reached saturation with respect to one or more of them (e.g. saleeite). When this groundwater continued to migrate laterally through the partially weathered barren schist, further chemical reactions would be expected with the unweathered parts of the schist. These would be similar to the reactions discussed above and could result in the precipitation of saleeite to form a dispersion fan.

Under present-day climatic conditions, present-day groundwaters migrating through the secondary uranyl phosphate zone are actively dissolving and destroying it. Uranium acquired from the uranyl phosphate part of the dispersion fan may thus be in the process of being transported further out into the dispersion fan where no visible phosphate mineralisation is present and where uranium may be removed from solution by sorption processes.

16.4 Sorption

As discussed earlier, the migration of radionuclides in water-rock systems is largely controlled by precipitation/dissolution and adsorption/desorption reactions. The relative importance of these processes is dependent on the concentration and redox state of the radionuclide present, the tendency of the radionuclide-containing minerals to precipitate, and the availability and type of sorbing surfaces.

Although numerous studies of the partitioning of uranium between solid and solution phases have been reported, most of the data relating to U sorption in the natural environment is only of relevance to a particular solid substrate and groundwater composition. Hence, distribution coefficients (K_d values) obtained from these studies are not suitable for predicting the migration of uranium through porous media of variable composition, and under solution conditions that exhibit major spatial and temporal variability.

There have been some attempts over the last ten years to develop more general models of the adsorption of U(VI) to solid substrates, but most studies have only been conducted on a few simple (single mineral phase) substrates under a limited range of conditions.

A two-stage process was therefore undertaken within the ARAP. In the first stage, factors that influence the sorption of U(VI) to well-defined mineral phases (ferrihydrite, crystalline silica, and kaolinite) and to selected natural substrates from Koongarra, were investigated experimentally. The surface properties of the materials were rigorously defined, then adsorption studies were carried out over a range of solution pH, ionic strength, carbonate content, adsorbent and adsorbate concentrations, and in the presence of uranium complexants and potentially competing adsorbates, such as phosphate and fluoride. In the second stage, models of uranyl sorption were developed on the basis of the wide range of chemical conditions studied experimentally.

16.4.1 Experiments

Uranium was added to a slurry of the phase being studied and the pH was adjusted to the value required. The solid and liquid phases were separated by centrifugation 48 hours later and the amount of uranium remaining in solution was determined by either α-spectrometry or kinetic phosphorescence analysis. The wide range of solution/suspension conditions over which pH edges were measured is summarised in Table 16.4.

An example of the results from the experimental study is shown in Figure 16.7 for the pH dependence of adsorption of U(VI) to 10^{-3}M ferrihydrite for total uranium concentrations of 10^{-8}M, 10^{-6}M, 10^{-5}M and 10^{-4}M over a pH range of 3-6.

Whilst most studies were made under atmospheric conditions, some were performed in a glove box at an elevated partial pressure of carbon dioxide using a mixture of air and CO_2 plus N_2 gas. The presence of oxygen derived from the air ensured the stability of the solid phases against reductive dissolution.

TABLE 16.4

RANGE OF CONDITIONS UNDER WHICH pH EDGES HAVE BEEN OBTAINED FOR URANYL ADSORPTION TO VARIOUS SUBSTRATES

Condition	Ferrihydrite	Nichika kaolinite	KGa-1 kaolinite	Quartz	W1 Core	W2 Core
Ionic Strength [$NaNO_3$], M	0.004 0.02 0.1 1	0.004 0.1 1	0.1	0.005 (1) 0.01 0.1	0.1	0.022 0.1 0.2 2.2
U(VI), M	10^{-8} 10^{-6} 10^{-5} 10^{-4}	10^{-6} 5.10^{-7} to $2.7.10^{-4}$ (2)	10^{-6}	10^{-6}	See text Volume 7 of this series	See text Volume 7 of this series
Solid to liquid ratio	10^{-3}M 2.10^{-2}M (as Fe)	1 g/L 4 g/L 16 g/L	4 g/L	100 g/L	20 g/L	4 g/L
CO_2, %	0.03 1	0.03	0.03	0.03	0.03 1	0.03 1
Phosphate, mM	0 2.5, 10, 30 (3), 100	0	0	0 2	0	0
Fluoride, mM	0	0	0	0 0.1 0.5	0	0
DCB leach	No	Yes	Yes	No	No	Yes

1 KNO_3 rather than $NaNO_3$ used to avoid NaF precipitation

2 Uranium adsorption determined at pH 6.5 only

3 Effect of phosphate at these concentrations examined only at pH 4.0

Given the importance of carbonate complexation to U(VI) speciation and the elevated partial pressures of carbon dioxide found in subsurface waters in the Koongarra region, investigation of the impact of CO_2 partitioning between solution and solid phases was considered to be a high priority. The effect of another potential uranyl ligand, phosphate, on the adsorption of U(VI) was also investigated.

A range of ancillary studies helped define important sorbing surfaces and elucidate the effects of chemical processes on uranium partitioning between the solid and solution phases. An examination of U(VI) uptake on preformed and co-precipitated iron oxides indicated very little difference in partitioning, and suggested that short term aging of amorphous iron oxide phases does not dramatically influence the sorbing capacity. Ferrihydrite aging (transformation to more crystalline forms such as goethite and hematite) resulted in a reduction in surface area with a concomitant decrease in adsorption of U(VI). Uranium present during the transformation process was partially incorporated into the resulting solid phase, with a consequent decrease in its availability for desorption.

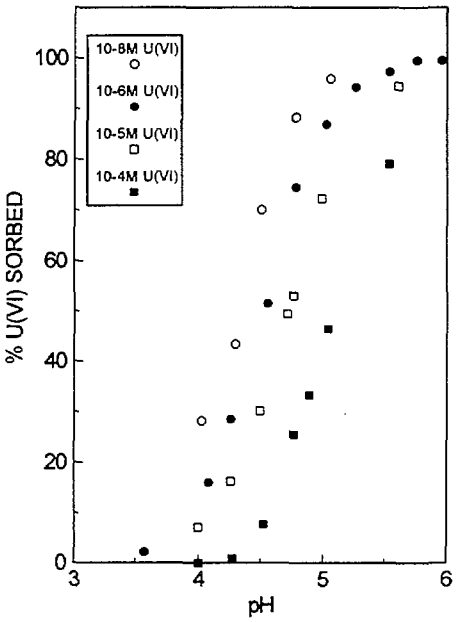

FIGURE 16.7 *U(VI) sorption to 10^{-3} ferrihydrite for total uranium concentrations* of 10^{-8}M, 10^{6}M, 10^{-5}M and 10^{-4}M over a pH range of 3-6. Experiments carried out in 0.1 M $NaNO_3$ in equilibrium with air.

Fine fractions (nominally < 10 mm) of natural substrates from Koongarra were also examined. These were taken from a depth of ~ 13m in boreholes W1 and W2 (see Figure 6.4) where groundwater had been sampled in the groundwater chemistry measurement program. In addition to measurements of partitioning between solution and solid phases, the relationship between ^{236}U in solution and ^{238}U leached from the samples was determined to provide information on the amount of accessible uranium present. The estimate of total accessible U(VI) was found to be in good agreement with the Tamms acid oxalate (TAO) (see Table 12.1) extractable uranium in these samples.

Results of the adsorption studies of uptake of U(VI) to fine fractions of the W1 (13m) sample can be seen in Figure 16.8. As observed for single phases, U(VI) is sorbed strongly to the natural substrate in the mid-pH region (5-8) but increasingly exhibits a preference for the solution state as the pH falls below 5 and as the pH rises above 8 (attributed to the strength of uranyl carbonate complexes).

16.4.2 Modelling

Models used to describe the equilibria of adsorption-desorption reactions at mineral surfaces can be classed into two main types: empirical partitioning relationships and conceptual models for surface complexation, which use a formalism of ion association reactions in solution to represent surface reactions.

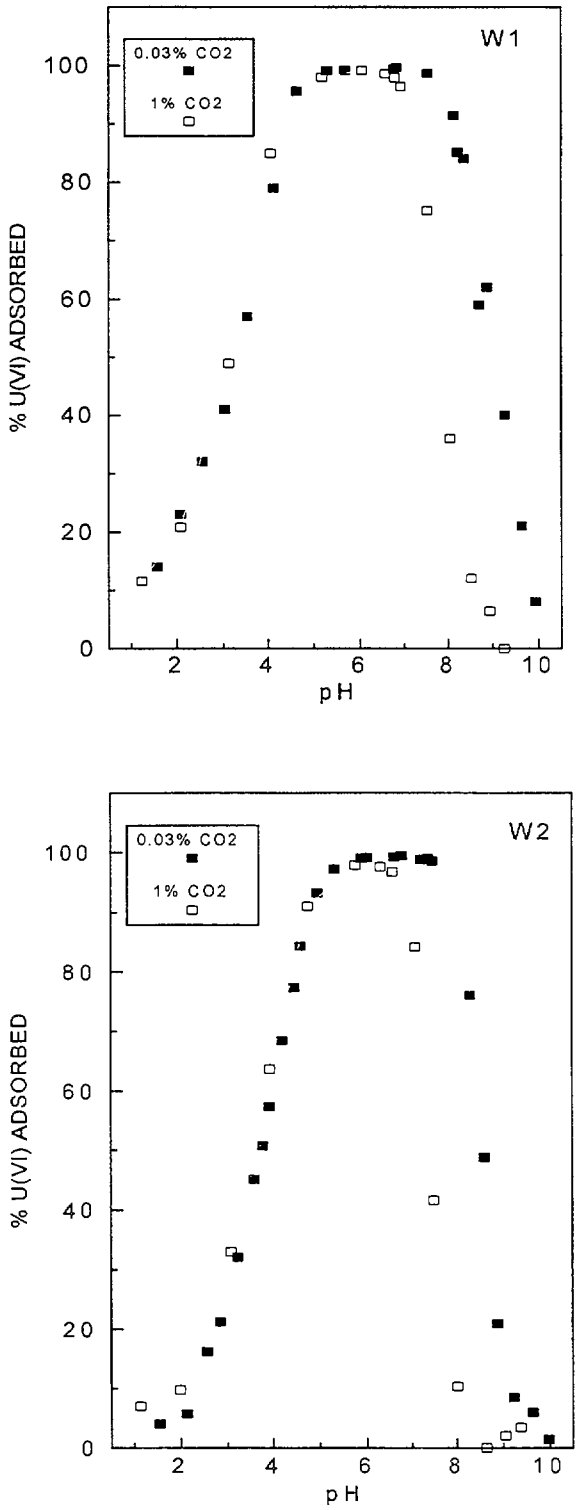

FIGURE 16.8 U(VI) adsorption to fine fractions of W1 (20 g/L) and W2 (4 g/L) core materials as a function of pH and at 0.03% and 1% CO_2. $[U]_{TOTAL}$ determined by concentration of accessible ^{238}U.

Because of the complexity of natural systems an empirical approach has been widely used to describe the partitioning of solutes between mineral and water phases in transport modelling (see Section 17). Many current models used for the assessment of the long-term fate of radionuclides rely on distribution coefficients (K_d); however, reversible conditions must be ensured, as must the linear dependence of adsorbed solute concentration on solution phase solute concentration.

There have been some attempts over the last ten years to develop more general models of the adsorption of U(VI) to solid substrates. Studies have been conducted on a few simple (single mineral phase) substrates but little agreement exists either between the data obtained or in the optimal modelling approach. However, surface complexation models have been finding increasing acceptance (e.g. see below an example of transport modelling using the computer code CHEMTARD).

The aim of the current work was to develop a predictive model of U(VI) partitioning between solution and the natural substrates which would build upon the preliminary surface complexation modelling of uranyl sorption to single minerals.

16.4.3 Modelling single minerals

Adsorption of U to ferrihydrite was modelled using the surface complexation approach with a diffuse double layer description of the electrical double layer. While a single site type was used initially, most success was achieved by assuming the presence of two site types. One site type corresponded to a small set of high affinity cation binding sites and the other type to the total reactive sites available for sorption of protons, cations and anions. Mononuclear uranyl surface species provided an adequate description of the adsorption results.

A combination of adsorption to "strong" and "weak" sites forming hydroxylated uranyl surface complexes, $SOUO_2OH$ and $TOUO_2OH$, respectively, i.e.

$$SOH + UO_2^{2+} + H2O \Leftrightarrow SOUO_2OH + 2H^+$$

$$TOH + UO_2^{2+} + H_2O \Leftrightarrow TOUO_2OH + 2H^+$$

gave excellent agreement between model and experiment (Figure 16.9); however, addition of $SOUO_2^+$ and $TOUO_2^+$ into the model reduced the variance further. Best-fit constants were derived using the non linear optimisation program, FITEQL. Adsorption under basic conditions, where uranyl carbonate species dominate the solution speciation of U(VI), was also satisfactorily described without recourse to specific adsorption of uranyl carbonate complexes, even under elevated partial pressures of carbon dioxide typical of Koongarra groundwaters.

A surface complexation model involving only uptake on "weak" sites (to form $TOUO_2OH$) provided a good description of U(VI) sorption to quartz and this simple model adequately described the competing effect of solution complexation of U(VI) by fluoride.

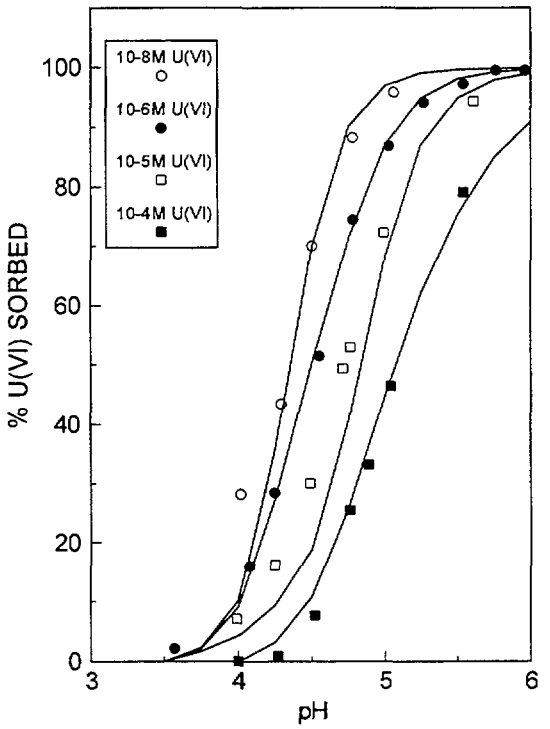

FIGURE 16.9 Results of surface complexation modelling assuming the formation of $SOUO_2OH$ and $TOUO_2OH$ at strong and weak adsorbing sites (SOH and TOH) of concentrations 7 x 10^{-7}M and 2 x 10^{-4}M, respectively with log (formation constants) at these sites of –1.60 and –5.21, respectively.

The results of modelling uranyl adsorption to kaolinite were less satisfactory. Reasonable correspondence between experiment and model results was obtained at low U(VI) concentrations with a model incorporating both ion exchange and specific adsorption to strong and weak sites, i.e.

$$NaX + UO_2^{2+} + H_2O \Leftrightarrow UO_2OHX + H^+ + Na^+$$

$$SOH + UO_2^{2+} \Leftrightarrow SOUO_2^+ + H^+$$

$$TOH + UO_2^{2+} + H_2O \Leftrightarrow TOUO_2OH + 2H^+$$

but this model did not adequately describe the experimental data obtained at high U(VI) concentrations. Further insight into the factors controlling uranyl uptake on kaolinite is still required.

16.4.4 Modelling the substrates

Preliminary modelling which assumed all U(VI) adsorption to the natural substrates could be accounted for by uptake on amorphous (TAO extractable) iron oxides, was reasonably successful. However, more detailed analysis indicated significant difficulties with this approach. The uniform site density per unit area assumed in the modelling also led to serious under-prediction of U adsorption (when reasonable site densities were used).

A reasonable fit (see Figure 16.10) to the experimental data was obtained using a more complex model with the following features:

- a large concentration of strongly acidic, strongly binding sites, and
- an even larger concentration of weakly binding sites, with acidic properties similar to ferrihydrite.

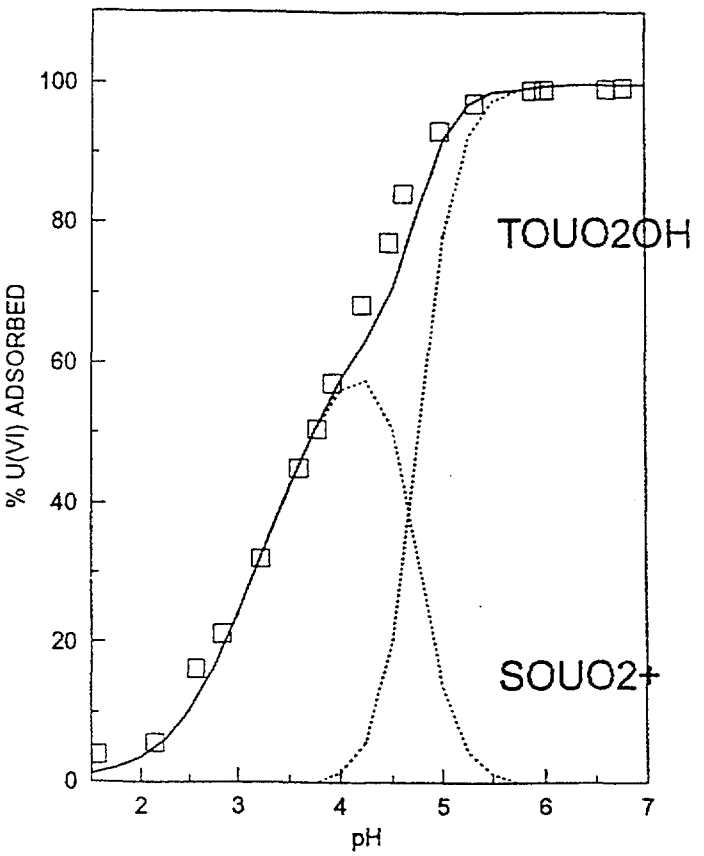

FIGURE 16.10 Comparison of experimental data and a model which contains both highly acidic strongly binding sites (forming $SOUO_2^+$) and sites more typical of iron oxyhydroxide (forming $TOUO_2OH$)

While the agreement demonstrates that it is possible to derive a model that adequately describes the experimental data, the parameter values were chosen by methods little better than trial and error.

16.4.5 Conclusions

The extensive database from the experimental study, with a number of parameters being varied over a wide range, has enabled more confidence to be placed in the modelling results. In the case of ferrihydrite, the model adequately accounted for the effect on U sorption of a number of parameters, most notably pH, P_{CO2} and total U present. Few (if any) earlier models are adequate in this respect.

Although the modelling of the natural Koongarra substrates is not as advanced, insights obtained in modelling the ferrihydrite data will be valuable in deriving a model for the more complex natural substrates. However, considerably more insight into the nature of surface binding groups on the natural Koongarra substrate is required before undertaking more detailed modelling work.

17 RADIONUCLIDE TRANSPORT MODELLING

The aims of the transport modelling were:

(a) to understand the processes that retard the migration of uranium series radionuclides, and

(b) to obtain bounds on the timescale over which the dispersion fan has been formed and to compare these bounds with constraints emerging from geomorphological studies.

A large number of models were used in the ARAP to interpret the large database available from Koongarra of concentrations of uranium series radionuclides in the groundwater and in the solid phases. The work, reported in Volume 14 of this series, focussed on the ^{238}U series, and to a lesser extent on the ^{232}Th and ^{235}U series; other studies of ^{239}Pu, ^{129}I, ^{99}Tc and ^{36}Cl have been discussed earlier in this report. All of these radionuclides are found in radioactive wastes, hence, the Koongarra ore deposit can be regarded as an analogue of a repository containing such wastes.

The modelling approaches had to deal with many uncertainties in representing the Koongarra site and its evolution with time. These have been discussed in earlier sections, but include the hydrogeology, the effect of climatic variations, and the heterogeneity of the weathered zone. Consequently, it was found that there are a number of models that fit the available data, hence it was not possible to conclude that any one particular model was correct and that the others were incorrect. Rather, it was possible to identify important processes affecting uranium transport and then apply a broad variety of modelling approaches. The different assumptions and concepts incorporated in the models are summarised in Table 17.1.

Many processes control the amount of radionuclides that are removed from the groundwater in the dispersion fan. These include equilibrium sorption modelled by a

simple K_d approach and sometimes by a more detailed model, chemical incorporation into iron oxides, uranium minerals or other crystalline phases, and recoil transfer of daughter products resulting from alpha-decay. Uranium in some of the crystalline phases is not in isotopic equilibrium with the groundwater, whereas in other phases it is in isotopic equilibrium, i.e. inaccessible and accessible phases, respectively.

It was, therefore, convenient to divide the one-dimensional models into three types involving:

- partitioning of uranium between groundwater and one solid phase
- partitioning between groundwater and more than one solid phase, and
- a more realistic representation of the geochemical processes determining partitioning between groundwater and rock.

17.1 Partitioning of Uranium between Groundwater and One Solid Phase

The first type of model is similar to simple models often used in performance assessments and is easy to represent mathematically. The transport equation usually contains a simple equilibrium sorption term that relates to the whole rock matrix. The distribution coefficient K_d describes the radionuclide equilibrium distribution ratio between the whole rock matrix and adjacent groundwater. However, this is not consistent with analytical measurements for the site, which have shown that most of the radionuclide in the rock is not directly accessible to groundwater and therefore cannot be treated as sorbed. A simple K_d based on the total amount of uranium in the rock can therefore be much too high.

The second type of transport model considered the separate groundwater accessible and inaccessible mineral phases in the rock, hence was more consistent with available analytical data. However, this model is more complicated mathematically, has more free parameters and requires more data on the system. The models developed incorporated recoil processes and kinetically limited chemical exchange between groundwater and a crystalline phase. To achieve anything more than a very crude representation of the processes controlling and retarding radionuclide transport at Koongarra, it is necessary to use a model with at least this degree of complexity. Models with more phases have also been attempted, although it was hard to obtain estimates of many of the relevant geochemical parameters.

A number of modelling attempts concentrated on data from specific horizons as it was considered this would minimise problems arising from heterogeneity. There is also some evidence for preferential flow in some layers. Data from one depth interval may correspond to one streamline, hence may be less heterogeneous.

TABLE 17.1

SUMMARY OF CONCEPTS INCORPORATED IN RADIONUCLIDE TRANSPORT MODELS

model		structure			transport processes			retardation processes			
name	sectn	dim	path	couplg	adv	disp	m.diff	sorpt	precip	phase	recoil
open system	5.1		1					x			
multiphase	5.2		1					x		x	x
retarded velocity	5.3	1			x			x			
transport time	5.3	1			x			x			
simple two phase	5.4	1			x			x		x	
simple models	6.1	1			x			x			
one phase, box	6.2	1	1		x	x		x			
access phase, box	6.2	1	1		x	x		x		x	
modif. tr. time	6.2r	1	1		x			x			
m.tr.time-access	6.2r	1	1		x			x		x	
perform. assess	6.3	1			x	x		x			
two-phase access	7.1	1	1		x	x		x		x	x
two-phase transp.	7.2	1			x			x		x	x
adv-disp-sorp-fix	7.3	1			x	x		x		x	
Th fixation	7.4	1			x			x		x	x
prefer. pathways	8.1	2(q)	2		x	x		x		x	
adv-disp-sorption	8.2	2(q)			x	x		x			
evolving tr. zone	8.3	2(q)			x			x		x	x
NAMMU	8.4	2			x	x		x			
saleeite dating	9.1	1							x		
CHEMTARD	9.2	1		x	x	x		x	x		

Some models considered flow concentrated in the lower part of the weathered zone but these models were unable to represent precisely the evolution of the weathered zone as the data were not sufficient to constrain the model. As there are many uncertainties in the system, 1D modelling was generally adequate. However, 2D models constructed out of a number of 1D models offer some potential to explore possible histories for the dispersion fan. These models can illustrate possible histories of the dispersion fan in a qualitative manner; however, at this stage it is not possible to calibrate these models unequivocally in a quantitative manner.

An example was developed to estimate the effects of chlorite weathering on uranium migration. It considered such factors as changes in distribution coefficients and porosities with time and was based on a one-dimensional advection-dispersion-sorption model. This model resulted from the chlorite weathering studies reported in Section 13. Chlorite weathering increases the retardation factor of uranium by a factor of 2.5 compared to that without weathering. By assuming a Darcy velocity and an initial uranium concentration in the groundwater similar to present-day values, the calculated uranium concentrations in the rock are in good agreement with the measured values (Figure 17.1). However, when time-dependent chlorite weathering was absent the calculated results did not agree with those observed.

Uranium movement in two dimensions has been modelled using the multi-dimension groundwater flow and radionuclide transport code, NAMMU (Atkinson et al., 1986). This built upon the earlier work discussed in Section 15.1 to explore the shape of the radionuclide plume and its evolution with time. The choice of hydrogeological parameters could be evaluated by comparing the shape of the calculated uranium profile with the current shape of the dispersion fan. The model is particularly sensitive to permeability contrasts between the weathered zone and the unweathered Cahill Schists. However, full data for a complete calibration of the model are currently lacking.

Nearly all of the models assumed constant groundwater flow parameters with time. However, models that simulated the end of uranium transport some hundreds of thousands of years ago showed that such fluctuations can have a considerable effect on activity ratio profiles.

Although the complicated nature of the hydrogeological system has been confirmed and there is evidence for present-day flow in another direction, most of the transport models have used time-averaged flow in a (Mine Grid) N-S direction, as there are more data available for these sections. Different selections of data were adopted in the various modelling approaches. One employed all the data, whereas others used only data from the region of the fan characterised by high uranium concentrations.

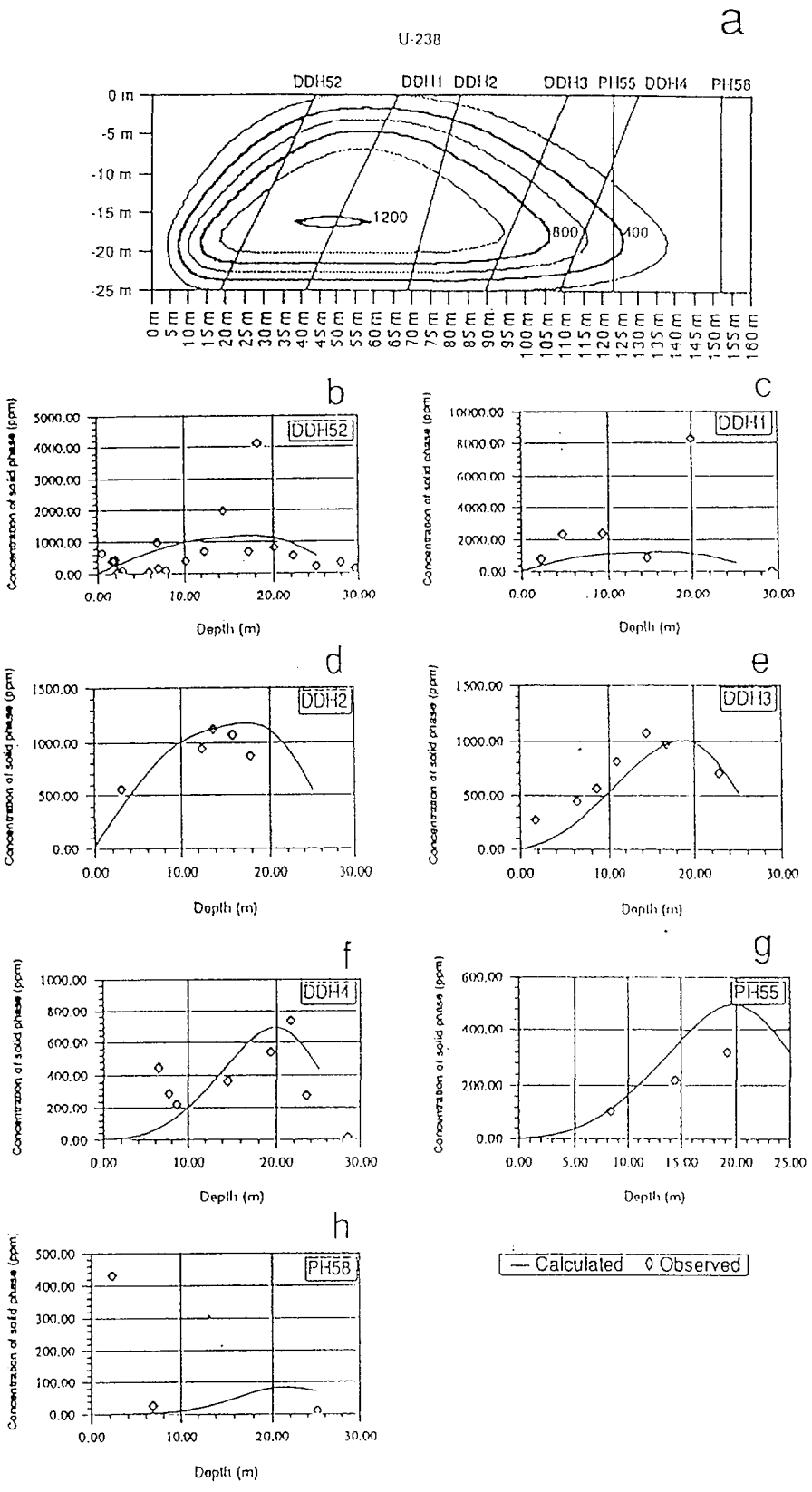

FIGURE 17.1 (a) Calculated uranium concentrations (μg/g) in Section 6109 mN, Comparisons of calculated and observed uranium concentrations: in (b) DDH52, (c) DDH1, (d) DDH2, (e) DDH3, (f) DDH4, (g) PH55, and (h) PH58.

Dispersion was omitted from many of the models, since it was considered to be of much less importance than advective transport. However, there is some evidence for back flow of waters from the dispersion fan towards the Koongarra Fault at certain times, which could be accounted for by incorporating dispersion in the models. Dispersion was included in several simple box models by allowing a component of the radionuclide transport to proceed in the direction determined by the local concentration gradient. Dispersion was also incorporated in the 2D NAMMU modelling (Atkinson et al., 1986). Matrix diffusion was not considered to be a primary mechanism in the formulation of the dispersion fan, hence it was not included in the modelling.

17.2 Partitioning between Groundwater and More than One Solid Phase

Multi-phase models incorporating recoil processes were able to reproduce the observed differences in isotopic composition between the accessible and the inaccessible phases and the separation of ^{238}U and ^{234}U isotopes. However, they employed a number of poorly known parameters and required a very high proportion of alpha-emitting radionuclides decaying in the water-accessible phase (up to 40%) to recoil the daughter radionuclide to the inaccessible phase. Although trends in the accessible phase activity ratios could be reproduced relatively well, simultaneous good fits for the inaccessible phase were more difficult to achieve (Figures 17.2 and 17.3). The model confirmed that partitioning of uranium into a crystalline phase was an important retarding process to uranium transport in the weathered zone.

An alternative model to those incorporating recoil proposed the chemical partitioning of ^{234}Th into an, as yet, unidentified phase. This mechanism differs from that usually proposed to explain the behaviour of uranium series radionuclides in rocks.

Both the ^{234}Th and recoil models were able to explain the decreasing $^{234}U/^{238}U$ activity ratios in rocks in the direction of transport. Models including recoil are also capable of explaining an increase of rock $^{234}U/^{238}U$ activity ratios in the direction of flow, as found in many other case studies (Osmond et al., 1983), with different parameter choices. However, the ^{234}Th model is not able to explain the progressive enrichment of $^{234}U/^{238}U$ in the groundwater in the direction of flow.

One-phase models incorporating equilibrium sorption cannot explain the differential transport of the two uranium isotopes except by assigning a different retardation to each isotope.

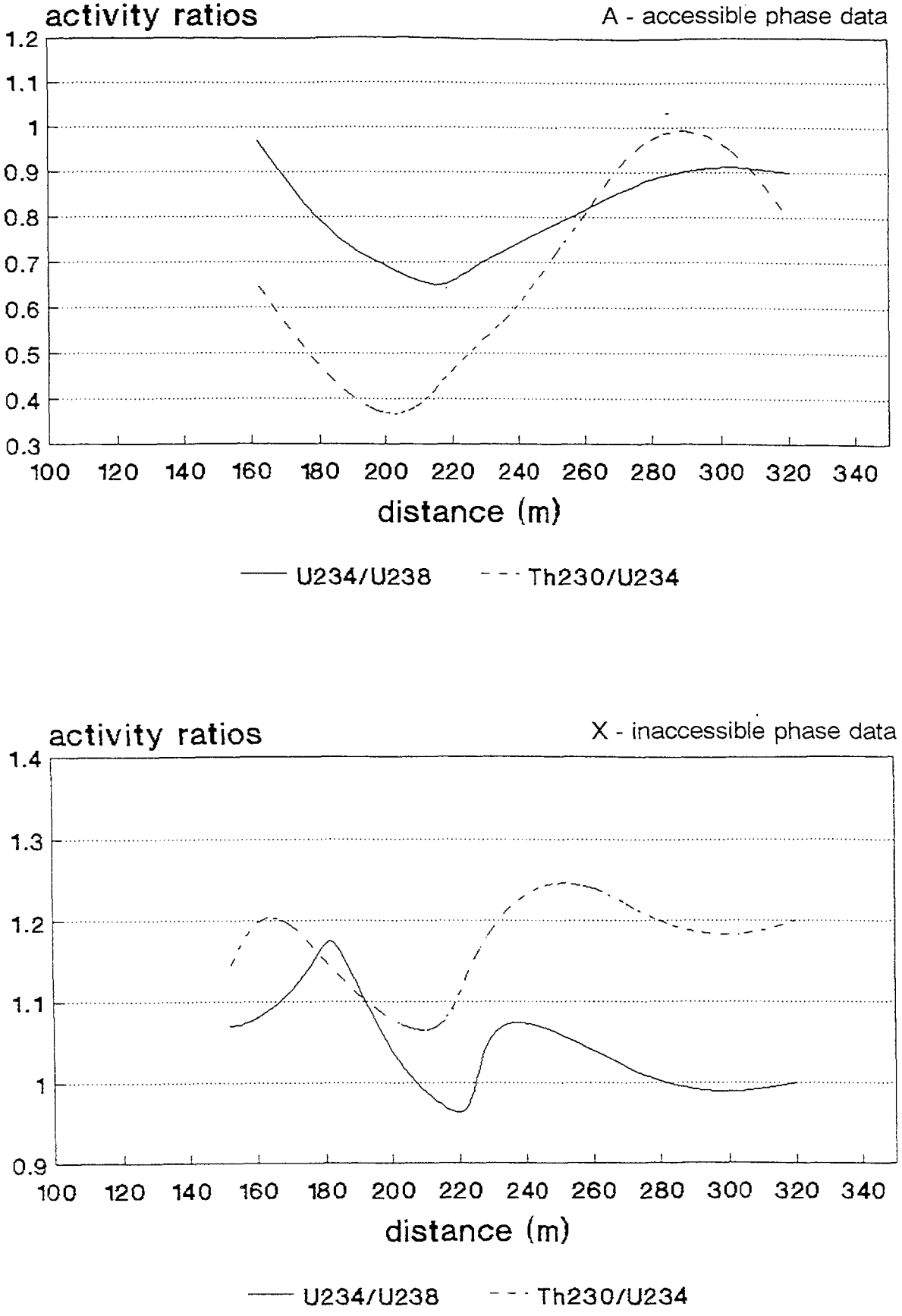

FIGURE 17.2 General trends in (observed) activity ratios along the dispersion fan

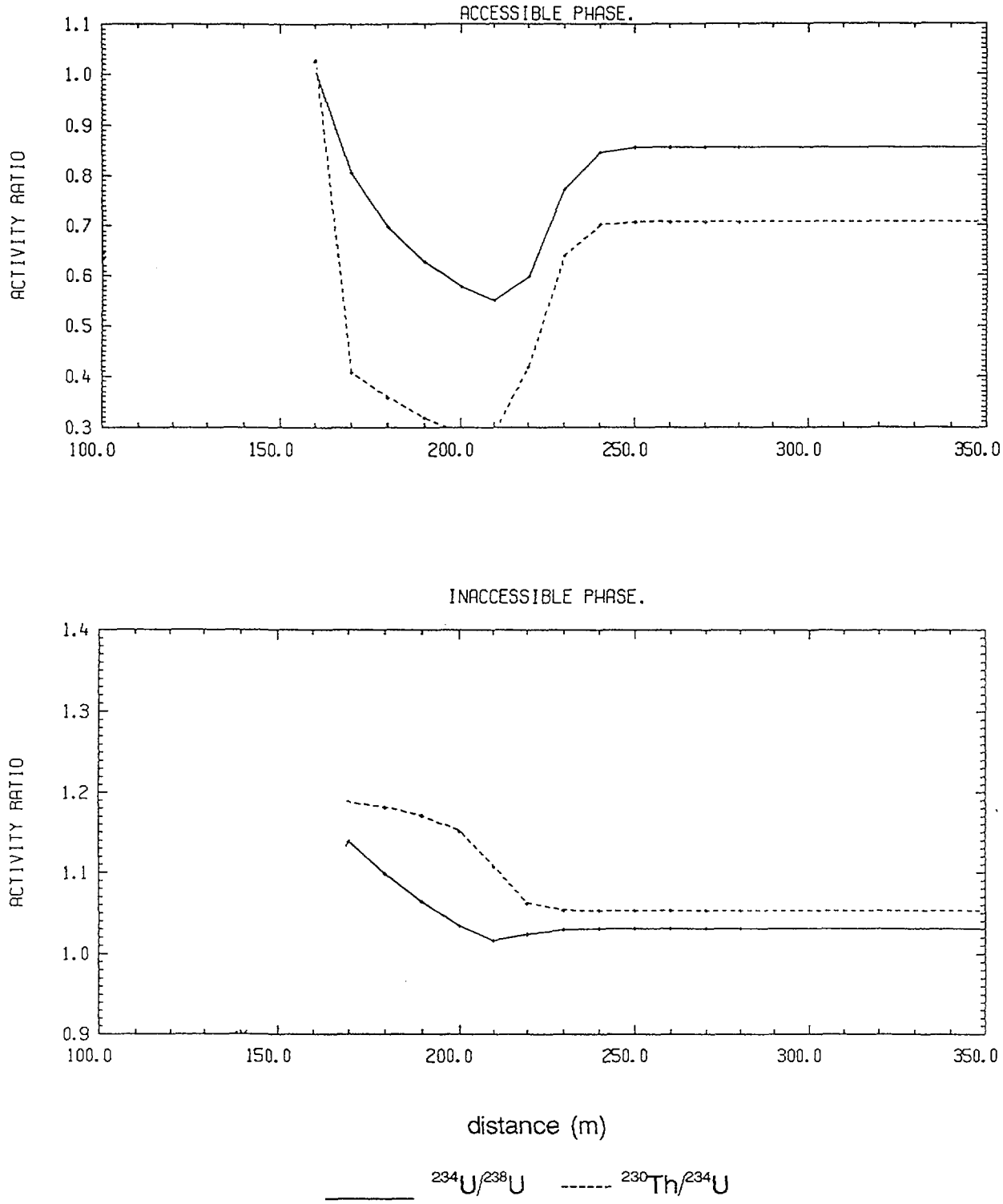

FIGURE 17.3 Calculated activity ratios for the two mineral phases
Total transport time t = 700 ka, K_d = 4000 mL/g

17.3 More Realistic Representation of Geochemical Processes Determining Partitioning between Groundwater and Rock

A quantitative one-dimensional coupled chemical transport model, CHEMTARD, was also applied. This is based on the retardation of uranium (VI) carbonate species during groundwater flow, by equilibrium sorption onto iron oxides, which was approximated using a Triple Layer Model representation of the sorbing surface. Calculated levels of sorbed uranium were in accordance with those observed in the dispersion fan at the Koongarra site.

Figure 17.4 shows the predicted distributions of uranium and thorium in the solid phase along the flow path, after flow at 0.01 m/year for 0.5 and 1 My. It can be seen that the model predicts greater mobility of uranium than thorium and that thorium gradually builds up to progressively higher concentrations at the beginning of the flow path with time, rather than simply migrating significantly along it. Maximum predicted concentrations of sorbed uranium fall in the range 400 to 450 μg/g which compare well with results of the measurement program for weathered rocks from the dispersed zone. These were in the range 100 to 600 μg/g.

17.4 Conclusions

There are considerable differences between the Koongarra No. 1 uranium orebody and a radioactive waste repository, particularly a deep waste repository. The Koongarra system is shallow, affected by seasonal hydrogeological changes as well as climatic variations on a longer timescale and transport is taking place in a zone of active weathering. Some of these features make the Koongarra system harder to characterise than a deep repository. However, there are nevertheless many analogies between the processes occurring at Koongarra and those occurring around a deep or shallow waste repository.

Thirteen models have been shown to be capable of representing different aspects of the system. The more complex models are more realistic, but require more data than are currently available. The simpler models are capable of representing the important features of the system and have the advantage of requiring fewer data. In general, the modelling did not enable a preferred "scenario" to be selected; however, it has illustrated the possible consequences of different processes and parameter ranges that are consistent with the analytical data.

The Koongarra system is heterogeneous and this has led to difficulties in selecting data for modelling. Some approaches have been adopted to minimise such uncertainties; for instance by selecting data from only one depth interval. The difficulties encountered because of the heterogeneity of the Koongarra weathered zone mirror those to be addressed in assessing radionuclide transport in repository systems.

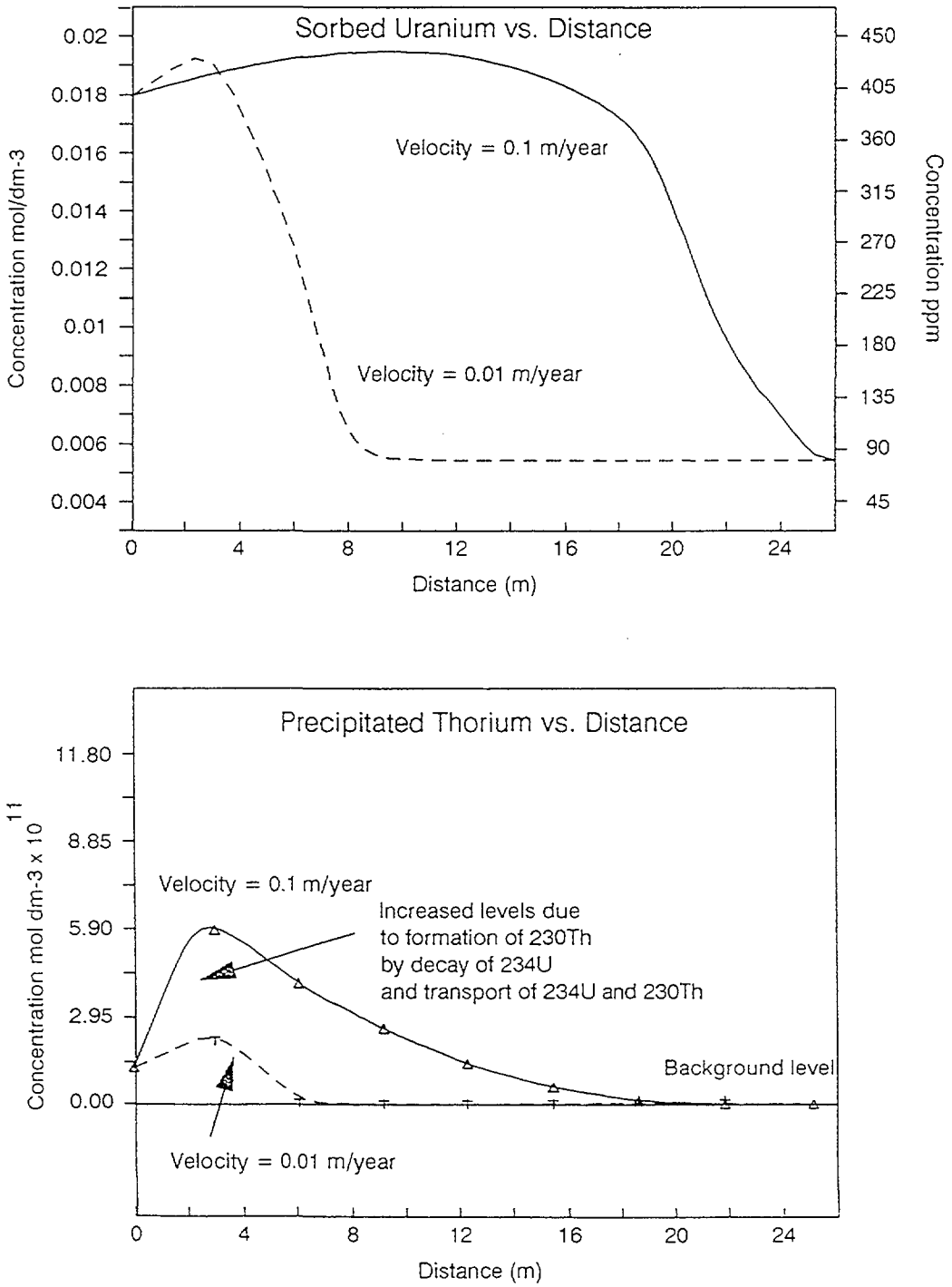

FIGURE 17.4 The predicted distributions of uranium and thorium in the solid phase along the flow path after flow at 0.01 m/yr for 0.5 and 1 Ma.

Recoil processes are believed to be of considerable importance in controlling the ratios of different radionuclides in solution. This process is not usually incorporated into performance assessments. However, in some circumstances it may significantly affect activity ratios of radionuclides in solution.

Considerable amounts of uranium are fixed in a phase where the uranium is inaccessible to the groundwater. Such fixation is not generally considered in safety assessment modelling, but is clearly sometimes important. To some extent, Koongarra may be atypical in that it is more chemically reactive than the geosphere through which radionuclides derived from a deep repository would move.

The Koongarra system is unusual in that $^{234}U/^{238}U$ activity ratios in rock samples from the dispersion fan decrease in the direction of groundwater transport, whereas in many other systems it has been reported that ^{234}U is preferentially mobile relative to ^{238}U. As most uranium resides in the rock rather than in the groundwater, the net recoil flux of uranium daughter radionuclides is usually from the rock to the groundwater, thus leading to $(^{234}U/^{238}U)_r$ less than one. Models involving recoil have explained the trend at Koongarra; other models explain the observations by invoking the presence of a phase in which ^{234}Th is irreversibly fixed.

One major uncertainty is the hydrogeological evolution of the fan. It is clear that the flux of groundwater and hence of uranium into the dispersion fan must be sufficient to explain the observed mass of uranium in the dispersion fan. Thus the models can be used to constrain the time-averaged Darcy flux. The shape of the dispersion fan, as predicted from 2D radionuclide transport modelling, could be used to constrain the permeability contrast between the weathered and unweathered zones.

The geometry of the dispersion fan could have changed over time as a result of downwards migration of the weathering front and erosion of the surface or deposition. These changes in geometry may also have been accompanied by changing hydrogeological properties. Such changes over time with active weathering have been investigated with a series of 1D models which had flow restricted to the region around the migrating weathering front. However, it was not possible to reproduce the uranium data using this model. It was therefore concluded that uranium has continued to be added at all levels of the dispersion fan within the recent past.

Estimates of the timescale for the evolution of the dispersion fan, assuming a constant Darcy flux of the groundwater, resulted in ages of the dispersion fan of the order of 0.5 to 3 million years. This was in accord with the geomorphological estimates of the rates of surface erosion over the Koongarra orebody discussed in Section 7, which suggested initiation of the dispersion fan between one and six million years ago. Over this period, it appears that the dispersion fan has moved some 50 to 100 m downstream in the predominant direction of groundwater flow. However, it is not known if some uranium-bearing groundwaters have been lost from the system. Uranium transport in the secondary dispersion fan has therefore taken place over fairly short distances over a timescale of the order of millions of years.

There are a number of influences on the system that have not been fully represented in the modelling. It is clear that modelling of the Koongarra System requires a representation of the influence of climate on hydrogeological and geochemical processes. The approach adopted here is to attempt to estimate the present-day values of relevant parameters and assume that they have been constant in time. This assumption is reasonable provided that the timescale for climatic fluctuations is short, relative to the radionuclide half-lives of interest.

Further progress in radionuclide transport modelling of the Koongarra natural analogue would require additional data on the hydrogeological system and its variation with time, on the form of uranium within the dispersion fan and on the heterogeneity of the system. It is particularly important to establish the proportion of uranium in the dispersion fan contained in uranium-rich phases. Additional modelling approaches could include, data permitting, some representation of heterogeneity of the system, a better representation of the evolving hydrogeology of the system and coupling between geochemical and transport codes.

17.5 Outstanding Issues and Uncertainties

There are a number of data requirements that would enable further progress to be made in radionuclide transport modelling. These are:

- a better quantification of climatic effects
- improved characterisation of the current and past hydrogeology (uncertainties in groundwater flow patterns and flow rates over geological timescales were a major unknown as climatic variations could have resulted in substantial lowering of the water table so that no horizontal uranium transport occurred)
- further consideration of the evolving geometry of the site as a result of geomorphological processes; eg, the relative positions of the surface and the base of the weathered zone
- additional information on the form of uranium within the dispersion fan and the nature of the processes resulting in the incorporation of uranium in crystalline phases, and
- statistical information on heterogeneity.

Given the availability of appropriate data, the following approaches may be beneficial:

- precipitation and dissolution be added to the current equations
- a proper coupling of transport and geochemical models
- a more sophisticated treatment of sorption
- better representation of the mineralogical processes accompanying the fixation of uranium in crystalline phases
- improved 2D models to constrain changes in the geometry and hydrogeology of the system with time, and

- additional 2D sections of the site should be considered.

18 SCENARIO DEVELOPMENT

Although the formation of the dispersion fan at Koongarra was discussed throughout the ARAP and has been frequently referred to in this report, an integrated approach to understanding the formation was also considered as a further stage of the modelling work.

The methodology was similar to that used by SKI/SKB in the Swedish nuclear waste isolation program, following a technique originally developed by Sandia National Laboratories (Cranwell et al., 1990). In performance assessments of repositories, a broad range of physical, chemical and mathematical models are used to assess long-term behaviour. Hence, the validation of these models is a major concern for regulatory authorities. Although it is now realised that validation in the strictest sense of the word can never be obtained, uncertainties continue to play an important role in the assessment of repository safety. By testing scenarios of the evolution of a site, it might be possible to test model concepts, to understand uncertainties in data, and to increase confidence in the use of the models in performance assessment of a waste repository.

The overall objective of the current work was not to validate scenario development methods but to apply them to describe the (past) evolution of the natural analogue by:

- providing a systematic description of the analogue, ie descriptions of how different processes contributed to and caused the development of the dispersion fan, and
- deriving alternative evolution scenarios for the analogue.

The preparation of systematic descriptions of the analogue provided a forum for exchange of information and ideas between the different scientific disciplines and modellers, and encouraged a more integrated approach in the conceptualisation of processes. It also focussed the evaluation to issues relevant for performance assessments.

18.1 Scenario Methodology as Applied in the Analysis of Koongarra

The initial activities comprised:

- identification of all features, events and processes (FEPs) that may have had an influence on the evolution of the analogue (this involved several of the ARAP research groups in order to cover all relevant disciplines)
- documentation of each FEP in a short memo-text containing a description of the FEP, the causes and effects of the FEP, modelling aspects and references to literature
- screening on the basis of well defined criteria regarding the FEP's importance and role in the evolution of uranium mineralisation, and

- classification of the remaining FEPs depending on the nature of the FEP and lumping of related FEPs into subgroups.

By going through the merged list of 242 primary FEPs it was found that each FEP could be screened into one of the following four groups:

- OUT - on the basis of duplication, poor definition, low probability or low consequence (52 FEPs)
- PROCESS SYSTEM - comprising all deterministic chemical and physical phenomena that might have influence the formation of the secondary uranium mineralisation and the dispersion in the weathered zone (Examples of major FEPS are "groundwater flow" and "adsorption") (138 FEPs)
- EXTERNAL CONDITIONS - having occurred independently of the phenomena in the PROCESS SYSTEM) (Examples are "rainfall range and intensity" and "erosion to major peneplanation") (39 FEPs), and
- EXTERNAL FEATURES - reflecting the history of the region but not influencing the evolution of the analogue such as "talus deposits" and "old coastline" (13 FEPs).

The FEPs in the PROCESS system were then used to systematically describe the Koongarra analogue in terms of schematic diagrams, which showed the interconnections and links of causes and effects between different processes. Two diagrams, shown in Figures 18.1 and 18.2 were prepared for:

- the source (the combination of phenomena which have influenced the distribution of uranium between solid and liquid phases at the location of the primary ore), and
- migration (the combination of processes directly involved in the formation of the dispersion fan).

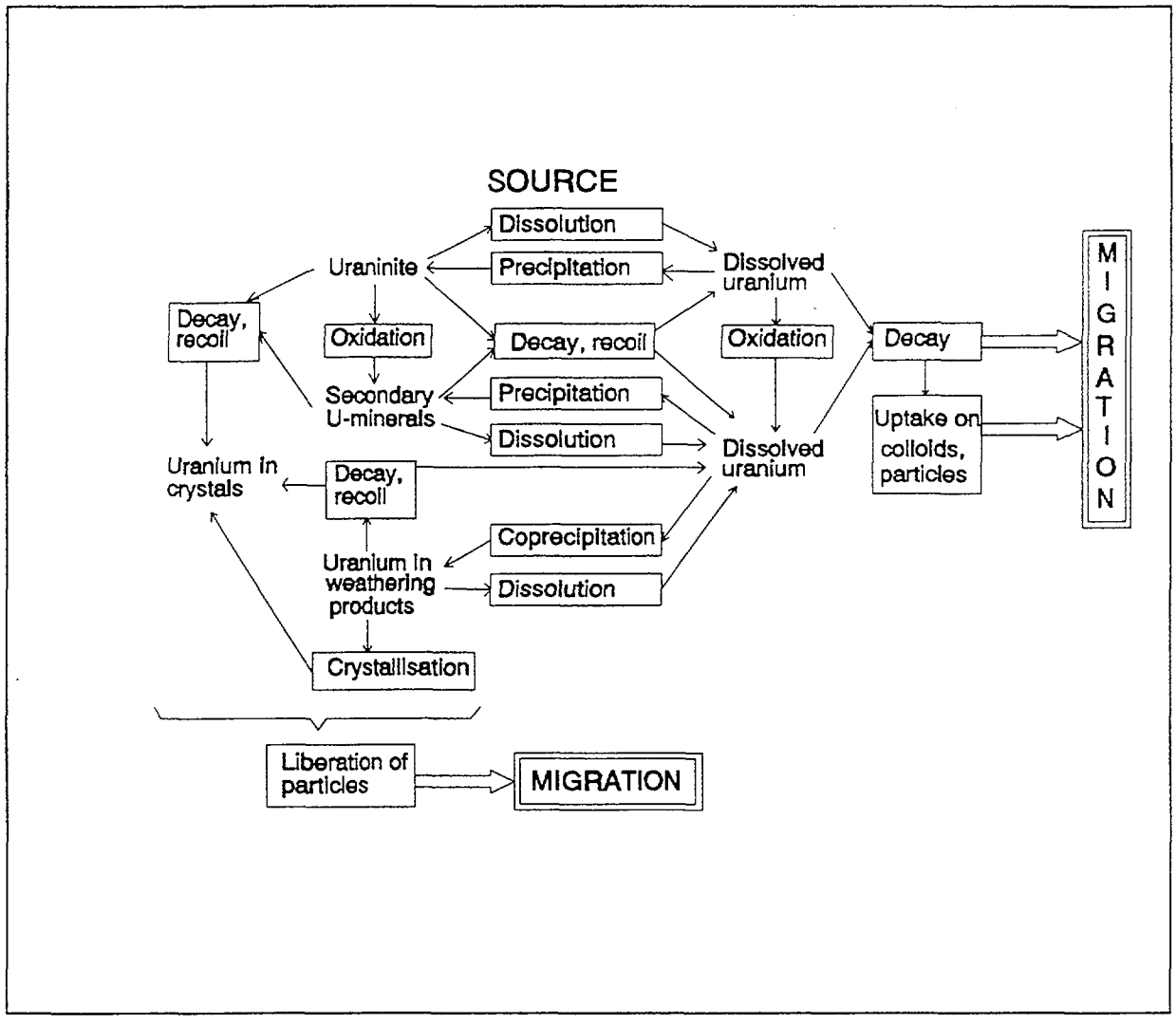

FIGURE 18.1 A schematic illustration of the source

The description of the source suggests that since the deposition of the primary uraninite orebody, there has been a redistribution of uranium between immobile and mobile phases. In addition to primary uraninite, the immobile phases are secondary uranium minerals (uranyl silicates and uranyl phosphates) as well as different forms of weathering products (amorphous and crystalline iron oxy-hydroxides and clays) and minerals such as quartz, which initially did not contain uranium. The identified mobile phases are dissolved uranium in different oxidation states and potentially also uranium in colloidal form and particles of uranium minerals, with the distribution of uranium resulting from the following phenomena:

- dissolution (leaching)/precipitation of uranium
- coprecipitation, crystallisation and dissolution of weathering products
- oxidation of uranium
- decay and α-recoil
- uptake on colloids/particles, and
- liberation of particles containing uranium.

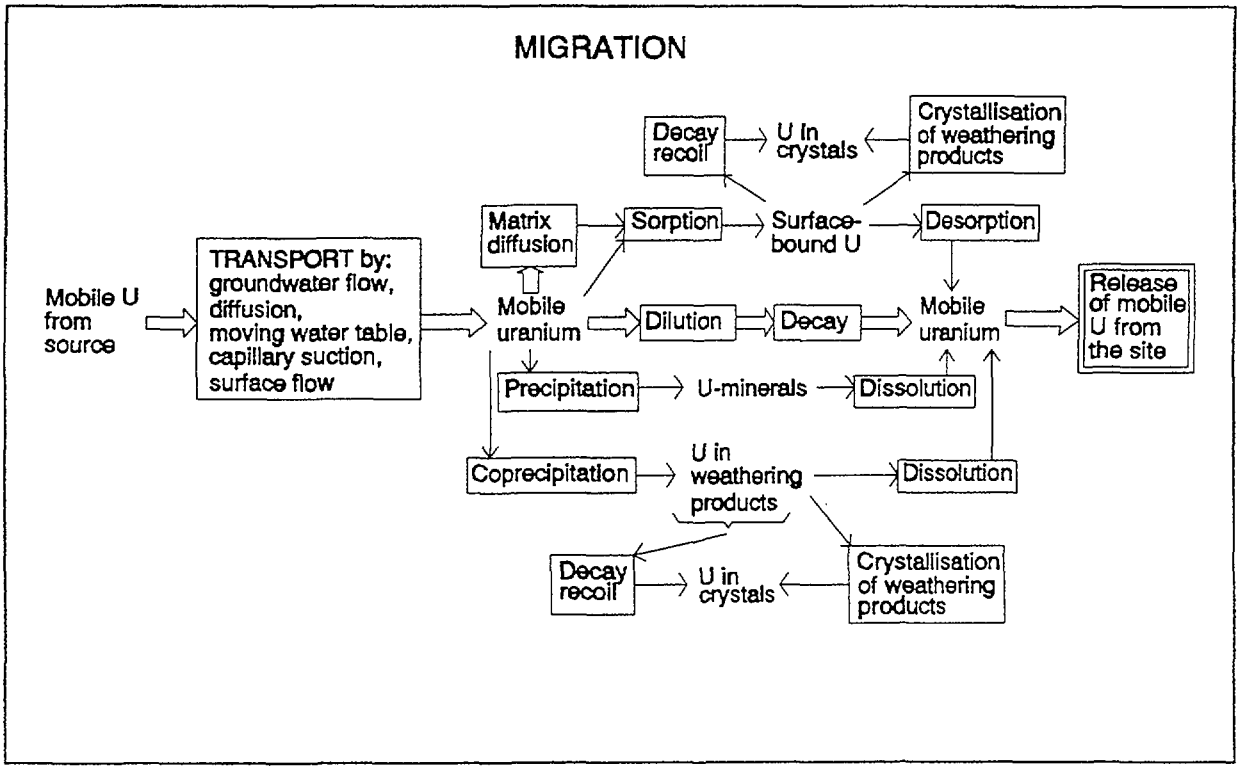

FIGURE 18.2 *A schematic illustration of migration*

Although not completed during the ARAP, initial work to formulate scenarios for the formation of the dispersion fan at Koongarra was carried out. These scenarios were developed on possible evolutions of External Conditions and External Events and on their impact on the important FEPs in the Process System. A rapid weathering of the host chlorite-schist rock was assumed to have started around the onset of the Pleistocene Ice Age (ca 1.6 Ma ago). The eventual oxidation and mobilisation of the uranium ore could then have occurred under unsaturated or saturated conditions leading to the following major scenarios, which are described in detail in Volume 16 of this series:

- uranyl phosphates formed under unsaturated conditions, with periodical evolution of the dispersion fan in conjunction with alternating dry (glacial) and wet (interglacial) periods during the Pleistocene
- uranyl phosphates formed under unsaturated conditions as a single event, taking place either early or late during the Pleistocene
- uranyl phosphates formed under saturated conditions, in conjunction with periods of higher and lower flow due to climatic cycling.

Additional scenarios to account for the occurrence of uranium in the weathered zone, in a direction coinciding with present-day groundwater flow but different from that of the uranyl phosphate occurrence, might be proposed. These could provide information on the result of changes in groundwater flow with time or might even suggest that assumptions on the initial shape of the ore body are wrong and the dispersion plumes originate from two different ore bodies located in different hydrologic regimes. A further scenario could address weathering processes and the interaction with both hydrology and mass transport, when for example, at an early stage of weathering, the rock might become more permeable, thereby increasing the size and number of paths available for water flow.

18.2 Conclusions

The original objectives of the work were only partially met; however, the work resulted in a checklist of phenomena of potential importance for both the evolution and evaluation of the analogue as well as first attempts to describe the process system and formulate scenarios. The work also contributed to a better understanding of the analogue. Although there had been detailed studies of individual processes by research groups during the ARAP, the scenario process encouraged all research groups to develop a much more integrated approach to the conceptualisation of processes relevant to Koongarra and the evolution of the dispersion fan.

19 IMPLICATIONS FOR PERFORMANCE ASSESSMENT MODELLING

Assessments of the long-term performance of geological repositories for radioactive wastes are being undertaken in many countries. In some countries, these assessments are for repositories that are either in operation or being built; in others they are for potential repositories that are being planned or considered. Four pathways have been identified internationally as being of importance in returning radionuclides to the biosphere: transport in groundwater; natural disruptive events; release of radioactive gases; and human intrusion into the repository.

The main pathway to which an analogue such as Koongarra is relevant is return by groundwater flow. It is therefore appropriate to consider the relevance of modelling of radionuclide transport in the Koongarra system to similar modelling undertaken for groundwater flow paths from proposed repositories. Most of the models used in the ARAP transport modelling are more complex than the simple modelling undertaken in performance assessments that assume equilibrium sorption and no interaction of radionuclides with crystalline phases.

It should be noted that there is a fundamental difference between modelling natural systems and assessing future performance of a waste repository. In the first the natural complexity of the system has to be addressed, whereas in the other scoping or bounding assessments may be sufficient. However, insights into natural processes may be gained from modelling the complexities of the analogue. Such insights may justify the simplifications in the performance assessments, or alternatively they may point to areas where more detailed modelling is required.

Many radionuclides have been studied in the ARAP. These include ^{238}U, ^{235}U and ^{232}Th series radionuclides and ^{239}Pu, ^{129}I, ^{99}Tc and ^{36}Cl. All these radionuclides are found in radioactive waste repositories, and can also be good analogues of other relevant radionuclides. In this sense the estimates of radionuclide mobility obtained in this study are of relevance to performance assessment modelling.

There are a number of significant differences between the Koongarra site and proposed radioactive waste repositories. One difference between an analogue such as Koongarra and most repositories for ILW, HLW or SF, is that there is no physical containment in a metallic canister. Some repositories are rather deeper than the Koongarra system, but shallow repositories either exist or are planned. The shallow situation of the Koongarra site means that there is likely to be a greater flux of groundwater through the orebody and geochemical conditions will be far more oxidising than in a deep repository. Uranium transport at Koongarra is taking place in a zone of active weathering. This is atypical as far as many waste repositories are concerned.

The geochemistry and geochemical processes at Koongarra associated with the uranyl phosphate zone can be conveniently divided into two categories according to their relevance to present-day geochemical processes and those that have operated in the geologic past. Information on the present-day geochemistry of soils, weathered rock, groundwaters, and the role of sorption processes forms a basis for a *present-day analogue for nuclear waste migration.* Information and inferred reconstructions of geochemical processes thought to have operated in the geologic past form a basis for a *paleoanalogue for nuclear waste migration.*

The extensive databases of present-day geochemistry and geochemical processes at Koongarra effectively form the basis for a present-day analogue for nuclear waste migration. They have enabled geochemical speciation and state of saturation models to be tested via comparison of the results of a series of calculations to be compared with the chemistry of the present-day groundwaters at Koongarra.

Studies of geochemical processes thought to have taken place in the geologic past provide a unique reference for our understanding of how uranium and other nuclides migrate in nature. Despite their inherent uncertainties, such studies provide a basis for assessing the way in which radionuclides will migrate in environments with a variety of geologic settings and over a range of different geologic timescales.

Uranium transport in the secondary dispersion fan has taken place over fairly short distances during a timescale of the order of millions of years. However, it is not possible to exclude the loss of some uranium bearing fluids from the system along flow paths through now eroded rocks. The fact that most of the uranium has moved only of the order of 50 to 100 m over a timescale of the order of millions of years suggests that the uranium is not very mobile, even in a chemically active system with relatively high groundwater flow.

Studies of the Koongarra system have emphasised the importance of partitioning of radionuclides into crystalline phases during transport. This process is not generally incorporated into performance assessment models, which often only include

retardation by linear equilibrium sorption. If the sorption coefficients are chosen appropriately by considering only those phases in equilibrium with the groundwater, then the neglect of crystalline phases will overestimate the rate at which such radionuclides are transported. Proper consideration of the kinetic processes leading to the incorporation of these radionuclides into crystalline phases would result in slower transport.

Recoil is an important process affecting radionuclide transport at Koongarra, in that it can affect the distribution of radionuclides between phases in equilibrium with the groundwater and crystalline or inaccessible phases. Recoil is not generally incorporated into current performance assessments.

The difficulties with heterogeneity of the Koongarra weathered zone mirror those encountered in assessing radionuclide transport in all geological systems. It is clear that the Koongarra System requires non-steady state models and that a representation of the influence of climate on hydrogeological and geochemical processes is required to develop a detailed understanding of the system. The Koongarra System is close to the surface and is particularly sensitive to such changes. However, this observation is illustrative of the need to consider climatic variations in performance assessments.

One of the great challenges of the ARAP, and therefore one of the great benefits because of the successful completion of the project, was that so many contrasting scientific disciplines had to work together to develop an understanding of the system. This was a valuable experience that similar teams will have to develop for the assessment of repositories, which will have to be founded on the characterisation of real sites.

20 REFERENCES

Airey. P.L., Golian, C. and Lever, D.A. (1986). Radionuclide Migration Around Uranium Ore Bodies – Analogue of Radioactive Waste Repositories. Topical report – An approach to the mathematical modelling of the uranium series redistribution within ore bodies. United States Nuclear Regulatory Commission Contract NRC-04-81-172. AAEC/C49, NUREG/CR-5060.

Atkinson, R., Herbert, A.W., Jackson, C.P., Robinson, P.C. and Williams, M.G. (1989) NAMMU Users Guide (Release 4). UKAEA Report AERE-R.12354.

Australian Groundwater Consultants (AGC) (1980) Koongarra Project, unpublished consultants report.

Birchard, G.F. (1989). International Alligator Rivers Analogue Project. Radioactive Waste Management and the Nuclear Fuel Cycle. Vol. 130-140, pp 325-337. Harwood Academic Publishers GmbH.

Bowler, J.M., Hope, G.S., Jennings, J.N., Singh, G. and Walker, D. (1976). Late Quaternary climates of Australia and New Guinea. Quaternary Research, 6, pp. 359-394.

Briesmeister, J. (ed) (1986). MCNP - A General Monte Carlo Code for Neutron and Photon transport, Version 3A, Los Alamos National Laboratory, LA-7396-M, Rev. 2 (manual), 583p.

Brown, D.S. and Allison, J.D. (1987). MINTEQA1, an Equilibrium Metal Speciation Model: User's Manual. Environmental Research Lab., Athens, GA. Report No.:EPA/600/3-87/012.

Chapman, N.A., McKinley, I.G. and Smellie, J.A.T. (1984). The potential of natural analogues in assessing systems for deep disposal of high-level radioactive waste. NAGRA Tech. Rept. NTB 84-41.

Chapman, N.A., McKinley, I.G., Shea, M.E. and Smellie, J.A.T. (1991). The Poços de Caldas Project: Summary and implications for radioactive waste management. NAGRA NTB 90-33, SKB TR 90-24, UKDOE WR 90-055.

CODATA Task Group Report (1978). Prepared by ICSU CODATA, Paris. J. Chem. Thermodynamics, Vol. 10(10), p.903-906.

Cowan, G.A., Bryant, E.A., Daniels, W.R. and Maeck, W.J. (1975). Some United States Studies of the Oklo Phenomenon. Proc. Int. Symp. on The Oklo Phenomenon, Libreville, IAEA (Int. At. Energy Agency), Vienna SM-204/5, pp. 341-356.

Cramer, J.J. and Smellie, J.A.T. (1994). Final report of the AECL/SKB Cigar Lake Analog Study. AECL-10851, COG-93-147, SKB TR 94-04.

Cranwell, R.M., Guzowski, R.V., Campbell, J.E., and Ortiz, N.R. (1990). Risk methodology for geologic disposal of radioactive waste: Scenario selection procedure, SAND80-1429, NUREG/CR-1667, Sandia Laboratories, Albuquerque, USA.

Curtis, D., Benjamin, T., Gancarz, A., Loss, R., Rosman, K., DeLaeter, J., Delmore, J.E. and Maeck, W.J. (1989). Fission product retention in the Oklo natural fission reactors. Applied Geochemistry, Vol. 4, pp. 49-62.

Giblin, A.M. and Snelling, A.A. (1983). Application of Hydrogeochemistry to Uranium Exploration in the Pine Creek Geosyncline, Northern Territory, Australia, Journal of Geochemical Exploration 19, pp. 33-55.

Grenthe, I., Lemire, R.J., Muller, A.B., Nguyen-Trung, C. and Wanner, H. (1989). Chemical Thermodynamics of Uranium. OECD/NEA Draft Report. [Published in 1992 by North Holland, Elsevier Science Publishers, Amsterdam for OECD/NEA.]

Gringarten, A.C. (1982). Flow-test evaluation of fractured reservoirs. Geological Society of America Special paper 189, pp. 237-260.

Ivanovich, M., Duerden, P., Payne, T.E., Nightingale, T., Longworth, G., Wilkins, M.A., Hasler, S.E., Edgehill, R.B., Cockayne, D.J. and Davey, B.G. (1988). Natural Analogue Study of the Distribution of Uranium Series Radionuclides between the

Colloid and Solute Phases in the Hydrogeological System of the Koongarra Uranium Deposit, Australia. UKAEA Report AERE-R.12975.

Kenna, B.T. and Kuroda, P.K. (1964). Technetium in nature. J. Inorg. Nucl. Chem., 26, pp. 493-499.

Kershaw, A.P. (1986). Climatic change and Aboriginal burning in north-east Australia during the last two glacial/inter-glacial cycles. Nature, 322, pp. 47-49.

Langmuir, D. (1978). Uranium solution-mineral equilibria at low temperatures with applications to sedimentary ore deposits. Geochim et Cosmochim. Acta, 42, pp. 547-569.

Loss, R.D., Rosman, K.J.R., DeLaeter, J.R., Curtis, D.B., Benjamin, T.M., Gancarz, A.J., Maeck, W.J. and Delmore, J.E. (1989). Fission-product retentivity in peripheral rocks at the Oklo natural fission reactors, Gabon. Chemical Geology, 76, pp. 71-84.

Magalhaes, M.C.F., Pedrosa de Jesus, J. and Williams, P.A. (1985). The chemistry of uranium dispersion in groundwaters at the Pinal Do Souto mine, Portugal. Inorganica Chimica Acta, 109, pp. 71-78.

Moskvin. A.I., Shelyakina, A.M. and Perminov, P.S. (1967). Solubility product of uranyl phosphate and the composition and dissociation constants of uranyl phosphato-complexes. Russ. J. Inorg. Chem., 12, pp. 1756-1760.

Needham, R.S. (1982). Cahill, Northern Territory. 1:100 000 Geological Map and commentary. Bureau of Mineral Resources, Geology and Geophysics. Canberra, Australia.

Needham, R.S. and Stuart-Smith, P.G. (1976). The Cahill Formation – host to uranium deposits in the Alligator Rivers Uranium Field, Australia. BMR Journal of Australian Geology and Geophysics 1, pp. 321-333.

Noranda Australia Limited (1978). Koongarra Project Draft Environmental Impact Statement, 3 Volumes, Noranda Australia Limited, Australia.

Osmond, J.K., Cowart, B. and Ivanovich, M. (1983). Uranium isotopic disequilibrium in groundwater as an indicator of anomalies. Int. J. Radiat. Isot., 34, pp. 283-308.

Papelis, C., Hayes, K.F. and Leckie, J.O. (1988). HYDRAQL: A Program for the Computation of Aqueous Batch Systems including Surface Complexation Modeling of Ion Adsorption at the Oxide/Solution Interface. Stanford Univ. Dept. Civil Eng. Tech. Report No. 306.

Parkhurst, D.L., Thorstenson, D.C., and Plummer, L.N. (1980). PHREEQE: A Computer program for Geochemical Calculations, USGS Water Res. Invest. Report 80-60, Revised, 1985.

Pedersen, C.P. (1978). The geology of the Koongarra deposits, including investigations of contained elements. In: Koongarra Project Draft Environmental Impact Statement, Appendix 5, Noranda Australia Limited, Melbourne.

Petit, J.C., (1992). Reasoning by analogy: rational foundation of natural analogue studies. Applied Geochemistry, Suppl. Issue No.1, pp 9-11.

Read, D. (ed). (1990). Chemval project report on stage 2: application of speciation models to laboratory and field data sets. CEC Report EUR 13124EN.

Snelling, A.A. (1980a). A geochemical study of the Koongarra uranium deposit, Northern Territory, Australia. PhD thesis (unpublished), The University of Sydney.

Snelling, A.A. (1980b). Uraninite and its alteration products, Koongarra uranium deposit. In: Uranium in the Pine Creek geosyncline, J. Ferguson and A.B. Goleby (eds), International Atomic Energy Agency, Vienna, pp. 487-498.

Snelling, A.A. (1990). Koongarra uranium deposits. In: The Geology of the Mineral Deposits of Australia and Papua new Guinea, F.E. Hughes (ed), The Australasian Institute of Mining and Metallurgy, Melbourne, pp. 807-812.

Townley, L.R. (1987). AQUIFEM-N: A Multi-Layered Finite Element Aquifer Flow Model. User's Manual and Description, Townley and Associates.

Tripathi, V.S. (1984). Uranium (VI) transport modelling: Geochemical Data and Submodels. PhD dissertation, Stanford University, Palo Alto, CA.

van de Weerd, H., Leijnse, A., Hassanizadeh, S. M. and Richardson-van der Poel, M.A. (1994). INTRAVAL phase 2, test case 8 – Alligator Rivers natural Analogue – Modelling of uranium transport in the weathered zone at Koongarra (Australia). RIVM Final Report 715206005.

von Maravic, H. and Smellie, J. (eds) (1992). 5th CEC Natural Analogue Working Group Meeting and Alligator River Analogue Project (ARAP) Final Workshop, Toledo,Spain. CEC EUR 15176 EN.

Wasson, R.J. and Donnelly, T.H. (1991). Palaeoclimate reconstructions for the last 30 000 years in Australia – A contribution to prediction of future climate. CSIRO Division of Water Resources. Technical Memorandum 91/3.

Westall, J. C., (1979). MICROQL, A chemical equilibrium program in basic, Swiss Federal Institute of Technology (EAWAG), Zurich 1979.

Wolery, T.J. (1983). A computer program for geochemical aqueous speciation-solubiligy calculations, user's guide and documentation. UCRL Report No. UCRL-5314. Lawrence Livermore Lab., Univ. Calif. 191 p.

APPENDIX 1

ARAP Agreement Funding Organisations

Participants	
Australian Nuclear Science and Technology Organisation	(ANSTO)
Japan Atomic Energy Research Institute	(JAERI)
Swedish Nuclear Power Inspectorate	(SKI)
UK Department of the Environment	(UKDoE)
US Nuclear Regulatory Commission	(USNRC)
ARAP Associate Participant	
Power Reactor and Nuclear Fuel Development Corporation of Japan	(PNC)
Additional Support	
Government of the Northern Territory of Australia	
US Department of Energy	(USDOE)
Central Research Institute for Electric Power Industry, Japan	(CRIEPI)

Collaborating Laboratories and Principal Investigators

AUSTRALIA		
ANSTO	Mineralogy/Colloids/Rock U Series	R Edis
	Transport Modelling	C Golian
	Groundwater Chemistry Sorption Experiments	T Payne
	Sorption Modelling	D Waite
	PIXE/PIGME Analysis	D Cohen
	Uranium Analysis – DNAA	T Wall
	Tritium Analysis	R Stokes
	^{14}C Measurements	L Smith
	Accelerator Mass spectrometry ^{36}Cl	J R Bird, D Fink, C Tuniz, A V Jenkinson
The Australian National University	Accelerator Mass Spectrometry ^{36}Cl	K Fifield and G Allen
Consultant	Geology	A Snelling
CSIRO – Division of Energy Chemistry (Lucas Heights)	ICP-AES/ICP-MS	L Dale
	Anions/Cu	G Batley
	TOC	R Matthews

CSIRO – Division of Water Resources (Adelaide, SA)	Hydrogeochemistry	A Herczeg
	Stable Isotope Measurements	F Leaney
CSIRO – Division of Water Resources (Perth, WA)	Hydrology Modelling	L Townley, M Trefry, R Salaama, A D Barr
Monash University	Mössbauer Spectroscopic Analysis	J D Cashion and L J Brown
Northern Territory Department of Mines & Energy	Groundwater Sampling/Hydrology	B Treloar
Northern Territory Power & Water Authority	Geomorphology/Groundwater/ Geophysics	P Jolly, D Pidsley, K Martin
The Sydney University Department of Geophysics	Petrofabric Analysis and Field Geophysics Measurements	D Emerson , K Mills, L Q Cao, M Hallett
The Sydney University Department of Soil Science	Pedology/Thin Section Analysis	T Koppi and D Klessa
The University of Western Australia	Geomorphology and Palaeoclimates	K-H Wyrwoll

	JAPAN	
Akita University	Uranium Redistribution	S Nakashima
Central Research Institute for Electric Power Industry	Borehole TV Investigations	K Miyakawa
Japan Atomic Energy Research Institute	Alteration	T Murakami, T Nagano
	Groundwater Chemistry	N Yanase
	Transport Modelling	T Ohnuki and H Kimura
	Sorption/U Series data	K Sekine
	Spectroscopy	T Nagano
Power Reactor & Nuclear Fuel Development Corporation	Groundwater and Rocks REE	T Seo
University of Tokyo	Transmission Electron Microscopy	S Nakashima
	SWEDEN	
KEMAKTA	Transport Modelling	K Skagius
	Hydrochemistry	K Pers, F Brandberg, M Lindgren
SKI	Scenario Development Validation	S Wingefors

UNITED KINGDOM		
W S Atkins	Geochemical Modelling	D Read and D Bennett
AEA Technology, Harwell Laboratory	Transport Modelling/ Hydrology Modelling	D A Lever, A J Baker, M Ivanovich, G Longworth, L D Connell
USA		
The Johns Hopkins University	Geochemical Modelling	D Sverjensky and J Raffensperger
Los Alamos National Laboratory	^{36}Cl, ^{99}Tc, ^{129}I, ^{239}Pu Analysis and Production Rate Modelling	D Curtis, J Fabryka-Martin, M Attrep, F Roensch
Batelle Pacific Northwest Laboratory	Hydrology (Fracture) Modelling	J Smoot
United States Geological Survey	Sorption Modelling	J A Davis
The University of Arizona	Hydrogeology	S N Davis, S Braumiller, B Marley, J Norris
The University of New Mexico	Alteration of Uranium Minerals	R C Ewing and H Isobe * (* On attachment from JAERI)
US Nuclear Regulatory Commission	Geochemical Modelling	G Birchard